RESEARCH REPORT

Copy 1

GUGGENHEIM AERONAUTICAL LABORATORY

CALIFORNIA INSTITUTE OF TECHNOLOGY

HYPERSONIC RESEARCH PROJECT

Memorandum No. 47
December 15, 1958

AN EXPERIMENTAL INVESTIGATION OF THE EFFECT OF EJECTING A COOLANT GAS AT THE NOSE OF A BLUNT BODY

by
C. Hugh E. Warren

PURDUE UNIVERSITY
MAY 15 1959
AERO LIBRARY

ARMY ORDNANCE CONTRACT NO. DA-04-495-Ord-19

GUGGENHEIM AERONAUTICAL LABORATORY
CALIFORNIA INSTITUTE OF TECHNOLOGY
Pasadena, California

HYPERSONIC RESEARCH PROJECT

Memorandum No. 47

December 15, 1958

AN EXPERIMENTAL INVESTIGATION OF THE EFFECT OF EJECTING A COOLANT GAS AT THE NOSE OF A BLUNT BODY

by

C. Hugh E. Warren

Clark B. Millikan, Director
Guggenheim Aeronautical Laboratory

ARMY ORDNANCE CONTRACT NO. DA-04-495-Ord-19
Army Project No. 5B0306004
Ordnance Project No. TB3-0118
OOR Project No. 1600-PE

ACKNOWLEDGMENTS

The author wishes to express his appreciation to Professor Lester Lees for his assistance, guidance and encouragement during this work, to Mr. Howard McDonald and other members of the Aeronautics Machine Shop for fabricating and maintaining the models and other items of equipment, to Mr. Paul Baloga and the staff of the Hypersonic Wind Tunnel for their assistance and advice during testing, to Mrs. Betty Laue for much computational work, and to Mrs. Gerry Van Gieson for typing the manuscript and piloting the report through after the author's departure.

Most of the work was done while the author was in receipt of a Harkness Fellowship of the Commonwealth Fund of New York, to whom thanks are due for the opportunity to spend a year on such an instructive and interesting program in such congenial surroundings.

ABSTRACT

An experimental investigation has been made of the effect of ejecting nitrogen and helium coolant gases at the nose of a blunt body in the GALCIT 5 inch x 5 inch hypersonic wind tunnel at a nominal Mach number of 5.8. The gases were ejected with "swirl", to encourage them to flow tangentially to the model surface at ejection, and also straight out. Measurements were made of pressure, temperature and heat flux on the surface of the model at incidences of 0, 4, 8 degrees, and for a range of coolant gas flows.

It was found that ejection with swirl did not in fact lead to an easement of the heating problem, because the high tangential velocity with which the coolant was injected into the boundary layer so increased the wall shear stress, and hence by the Reynolds analogy, the heat flux, that it predominated over the reduced driving temperature difference associated with the cooled boundary layer.

With straight-out ejection it was found that the heat alleviation capabilities of the ejected coolant were reduced considerably if the momentum flow was sufficiently high that the bow shock wave was bulged out. For the size of ejection orifice in the present study it was possible to eject only nitrogen coolant without disturbing the external flow appreciably. The results suggest, however, that straight-out ejection could provide an effective way of reducing the heat flux provided that the external flow is not disturbed, and tests with a larger ejection orifice are indicated.

A technique is proposed for making steady-state heat-flux measurements by measuring the temperature difference across a uniformly thin skin of uniform, low thermal conductivity.

TABLE OF CONTENTS

LIST OF TABLES

LIST OF FIGURES

LIST OF SYMBOLS

$C_{\dot{m}}$	coolant gas mass flow coefficient, $\dot{m}/\rho_\infty V_\infty \pi (D/2)^2$
C_P	pressure coefficient, $(P - P_\infty) / \frac{1}{2} \rho_\infty V_\infty^2$
c_p	specific heat at constant pressure
$C_{\dot{\mu}}$	coolant gas momentum flow coefficient, $\dot{m} V_{ej}/\rho_\infty V_\infty^2 \pi (D/2)^2$
D	model base diameter
k	thermal conductivity
M	Mach number
$\dot{m}$	coolant gas mass flow
P	static pressure, on model surface unless otherwise stated
$\dot{q}$	heat flux, on model surface unless otherwise stated
R	model nose radius
s	distance from the model nose along a meridian
T	static temperature, on model surface unless otherwise stated
V	speed
x	distance aft of the model nose, measured parallel to the model axis, except in Appendix 2
y	distance laterally from the model axis, except in Appendix 2
y_1	skin thickness
α	angle of incidence
γ	ratio of the specific heats
η	angle of the surface to the direction of motion
θ	angle of the surface profile to the model axis
μ	dynamic viscosity
ρ	density
σ	Prandtl number, $\mu c_p/k$
τ	wall shear stress

Subscripts

a	implies adiabatic wall conditions
e	refers to conditions at the external edge of the boundary layer
ej	refers to conditions at the point of ejection from the model
ent	refers to conditions at the entry to the final ejection pipe
i	refers to conditions on the inner surface of a skin
i_o	refers to conditions on the inner surface of a skin at $x = 0$
plen	refers to conditions in the plenum chamber
stag	implies tunnel stagnation conditions
w	refers to conditions on the wall, or outer surface of a skin
w_o	refers to conditions on the wall, or outer surface of a skin, at $x = 0$
o	refers to conditions at the model nose at zero incidence and with no coolant ejection
∞	refers to conditions in the free stream

1. Introduction

In a recent investigation McMahon[1] studied the effects of ejecting* a coolant gas from the nose of a blunt body. His results showed that the average heat transfer over a segment near the nose was reduced considerably for quite small flows of coolant, but with the transient technique employed it was not possible to determine the local rates of heat transfer. The purpose of the investigation reported here was to employ the steady state technique using heatmeters, developed by Hartwig[2, 3] and subsequently used by Richards[4], to determine the local rates of heat transfer associated with ejection from the nose, and to explore the effects of incidence.

The heatmeters developed by Hartwig are miniaturized thermopiles, about one-eighth of an inch by one-sixteenth in area, which in effect sense the temperature difference across a piece of glass about 0.007 in. thick. By suitably installing them close to the surface of a model they become instruments which are sensitive to normal temperature gradient, and hence to the heat transfer rate normal to the surface. The heat transfer equivalent of the millivolt output of a heatmeter can be found by proper calibration when installed. Proper calibration is, in fact, the key to the successful use of these instruments. Both Hartwig and Richards calibrated their heatmeters by placing the model in an oven which, in principle, exposed them to a known, and uniform, heat flux, and this technique has been followed here.

---

* McMahon used the term "injecting", in the sense of injection into the boundary layer, but the process is so very much stronger that here we shall use the term "ejecting", in the sense of ejection from the nose.

The investigation consisted of ejecting varying amounts of both nitrogen and helium from the nose of a blunt body of the same profile as that employed by Richards[4]. Measurements were made of surface temperature and heat flux, and some measurements of surface pressure, both at zero incidence and at incidences of 4 and 8 deg. Initially an attempt was made to eject the coolant gas in such a way that it was flowing tangential to the model surface at ejection, but the results showed that this method of ejection in fact tended to lead to an increase in heat flux, so later tests were made with straight-out ejection. The pressure and temperature of the ejected gas were measured just prior to ejection.

The tests were made in the GALCIT 5 inch x 5 inch hypersonic wind tunnel (leg 1) at a nominal Mach number of 5.8 and at a Reynolds number per inch of about 0.2 million based on free stream conditions. At this Reynolds number and Mach number it was assured that the boundary layer on the model was laminar.

2. Description of the Models

The model chosen for the present investigation was of identical profile to that previously tested by Richards[4], and the present tests were envisaged as extending that work by investigating the effects of ejecting a coolant gas at the nose. Relevant details regarding the profile are given in Table 1: basically the model has an oblate spheroidal forebody, of eccentricity 0.7315, and a conical afterbody of 10 degrees semi-angle.

Two models were constructed: one to obtain pressure distributions and to make preliminary studies of the method of ejection, and the other to obtain distributions of temperature and heat flux. Photographs of the models are shown in Figure 1.

The pressure model was constructed of brass with nine conventional static pressure orifices of 0.016 in. diameter. Figure 2 shows the internal construction of the model, and Figure 3 the positions of the pressure orifices, which were located helically on eight meridians.

The heat-flux model was constructed of a mild steel with a wall thickness of 0.050 in., and coated with a layer of porcelain of thickness 0.020 in. The porcelain served a dual purpose: it provided an electrical insulator for the circuits associated with the thermocouples and heatmeters, and it increased heatmeter sensitivity as compared to installation of the meters in the steel wall itself by virtue of its low thermal conductivity (about 0.00015 Btu/ft. sec. degR.). Figure 2 shows the internal construction of the model.

Along one meridian of the heat-flux model nine thermocouples were formed by cementing a constantan wire of 0.001 in. diameter on the model, and then removing the cement coating at nine precisely-located

points with a knife blade. It thus became possible to make contact with the wire by means of silver paint at these nine points, thereby forming nine silver-constantan junctions. (See Figure 3.) Painted silver leads connected the thermocouples so formed to turret posts set in fibre-glass on the base of the model.

The heatmeters are essentially miniaturized thermopiles. Fifty turns of 0.001 in. constantan wire spaced 0.001 in. apart were wound on a piece of microscope slide glass one-eighth of an inch by one-sixteenth in area, and 0.007 in. thick. One half of each loop was silver-plated, resulting in silver-constantan junctions with a thermocouple spacing of 0.008 in. For protection and electrical insulation the finished meters were given a thin coat of adweld. Installation of the nine heatmeters in the model, three on each of three meridians (see Figure 3), was accomplished by grinding a small indentation in the porcelain and cementing the meter in place with adweld. The constantan leads coming from the meter were laid in small grooves cut in the porcelain, contact made with them by silver paint, and they were then held down by a thin application of adweld. Painted silver leads connected the heatmeters to turret posts on the base as with the thermocouples, one lead being common to all meters.

There were therefore twenty turret posts on the base of the model -- one connected to the constantan common of the thermocouples, nine to the silver sides of the thermocouples, one to a silver common for the heatmeters, and nine to the individual silver leads from the heatmeters. From the turret posts connection was made by means of constantan or silver leads as appropriate. The leads were soft-soldered

to the turret posts, and, except for the early tests, were insulated by teflon.

The heat-flux model was cooled by water conveyed through coaxial tygon tubing and rubber hose, and coaxial pipes within the sting, the inflow being within the return-flow. (See Figure 2.) The inflow was fed from the water mains, and as no flow regulator was used the flow rate tended to vary with the daily fluctuations in mains water pressure, etc. However, measurements showed that the flow rate was on the average about 0.17 gallons per minute, the maximum variation measured being about twice or half this amount, but usually much less. The inflow water temperature whenever measured was always within $1^{\circ}F$ of $76^{\circ}F$, and the maximum measured temperature rise overall, that is due to the heat picked up not only in the model but also in the attendant piping, was never greater than $7^{\circ}F$, and usually less than $3^{\circ}F$.

The nitrogen and helium gases used in the ejection studies were fed into the model via a pipe within the inflow water pipe. This procedure ensured that the coolant gas reached the model at a fairly constant temperature. Within the model the gas entered a plenum chamber (see Figure 2) where a pressure probe and an iron-constantan thermocouple enabled the pressure and temperature of the gas to be determined. From the plenum chamber the gas was conveyed to the nose of the model through a pipe of 0.081 in. inside diameter and half an inch long, the edges of the ejection hole being rounded to a radius of about 0.02 in. The same physical parts for the coolant ejection were used in both the pressure and the heat-flux models.

When the experiment was conceived it was felt that the coolant

gas should be directed tangential to the model surface with the object of introducing the coolant in such a manner as would cause minimum disturbance to the external flow field. McMahon[1] in his investigation had attempted to do this by fitting a deflector cap at the nose over the ejection orifice, so that the coolant struck the back of the cap and was thereby deflected radially outwards. It was felt that this was not an entirely happy way of achieving the desired end, because in practice any easement of the heating of the nose achieved in this way would merely be replaced by the problem of how to cool the cap. It was therefore decided to encourage the ejected coolant to flow tangentially to the model surface by giving it some swirl in the ejection pipe, in the hope that the centrifugal effect of the swirl would cause the coolant to flow radially outwards at ejection, and that the Coanda effect would subsequently cause it to follow the surface profile. The necessary swirl was given to the coolant by inserting in the half-inch ejection pipe a twisted strip of brass, 0.01 in. thick and half an inch long. The strip was twisted through one complete turn clockwise, in the half inch, so that the helical advance angle at the wall was about 63 degrees. It was appreciated that such a device would not produce initially a rotationally symmetric coolant flow, but it was hoped that, once away from the ejection orifice, the flow would even out.

It subsequently transpired that the swirling device worked in so far as it caused the coolant to be ejected tangentially, at least at the smaller flow rates, but that the rotational distribution was probably poor. However, interest was by then centered on straight-out ejection, and for these tests the "swirler" was merely removed: it was held

merely by the tightness of the fit. Since it is a relevant parameter, insofar as it is related to the rotational asymmetry of the coolant flow, the setting of the swirler at the ejection orifice was recorded. On the pressure model it made an angle of about 40 degrees with the meridian through pressure orifices 1 and 9, on the side towards the meridian through pressure orifice 2, as indicated in Figure 3. On the heat-flux model two positions were tested: one made an angle of about 45 degrees with the meridian through the thermocouples, in the direction indicated in Figure 3 (referred to as "swirler at 45 degrees"); and in the other position it was aligned with the meridians through heatmeters 1, 4, 7 and 3, 6, 9 (referred to as "swirler at 90 degrees"). During the tests on the heat-flux model with the swirler at 45 degrees considerable difficulties were experienced with the heatmeters, such as short and open circuits, as well as meters becoming loose during test and blowing away down the tunnel. In such cases it was not possible to recheck the calibration of these meters after test, so the information with the swirler at 45^{o} is considerably less reliable, and less complete, than the remainder of the information obtained later with the heat-flux model after it had been completely rebuilt with fresh meters.

3. Experimental Equipment

3.1. Description of Wind Tunnel and Mounting of the Model

The GALCIT 5 inch x 5 inch hypersonic wind tunnel is of the continuous flow type, having a closed working section and a closed return. A description of the wind tunnel and the associated plant is given in Reference 5, and pertinent data is listed in Table 2. The nominal Mach number in the test section is 5.8. For all tests the tunnel stagnation pressure, which was measured just upstream of the throat, was maintained at 6 atm. absolute within very close limits. For the tests on the heat-flux model the tunnel stagnation temperature, which was measured just upstream of the throat, was 316°F with a standard deviation, based on the periodic measurements made, of just over 2°F. For the tests on the pressure model the stagnation temperature was nominally 250°F, which was probably within 10°F of the true value.

The model was mounted with the nose 21.75 in. aft of the throat. Incidence was produced by differential movement of the two vertically actuated struts on which the sting of the model was mounted, in such a way that the nose of the model remained in the same position in the tunnel. To obtain a complete knowledge of the characteristics at incidence it was necessary to rotate the models on their stings through 360 degrees, in order to bring each pressure orifice, thermocouple, and heatmeter into the windward, leeward and side meridians, etc.

3.2 Metering of the Coolant Gas

The nitrogen and helium gases used as coolants were fed from commercial bottles, passed through a pressure regulator, then through a Fischer and Porter variable-area gas flowmeter, then through a needle valve and into the model through a tube within the inflow water line. A pressure gage upstream of the flowmeter indicated the metering pressure, which was either 20 lb./in.^{2} or 50 lb./in.^{2} gage. The needle valve permitted the mass flow to be varied without changing the metering pressure appreciably.

The smaller mass flow rates were metered with a tube and ball-float meter which was calibrated for the two gases by running it in series with either a wet-test gas meter or a previously calibrated flowmeter. The larger mass flow rates were metered with a "tri-flat" tube and ball-float meter for which calibration curves could be predicted for the two gases. It is estimated that the probable error in the quoted mass flow rates is about 6 per cent, based on the differences in different calibrations, but the variations in mass flow rates which are nominally the same should be less than this.

The mass flows have been quoted as mass flow coefficients $C_{\dot{m}}$ based on the free stream mass flow through a capture area equivalent to the frontal area of the model, so that

$$C_{\dot{m}} = \frac{\dot{m}}{\rho_\infty V_\infty \pi (D/2)^2}$$

Pertinent information on the properties of the coolant gases is given in Table 3.

3.3. Measurement of Pressure

The steel tubes at the base of the pressure model were connected by saran tubing to vacuum-referenced manometers using silicone oil for the lower pressures and mercury for the higher pressures. Likewise the steel pressure probe in the plenum chamber was connected by saran tubing to a vacuum-referenced mercury manometer.

All pressures have been quoted as pressure coefficients, C_P, defined by

$$C_P = \frac{P - P_\infty}{\frac{1}{2} \rho_\infty V_\infty^2} ,$$

and normalized by dividing by the pressure coefficient, C_{P_o}, at the nose for zero incidence and no coolant ejection, which is of course the pressure coefficient behind a normal shock at the tunnel Mach number.

3.4. Measurement of Temperature

The thermocouple turret posts at the base of the heat-flux model were connected by silver or constantan leads, insulated by teflon, to a jack panel, which enabled the millivolt outputs of the thermocouples to be sampled in turn using a Leeds and Northrup potentiometer. A thermometer in the jack panel recorded the effective cold-junction temperature. The millivolt readings were converted to temperatures using the calibration for silver-constantan thermocouples previously obtained by Hartwig[2], and given in Table 4.

The iron-constantan thermocouple probes in the plenum chamber and upstream of the tunnel throat were likewise connected to the jack

panel and their outputs sampled. Their readings were converted to temperatures using standard calibration tables.

3.5. Measurement of Heat Flux and Calibration of Heatmeters

The heatmeter turret posts at the base of the heat-flux model were connected by silver leads, insulated by teflon, to the same jack panel as for the thermocouples, and the millivolt outputs of the meters sampled with the same Leeds and Northrup potentiometer.

As Hartwig[2] has pointed out, the key to the success of an experiment employing these heatmeters lies in their calibration. Hartwig's method was to construct an oven, which, when the model was inserted, would expose the surface of the model to a uniform heat flux. This end was not too difficult to achieve, but of course not all the power that was put into the oven flowed inwards into the model, even although the oven was heavily lagged. Hartwig attempted to measure his losses by employing commercial heatmeters on the walls of the box containing his oven. Richards[4] attempted to improve on this technique by surrounding his main heater elements by bucking heaters, with specially made heatmeters inserted between the main heater and the bucking heaters. The principle here was to adjust the power into the bucking heaters until their associated heatmeters were nulled. At this point it was assumed that there was no net heat flux outwards from the main heater, and thus all the power that was going into the main heater was going as heat into the model, uniformly as before.

It was originally intended to use the Richards oven to calibrate the model of the present investigation, since it was of identical external

geometry, but unfortunately the Richards oven burned out, and a new one on the same principle had to be constructed. Details are given in Appendix 1, and a sketch of the oven is given in Figure 4.

Power for the main oven heater was obtained from a variable d. c. supply and measured by means of an ammeter and voltmeter. Power for the two bucking heaters was obtained through powerstats from the a. c. mains and the amps recorded. For a given power input in the main heater, the power input into the bucking heaters was adjusted until the appropriate heatmeter was nulled, when it was hoped that the power input into the main heater could be treated as all going into the model.

The measurements of model surface temperature during calibration, expressed as an excess over the internal water temperature, differed by at most 5 per cent from the average surface temperature, so that it was assumed that the oven provided a fairly uniform heat flux meridianwise, although small corrections were applied for such non-uniformity as there was. The model was also tested in three rotational positions, for each power input, but here no appreciable variation was found, so that it was concluded that the oven provided an almost nearly uniform heat flux rotationwise.

However, the measurements of heat transfer obtained in the wind tunnel based on the calibration made in the oven were considerably less than was expected theoretically for the stagnation point heat transfer rate, and from the results of Richards[4] for the case of no injection. It was therefore concluded that, although the oven provided a fairly uniform heat flux to the model, the actual value of the heat flux differed considerably from that expected, because of a flow of heat from the bucking heaters

to the main heater even when the heatmeters read null. The explanation for this is far from certain; but it may be associated with various "battery" effects that were noted in connection with the oven. For example, after the oven had been heated for some time it was found that the main heater, the oven heatmeter and the oven bucking heater were at different electric potentials, by as much as 200 millivolts, and that currents of up to 20 microamps could be obtained. There was not time to resolve this matter, but it is probably associated with the sauereisen in which the heatmeters were embedded.

The difficulty was overcome in the following way. In Appendix 2 it is shown that the heat flux, $\dot{q}$, across a thin skin of low thermal conductivity is given very closely by

$$\dot{q} = \frac{k}{y_1} (T_w - T_i) ,$$

where

k is the thermal conductivity of the skin material

y_1 is the thickness of the skin

T_w is the temperature of the outer surface

T_i is the temperature of the inner surface.

Now the model is made up of a 0.020 in. layer of porcelain on a 0.050 in. steel shell, which is cooled on the inside by water which, during calibration, was never more than a degree or so from 79°F. Since the thermal conductivity of the porcelain is about one-sixtieth of that of steel, it is not unreasonable to assume that most of the temperature drop across the wall of the model occurs in the porcelain, and that the inner surface of the porcelain was not far removed from the water temperature,

namely 79°F. On this argument we would expect the heat flux into the model to be proportional to the amount by which the model surface temperature exceeded 79°F. It was in fact found that the excess of the model surface temperature over 79°F increased in proportion to the power that was put into the main heater. It was therefore concluded that the oven provided a uniform source of heat flux, and one in which the actual heat flux was indeed proportional to the power put into the main heater, but that quantitatively the factor of proportionality was not known. It is not possible therefore to present absolute rates of heat transfer, $\dot{q}$, from the present experiments, but only relative values, obtained by normalizing the results by dividing them by a suitable reference rate of heat transfer, namely that at the nose for zero incidence and no ejection, $\dot{q}_o$.

The argument presented above equally implies that the rates of heat transfer could be obtained from the measurements of temperature alone. This point is pursued further in Section 6.2.

4. Reduction of Data

Because of flow irregularities across the test section it was found that the measurements of pressure, temperature, and heat flux varied systematically as the model was rotated at zero incidence. The maximum difference between the highest and lowest values amounted to about 10 per cent on pressure, to almost $10^{\circ}F$ on temperature, and to about 30 per cent on heat flux. However, these differences were systematic in that the changes in pressure, temperature and heat flux produced by ejection showed very much less variation as the model was rotated than the readings themselves.

The data presented here for zero incidence is that averaged over the eight rotational angles tested for the pressure model, and over the four rotational angles tested for the heat-flux model, and the accuracy of this averaged data should therefore be much greater than that of the individual readings. The extent to which individual readings could be repeated for nominally the same conditions was within about 1 per cent on pressure, about $5^{\circ}F$ on temperature, and about 10 per cent on heat flux.

The data at incidence was corrected for the effects of the flow irregularities mentioned above, by adding to, or subtracting from, the measured values of pressure, temperature, or heat flux, the amounts by which the measured values at zero incidence differed from the averaged values.

It would have been possible to correct further the data at incidence by testing at both positive and negative angles, and averaging, but the extra work involved would have been prohibitive.

5. Results

The experimental results on pressure, temperature and heat flux are given in full in Tables 5 to 41, and only a representative selection are presented in the figures.

A full range of measurements of the effects of ejection with swirl and of straight-out ejection on temperature and heat flux were made at incidences of 0, 4, and 8 degrees, and for coolant gas mass flow coefficients of up to 0.008 for nitrogen and 0.005 for helium. Ejection with swirl was made with the swirler at two different angles relative to the positions of the thermocouples and heatmeters (see Section 2).

In regard to pressure, measurements were made only of the effects of ejection with swirl, and in the case of helium only at zero incidence, although for nitrogen incidences of 0, 4, and 8 degrees were covered. No measurements were made of the effects of straight-out ejection on pressure.

Schlieren photographs of all the flow patterns were taken, but only those needed to illustrate the arguments are presented in the figures.

At the end of the main program of tests some measurements were made of temperature and heat flux for various rates of straight-out ejection with no coolant water flow. These measurements were intended to give some idea of the "blanketing" effect of the separate coolant gases, although of course with no coolant water flow one had no control over the ejection temperature of the coolant gas.

6. Discussion

6.1. Pressure Distributions with No Ejection

Distributions of pressure in the plane of incidence with no ejection at incidences of 0, 4, and 8 degrees are shown in Figure 5. In Figure 6 are shown cross-plots of pressure against incidence for the various stations, together with curves deduced from the measurements of Richards[4], which they should duplicate. It will be seen that there is good agreement between the two sets of results except just ahead of the shoulder, where the results of Richards seem somewhat implausible. It will be recalled that Richards found that the experimental results were in fair agreement with the so-called modified Newtonian theory, which states that the pressure is given by

$$\frac{C_P}{C_{P_o}} = \sin^2 \eta \quad ,$$

where η is the angle of the surface to the direction of motion, except on the conical afterbody, where the Newtonian approach underestimates the pressure.

Distributions of pressure in the meridian plane normal to the plane of incidence are shown in Figure 7. As found by Richards, the measurements at incidence do not differ noticeably from those at zero incidence in this plane, at least over the range of incidence covered.

6.2. Temperature and Heat-Flux Distributions with No Ejection

Distributions of temperature and heat flux in the plane of incidence with no ejection at incidences of 0, 4, and 8 degrees are shown in Figure 5. These results cannot be expected to duplicate those of Richards[4], because of the different tunnel stagnation temperatures at which the two series of tests were made, but they do confirm his finding that the local temperatures and heat fluxes vary linearly with the angle of incidence over the range covered. Figure 7 shows that distributions of temperature and heat flux in the meridian plane normal to the plane of incidence do not vary noticeably with incidence, as was found in Section 6.1 for pressure.

The results on heat transfer can be compared with those of Richards by expressing them as Nusselt numbers, formed by dividing the product of the heat flux, $\dot{q}$, and a typical length, by the product of the driving temperature difference, $(T_a - T)$, and the thermal conductivity of the fluid, where T_a is the adiabatic wall temperature, or wall temperature for which the local heat flux would be zero. This adiabatic wall temperature is given by

$$T_a = T_e + \sigma^{\frac{1}{2}} (T_{stag} - T_e) \quad ,$$

where

T_e is the temperature at the external edge of the boundary layer

T_{stag} is the stagnation temperature

σ is the Prandtl number (see Table 3).

The temperature T_e depends upon the pressure distribution, and is given by

$$T_e = T_{stag} (P/P_o)^{(\gamma/\gamma - 1)} \quad ,$$

where

P is the local pressure

P_o is the pressure at the stagnation point at the nose.

Values of Nusselt number at zero incidence, normalized* by division by the Nusselt number at the nose, are shown as circles in Figure 8, together with a curve deduced from the measurements of Richards, and plotted against the complement of the profile slope angle, as being perhaps a more relevant parameter in this context than s/D. In the experiments of Richards the Reynolds number based on the free stream velocity, the base diameter, and the fluid properties at the nose was 0.24 million; in the present experiments it was 0.22 million, which is not significantly different. A possible explanation of the discrepancy was provided by comparison of the profiles of the two models in an optical comparator. It was found that, whereas the present model was of the design profile to within about 0.001 in., the model of Richards was small by about 0.012 in. The effective values of s/D for his heatmeters are therefore greater than he quoted: this has the effect of moving the curve for his measurements to the right in Figure 8, but not by an amount sufficient to explain fully the discrepancy, which may well be associated with some non-repeatability of the meters themselves, as will be mentioned below.

Also shown in Figure 8 are two theoretical curves of different degrees of approximation, calculated from the theory of Lees.[6] A

---

* When normalized the Nusselt number becomes independent of the typical length and the thermal conductivity of the fluid.

theoretical curve calculated from the theory of Cohen and Reshotko[7] was in substantial agreement with those derived from the theory of Lees. It will be seen that the discrepancy between experiment and theory is far greater than that between the experiments themselves, or between the two degrees of theoretical approximation. Now it is shown in Appendix 2, and has already been referred to in Section 3.5, that, for a model having a thin skin of uniform thickness and thermal conductivity, the heat flux across the skin should be very closely proportional to the difference between the wall temperature, T, on the outer surface of the skin, and the temperature, T_i, on the inner surface. By the argument given in Section 3.5, the effective inner surface temperature should not be far removed from the water temperature, which, in the wind tunnel, was about 80°F. Accordingly the Nusselt number should be proportional to $(T - T_i)/(T_a - T)$, where T_i is roughly 80°F. Values of normalized Nusselt number derived in this way are shown as triangles in Figure 8. Admittedly there is some scatter, but this is only to be expected in view of the assumptions upon which this method of determining the heat flux is based, but the agreement with theory up to an angle of about 45 degrees is remarkable. At greater angles of course the difference, $(T - T_i)$, is smaller and thus much more sensitive to the precise value of inner surface temperature used, which, it should be remembered was not measured, but crudely assumed to be equal to the probable water temperature.

This result indeed raises the question of the meaning of the results obtained with the heatmeters. It could be of course that the theories of both Lees and Cohen and Reshotko are in error, and that

the agreement between them and the experimental results deduced from the temperature measurements is fortuitous. But if one considers a body of spherical shape, which Hartwig[2] tested, and for which there is a fair amount of agreement between theory and experiments employing other techniques[8], one finds that far better agreement is obtained between theory and the heat fluxes derived from Hartwig's temperature measurements, on the lines outlined above, than between theory and the heat fluxes yielded by his heatmeter results. No explanation is at present forthcoming as to why the heatmeters do not give the correct heat flux in the tunnel, as would seem to be the implication, but it may be associated with the method of calibration, which is done under conditions of uniform heat flux only. It should be noted that in the present investigation and in those of Hartwig and Richards essentially the same method of calibration was used. Some experiments are at present in progress at the Jet Propulsion Laboratory using these heatmeters but employing an entirely different method of calibration. It is suggested that judgment on the meaning of the results obtained with these heatmeters be delayed until further evidence from this source is forthcoming.

In passing, however, it should be noted that the method whereby the heat fluxes have here been deduced from the temperature measurements could very well be an extremely effective method in its own right. What is required is an accurate knowledge of both the outer and inner surface temperatures of the skin, which should be of uniform thickness and thermal conductivity. In the present experiments the inner surface temperature was not measured, only deduced, and that somewhat crudely, but if necessary it could be measured as accurately as the outer surface

temperature. A skin of homogeneous material should ensure reasonably uniform thermal conductivity, and Hartwig[2] has shown that porcelain models can be manufactured so as to have a skin thickness uniform to within 3 per cent. The philosophy of the technique appears to lie in the thin skin of low thermal conductivity. The thinness of the skin is necessary to ensure that the effects of longitudinal temperature gradients are negligible (in the transient technique even a thin skin does not ensure this[1, 9]); the low thermal conductivity is necessary to ensure that, even although the skin is thin, there is a reasonable and measurable temperature difference across it. In practice the thickness of the skin would be a compromise between making it thin enough that the longitudinal temperature gradients would be negligible, and thick enough that the fractional departure from uniformity of thickness would be low.

It is suggested, therefore, that, in view of the uncertainty associated with the results obtained using the heatmeters, the most reliable, albeit rough, indication of the rates of heat transfer from the present experiments can be obtained from the measurements of surface temperature, by assuming that

$$\frac{\dot{q}}{\dot{q}_o} = \frac{T - T_i}{T_o - T_i} \quad ,$$

where

T is the measured surface temperature

T_i is the inner surface temperature, assumed to be $80^{\circ}F$

T_o is the surface temperature at the nose for zero incidence and no ejection, namely $130^{\circ}F$.

6.3. Effect of Ejection on the Flow Pattern

The variation of plenum chamber pressure with mass flow rate of coolant is shown in Figure 9. It will be noted that for small mass flow rates of both nitrogen and helium with straight-out ejection the plenum chamber pressure is less than the stagnation pressure at the nose for no ejection ($C_P/C_{P_o} < 1$). In this case the ejected gas acts as a "gas spike", causing the bow shock wave to bulge out. The normal flow pattern is replaced by one in which, in the vicinity of the nose, there is a roughly conical dead-air region behind a roughly conical shock wave. The pressures in the vicinity of the nose associated with this flow pattern are considerably less than those with a conventional non-bulged-out shock, as McMahon[1] found, which is why there is a corresponding drop in plenum chamber pressure. Figures 10(a) and 10(c) show the bulging-out of the bow shock wave by nitrogen and helium ejected straight out respectively, whereas Figures 10(b) and 10(d) show that at the same or greater mass flow rates with swirl there is no indication of such bulging out. In this sense the swirler may be said to be achieving its desired effect.

It will also be noted in Figure 9 that with straight-out ejection the plenum chamber pressure varied appreciably with incidence for the smaller mass flow rates. This is presumably because the conditions at the ejection orifice vary appreciably with incidence. For mass flow rates of helium corresponding to $C_{\dot{m}} = 0.004$ and higher this dependence on incidence disappears: this behavior is no doubt associated with the fact that at these mass flow rates the flow in the ejection pipe is choked, as will

be mentioned below. Figure 9 shows also that for ejection with swirl the plenum chamber pressure does not vary noticeably with incidence at all: this is no doubt because with swirl the flow ahead of the body is very little affected by ejection, and, as will be shown in Section 6.4, the pressures even in the vicinity of the nose do not vary much with either incidence or coolant ejection.

The above arguments are supported by examination of the schlieren photographs, a selection of which are shown in Figure 10. With the straight-out ejection of nitrogen the bow shock wave was bulged out slightly at zero incidence for a mass flow coefficient of 0.004, even less so at 4 degrees incidence, and hardly at all at 8 degrees incidence. At all three incidences it was bulged out appreciably for a mass flow coefficient of 0.006. With the straight-out ejection of helium the bow shock wave was bulged out slightly at zero incidence for a mass flow coefficient of 0.001, and less so at the higher incidences; and bulged out appreciably for a mass flow coefficient of 0.002 at all incidences. Helium tends to cause the bow shock wave to bulge out at a smaller mass flow rate than for nitrogen; since helium is one-seventh of the density of nitrogen, the speed of ejection is greater for the same mass flow rate. Ejection with swirl tended to cause the bow shock wave to bulge out more at incidence than at zero incidence. At zero incidence a noticeable bulging-out due to ejection with swirl does not appear until a mass flow coefficient of about 0.008 for nitrogen or 0.003 for helium. At incidences of 4 and 8 degrees the bulging-out appears at a mass flow coefficient of about 0.006 for nitrogen or 0.002 for helium.

On the assumption of one-dimensional flow in the coolant gas

line, the Mach number in the plenum chamber never exceeded 0.03, based on the measurements of mass flow rate, and of pressure and temperature in the plenum chamber, so that these pressures and temperatures can be treated as representing total conditions. On this assumption, and again that of one-dimensional flow, the Mach number at the entry to the final ejection pipe can be calculated (see Figure 3). This Mach number is shown in Figures 11 and 12. Figure 11 shows that for mass flow coefficients above about 0.005 for nitrogen or 0.002 for helium there is evidence that the flow in the swirl pipe was choked, although with the swirler removed (see Figure 12) the onset of choking is delayed to beyond a mass flow coefficient of 0.008 for nitrogen and to 0.0025 for helium for straight-out-ejection. The Mach numbers themselves should be treated as qualitative only, owing to the assumption of one-dimensional flow made in their derivation, and the fact that the Mach number is extremely sensitive to area ratio near a Mach number of unity.

For straight-out ejection, that is with the swirler removed, the momentum flow of the ejected gas can be calculated, again on a one-dimensional flow assumption, and ignoring any losses in the final ejection pipe, which are estimated to be small. The calculated momentum flow rates are shown in Figure 13 as momentum flow coefficients $C_{j\mu}$ defined as

$$C_{j\mu} = \frac{\dot{m}\, V_{ej}}{\rho_\infty V_\infty^2 \pi (D/2)^2}$$

It will be noted that, for a given mass flow rate, the momentum flow rate, and hence the speed of ejection for helium is about seven times that for nitrogen, as mentioned earlier, provided that the flow in the ejection pipe is not choked.

6.4. Effect of Ejection on Pressure

McMahon[1] has shown that straight-out ejection has a profound effect on the pressure distribution back to a value of s/R for a model having a spherical nose of about 0.6, where R is the nose radius.* In the vicinity of the nose the value of C_P/C_{P_o} was reduced by as much as 0.6. This is because the ejected gas acts as a "gas spike", as has been pointed out in Section 6.3, and causes the bow shock wave to bulge out. No measurements of pressure with straight-out ejection were made in the present investigation, partly through lack of time, and partly because McMahon has already demonstrated the main effects.

Typical results for ejection with swirl are shown in Figures 14, 15, and 16.** It will be seen that the changes in pressure due to ejection are far less than those found by McMahon for straight-out ejection, particularly for the mass flow rates for which the bow shock wave is not bulged out (namely, $C_{\dot{m}}$ less than about 0.006 for nitrogen, or less than about 0.002 for helium, see Section 6.3). Even at the higher mass flow rates the changes in pressure coefficient are less severe, being for all conditions tested less than a tenth of C_{P_o} for points aft of s/D = 0.177, and negligible aft of s/D = 0.357. Only at the first measuring station (s/D = 0.117) was there an appreciable effect, and even then it was much less than that found with straight-out ejection. These results

---

* For the model of the present investigation s/R = 1.86 s/D, where D is the base diameter.

** In the figures the vertical scale is everywhere such that half an inch corresponds to 0.2 in $\Delta C_P/C_{P_o}$.

confirm the conclusions drawn in Section 6.3 from a study of the schlieren photographs that the swirler is achieving some success by enabling the coolant to be ejected without too much disturbance to the flow external to the boundary layer.

6.5. Effect of Ejection with Swirl on Temperature and Heat Flux

The changes in temperature and heat flux for ejection with swirl at zero incidence are shown in Figures 17 and 18.* If one studies Figure 18 one observes, for example, that for helium with the swirler at 90 degrees (points represented by a multiplication cross), the heat flux is considerably reduced at stations 2, 5, and 8 (corresponding to $s/D = 0.177$, 0.357, 0.710), whereas it is appreciably less reduced, or even increased, at stations 1, 4, 7; 3, 6, 9 (corresponding to $s/D = 0.117$, 0.297, 0.477; 0.237, 0.417, 0.943). Reference to Figure 3 shows that stations 2, 5, 8 lie in one meridian plane, whereas the other six stations lie in another meridian plane. This dependence of the results upon the meridian plane of the heatmeter stations is because the swirler is not giving a rotationally symmetric distribution of coolant gas over the model. This implies that the results must be interpreted in the light of the location of the various thermocouple and heatmeter stations with respect to the swirler. (See Figure 3 and Section 2.) With helium in particular, at high mass flow rates, having the swirler at 90 degrees leads to a reduction in temperature at station 1 (corresponding to $s/D = 0.117$, see Figure 17), and at the same time to an increase in heat flux (see Figure 18), whereas

---

* In the figures the vertical scales are such that half an inch corresponds to $20^{\circ}F$ in temperature, or to 0.2 in $\Delta \dot{q}/\dot{q}_o$.

having the swirler at 45° leads to the opposite effect. This is because the thermocouple and heatmeter corresponding to station 1 lie on different meridians.

In view of these results, either an attempt should have been made to obtain a more nearly rotationally symmetric distribution of coolant gas, or else measurements should have been made with the swirler at many more angles. However, the general impression obtained from Figures 17 and 18 is that ejection with swirl seems, if anything, to lead to an increase in heat flux, and accordingly the matter was not pursued, but instead attention directed to straight-out ejection, which will be discussed in Section 6.6.

An explanation of the increase in heat flux produced by ejection with swirl is provided by the Reynolds analogy, which states that the ratio of the Nusselt number to the product of the surface friction coefficient and the Reynolds number is a constant depending upon the wall temperature and the longitudinal pressure gradient, or

$$\dot{q} \propto \frac{k\,(T_a - T)}{\mu\, V_e}\ \tau\ ,$$

where

τ is the wall shear stress

k is the thermal conductivity

μ is the dynamic viscosity.

Now the main effect of the introduction of a coolant is to reduce the driving temperature difference, $(T_a - T)$, and this is the basis on which it works, but in ejection with swirl the coolant is injected tangentially into the boundary layer at the nose with very high velocity, much greater

than the average velocity of the uninjected boundary layer, with the result that the wall shear stress is increased manyfold. The results obtained would seem to indicate that the increase in τ outweighs the reduction in $(T_a - T)$ and the changes in the other quantities, particularly, k, μ . If tangential injection into a boundary layer is to be instrumental in reducing heat flux it must be done with much less momentum flow for a given mass flow than was achieved in these experiments.

In the light of the above remarks concerning the effects of ejection with swirl at zero incidence little will be said concerning the results at incidence, although the data is given in full in Tables 16 to 31. Figures 19 and 20, for example, show the changes in temperature in the plane of incidence for an incidence of 4 degrees. These changes in temperature can be interpreted as changes in heat flux by the relation

$$\left(\frac{\Delta \dot{q}}{\dot{q}_o} \right)_{\text{deduced}} = \frac{\Delta T^{\circ}F}{50} ,$$

in keeping with the suggestion made at the end of Section 6. 2.

6. 6. Effect of Straight-Out Ejection on Temperature and Heat Flux

The changes in temperature and heat flux for straight-out ejection at zero incidence are shown in Figures 21 and 22.* According to both the temperature and heat flux results, the main feature is the initial increase in heat flux at stations 2, 3, 4 (corresponding to s/D = 0. 177, 0. 237, 0. 297) produced by the ejection of helium, prior to an eventual decrease at the higher mass flow rates. The corresponding results for

---

* In the figures the vertical scales are such that half an inch corresponds to $20^{\circ}F$ in temperature, or to 0. 2 in $\Delta \dot{q}/\dot{q}_o$.

nitrogen show an initial decrease, then an increase, with indications of an eventual decrease at the higher mass flow rates. This difference is no doubt associated with the different shock-bulging characteristics of the two gases. In Section 6.3 it was reported that with helium the bow shock wave was bulged out at a mass flow coefficient of 0.001, whereas with nitrogen it was not bulged out until the mass flow coefficient reached 0.004.

The point is probably illustrated better in Figures 23 and 24, in which are shown distributions of heat flux deduced from the temperature measurements on the lines suggested at the end of Section 6.2. The curve for nitrogen at $C_{\dot{m}} = 0.002$ (Figure 23) is of a markedly different shape from the curves for the other three cases of ejection. Moreover it corresponds to a reduction in heat flux along the entire body profile. As we have seen this case corresponds to the coolant being introduced with sufficiently little momentum that it does not cause the bow shock wave to bulge out. The other three cases (nitrogen at $C_{\dot{m}} = 0.006$ in Figure 23, and helium at $C_{\dot{m}} = 0.002$ and 0.004 in Figure 24) all correspond to bulged-out bow shock waves. We note that although large reductions in heat flux are obtained in the vicinity of the nose, there is an increase further round the profile, corresponding to $s/D = 0.25$ roughly. This is all in keeping with the results of McMahon[1]. He found large reductions in the average heat flux over the nose sector of a sphere of 60° included angle, but considerably smaller reductions over a sector of 120° included angle.

The explanation for these results is to be found in the changed flow pattern. As has already been pointed out in Section 6.3, when the ejected gas acts as a gas spike there is a roughly conical dead-air region

in the vicinity of the nose. The flow external to the boundary layer, instead of giving rise to a stagnation point at the nose, now has a "stagnation circle" at the base of the conical dead-air region, along which the heat flux is increased, compared with that at the same station for no ejection. Inside the dead-air region McMahon has shown that the pressure is greatly reduced (see Section 6.4), and this reduction in pressure is probably responsible for the reduced heat flux in the immediate vicinity of the nose.

It is of interest to consider the ratio of the reductions in heat transfer to the "heat capacity" of the ejected gas. The reduction in heat transfer is given by

$$\int - \Delta q \cdot 2\pi y \cdot ds \quad ,$$

and we will take as the "heat capacity" of the ejected gas the expression

$$\dot{m} \cdot c_p \cdot (T_{stag} - T_{plen}) \quad .$$

This expression represents the amount of heat that the gas can absorb when its temperature is raised from that in the plenum chamber to the stagnation temperature of the main air flow. For nitrogen ejected straight out at $C_{\dot{m}} = 0.002$, in which case the bow shock wave is not bulged out, the ratio of the reduction in total heat transfer up to the station $s/D = 1$ to the "heat capacity" of the gas is about 1.1. That this is more than unity implies that the nitrogen is acting more than as a blanket; that is, a greater reduction in heat transfer is being achieved than would correspond to the absorption by the nitrogen of the heat that would otherwise have been transferred to the model. The ratio of the reduction in the total heat transfer up to the shoulder ($s/D = 0.459$) to the "heat capacity" of the gas is about 0.4, which is still remarkably high. These

figures should be compared with those for helium for the same mass flow rate, but now for a flow corresponding to a bulged-out bow shock wave. The ratio of the reduction in total heat transfer up to the station $s/D = 1$ to the "heat capacity" of the gas is about 0.1, which is less than one tenth of the value with nitrogen, and the ratio based on the total heat transfer up to the shoulder is roughly zero.

The implication would seem to be that if the gas can be ejected without causing the bow shock wave to bulge out, as is the case with nitrogen ejected at $C_{\dot{m}} = 0.002$, then a steady reduction in heat flux with increase in mass flow should be achieved. In other words, the momentum flow for a given mass flow should be kept down, so that on impingement with the air the coolant can be directed around the body without too much mixing and consequent reduction of its heat alleviation properties. The importance of this observation is brought out by the results for nitrogen and helium ejected at a mass flow coefficient of 0.002. Although it has five times the heat capacity and is one-seventh of the density, implying a thicker layer for the same mass flow and velocity, helium is not as effective as nitrogen in reducing the heat flux, simply because its heat alleviation properties are drastically reduced by mixing in this case. It would obviously be extremely interesting to perform some experiments with an ejection pipe of twice the diameter of that used in these experiments. A pipe of this size would enable the momentum flow to be reduced to one quarter for the same mass flow, thereby delaying the bulging-out of the bow shock wave to higher mass flow rates, and thus probably achieving substantial reduction in heat flux for quite small mass flow rates.

The effects of incidence on the changes in temperature for

straight-out ejection are shown in Figures 25, 26, 27, and 28, and from them the changes in heat flux can be deduced by the relation

$$\left(\frac{\Delta \dot{q}}{\dot{q}_o} \right)_{\text{deduced}} = \frac{\Delta T^{\circ}F}{50} \quad ,$$

as suggested at the end of Section 6.2. Figures 25 and 26 show that ejection tends to increase the temperature, and hence heat flux, on the windward meridian, presumably for the same reason that it tends to increase it at zero incidence. The heat flux in the neighborhood of the "stagnation circle", which is now eccentric with respect to the nose of the model, is increased compared with that at the same station for no ejection. We note in Figure 25, for example, that the further back the station the greater the mass flow rate corresponding to the peak in the curves, presumably because the further back the station the greater the mass flow rate has to be to make the "stagnation circle" fall at that station.

The importance of avoiding a bulged-out bow shock wave is brought out by the results for nitrogen at an incidence of 8 degrees (see Figure 26). It will be noted that the increase in temperature occurs only above a mass flow coefficient of 0.004, which is the mass flow coefficient above which the nitrogen emerges as a gas spike and causes the bow shock wave to be bulged out (see Section 6.3). Figure 27 shows that on the side meridian the results for 4 degree incidence are somewhat similar to those at zero incidence (see Figure 21). Figure 28 shows that on the leeward meridian a not unexpected reduction in temperature occurs. The results for the side and leeward meridians at an incidence of 8 degrees are similar.

6.7. Effect of Straight-Out Ejection on an Uncooled Model

Figure 29 shows the temperature distribution for various mass flow rates of the two coolants with no coolant water flow. In this case the temperature of the coolant gas could not be controlled, and it will be noted that the plenum chamber temperature, shown plotted along the ordinate axis in Figure 29, tended to rise as the mass flow rate was reduced, owing to the heat acquired by the gas on its passage through the tunnel to the model. The results are similar to those obtained by McMahon[1]. We note in particular that four or five times the mass flow of nitrogen is required compared to that of helium to achieve the same reduction in temperature. Most of the cooling effect of helium is obtained at a mass flow coefficient of 0.002; increasing it to 0.005 reduces the temperature only by a further 60 per cent.

It will be noted in Figure 29 that the temperatures for $C_{\dot{m}} = 0$ and for nitrogen with $C_{\dot{m}} = 0.002$ decrease monotonically with distance back from the nose, whereas all the other curves have a peak around $s/D = 0.25$. It will be recalled that the first two cases correspond to non-bulged-out bow shock waves, whereas the remainder correspond to flow patterns having bulged-out bow shock waves (see Section 6.3). A much greater reduction in temperature was obtained with nitrogen in going from $C_{\dot{m}} = 0.002$ to 0.004, the bow shock being bulged out in the latter case, than in going from $C_{\dot{m}} = 0$ to $C_{\dot{m}} = 0.002$. However, for the same increments in mass flow coefficients greater than 0.004 the reductions achieved get appreciably less. It is indeed possible that if a mass flow coefficient of 0.008, say, could be achieved without bulging out the bow shock wave, (by having a larger ejection orifice, for example,)

then the reductions in temperature might well be greater than those obtained with a mass flow coefficient of 0.008 and a bulged-out shock wave. This matter is being investigated further.

Figure 30 shows the corresponding distributions of heat flux. It will be noted that there is an inflow of heat ahead of $s/D = 0.4$, roughly, and an outflow aft of this station, in keeping with the temperature distributions.

During these tests with no coolant water flow the model got sufficiently hot over the base that the radio cement joint started to leak (see Figure 2), and water seeped out into the dead air region behind the base. Here, because of the low pressure, it evaporated, and the associated cooling caused ice to form. In a few minutes the hitherto dead air region was a block of ice. Figure 31 is a photograph taken shortly after. After a while the leak stopped, but it took some twenty or thirty minutes for the ice to disperse.

7. Conclusions

In the course of the investigation three ways of ejecting a coolant gas from the nose of a blunt body have become apparent, and something has been learned about the heat transfer rates associated with them.

The method that was tried initially was to encourage the coolant gas to flow tangentially to the model surface at ejection by giving it some swirl in the ejection pipe. The method was successful in the sense that, except at the highest mass flow rates, the coolant gas was ejected with very small disturbance to the flow external to the boundary layer, as witnessed by the pressure distributions and schlieren studies. Unfortunately the swirling device employed was a little too crude to give a rotationally symmetric flow. The results obtained are therefore mainly qualitative, but they do indicate that this method of ejection is not a happy one as a means of easing the heating problem. Although the cool layers of coolant gas reduce the driving temperature difference, $(T_a - T)$, the high tangential velocity with which the coolant is injected into the boundary layer increases the wall shear stress considerably, and hence, by the Reynolds analogy, the heat flux. The results seem to indicate that the increased shear predominates, at least for the conditions considered here. The matter was not therefore pursued further.

Attention was then centered on "straight-out" ejection, but here two flow regimes were found. Except at the lower mass flow rates the coolant gas emerged as a "gas spike", causing the bow shock wave to bulge out. The normal flow pattern is replaced by one in which, in the vicinity of the nose, there is a roughly conical dead-air region behind a roughly conical shock wave. The flow external to the boundary layer,

instead of giving rise to a stagnation point at the nose, now has a "stagnation circle" at the base of the conical dead-air region. Inside the dead-air region we know from McMahon's results[1] that the pressure is greatly reduced compared with the case of no ejection, and it is found that, associated with this reduced pressure, there is a greatly reduced heat flux. However, in the vicinity of the "stagnation circle" the pressure is somewhat above its value for the case of no ejection, and this fact, together with the greater heating ability of the impingent stream, leads to an increased heat flux in a region around the "stagnation circle". The net result is that, although the region of severest heating is shifted, the overall heat transfer rate is not greatly reduced, at least not unless high mass flow rates are employed.

Because of its density the momentum flow rate of ejected helium was always sufficient to cause the bow shock wave to bulge out, even at low mass flow rates. With nitrogen on the other hand, it was found that at the lower mass flow rates the momentum flow rates were not sufficient to disturb the external flow appreciably. With this method of ejection relatively large reductions in heat flux were obtained as long as the external flow was sensibly undisturbed, as was the case with nitrogen ejected at a mass flow coefficient of 0.002. These reductions in total heat transfer over the model were of the order of the "heat capacity" of the coolant nitrogen, where the "heat capacity" is defined for this purpose as the amount of heat that the gas can absorb in having its temperature raised from that at the source (i.e., in the plenum chamber) to the stagnation temperature of the main air flow. For helium ejected at a mass flow coefficient of 0.002, for which the bow shock wave is bulged out, the reduction in total heat transfer over the model was no more than one tenth of the "heat capacity" of the coolant gas.

Clearly the method of ejecting straight out, but without sufficient momentum flow to cause the bow shock wave to bulge out, seems extremely promising as a means of alleviating the heating problem. For a given mass flow the momentum flow can only be reduced by increasing the size of the ejection orifice. Varying the momentum flow for a given mass flow by this means would provide an extremely interesting experiment.

The results obtained at incidence are qualitatively what would be expected on the basis of the results at zero incidence, when allowance is made for the fact that the stagnation point moves away from the nose; or, in the case of flow corresponding to a bulged-out bow shock wave, that the "stagnation circle" is now eccentric.

The investigation was started in the belief that the necessary heat flux information would be obtained from the use of the Hartwig heatmeters[2], but spurious and unexplained results were obtained with them, and instead the necessary information was obtained from the measurements of surface temperature. The philosophy of obtaining the heat flux by this means appears to lie in having a model with a thin skin of low thermal conductivity. The thinness of the skin ensures that the effects of longitudinal temperature gradients are negligible (at least in the steady state); the low thermal conductivity is necessary to ensure that, even although the skin is thin, there is a reasonable and measurable temperature difference across it. What is required in this technique is an accurate knowledge of both the outer and inner surface temperatures of the skin which should be of uniform thickness and thermal conductivity. In the present experiments the inner surface temperature was not measured, only deduced, and that somewhat crudely, but if necessary it could be measured as accurately as the outer surface temperature.

REFERENCES

1. McMahon, H. M.: An Experimental Study of the Effect of Mass Injection at the Stagnation Point of a Blunt Body. GALCIT Hypersonic Research Project, Memorandum No. 42, May 1, 1958.

2. Hartwig, F. W.: Development and Application of a Technique for Steady State Aerodynamic Heat Transfer Measurements. GALCIT Hypersonic Research Project, Memorandum No. 37, June 1, 1957.

3. Hartwig, F. W., Bartsch, C. A., and McDonald, H.: Miniaturized Heat Meters for Steady State Aerodynamic Heat Transfer Measurements. Journal of the Aeronautical Sciences, Vol. 24, No. 3, p. 239, March, 1957.

4. Richards, H. K.: An Experimental Investigation of Heat Transfer Rates on a Blunt Body in Hypersonic Flow. California Institute of Technology, Ae. E. Thesis, June, 1957.

5. Baloga, P. E. and Nagamatsu, H. T.: Instrumentation of GALCIT Hypersonic Wind Tunnels. GALCIT Memorandum No. 29, July 31, 1955.

6. Lees, L.: Laminar Heat Transfer over Blunt-Nosed Bodies at Hypersonic Flight Speeds. Jet Propulsion, Vol. 26, No. 4, pp. 259-269, April, 1956.

7. Cohen, C. B. and Reshotko, E.: The Compressible Laminar Boundary Layer with Heat Transfer and Arbitrary Pressure Gradient. N. A. C. A. Report 1294, 1956; superseding N. A. C. A. T. N. 3326, 1955.

8. Diaconis, N. S., Wisniewski, R. J., and Jack, J. R.: Heat Transfer and Boundary-Layer Transition on Two Blunt Bodies at Mach Number 3.12. N. A. C. A. T. N. 4099, October, 1957.

9. Crawford, D. H. and McCauley, W. D.: Investigation of the Laminar Aerodynamic Heat-Transfer Characteristics of a Hemisphere-Cylinder in the Langley 11-Inch Hypersonic Tunnel at a Mach Number of 6.8. N. A. C. A. T. N. 3706, July, 1956.

APPENDIX 1

CONSTRUCTION OF OVEN

A brass former, 3/16 inch larger than the model in profile, but somewhat shorter, was made. On this was built a 1/16 in. thickness of sauereisen, on top of which was wound the main heater of 20 gage (0.032 in.) nichrome wire at a spacing of 0.15 in. (see Figure 4). The heater was wound in such a way that the wire entered near the top of the oven, was wound to the bottom where it reversed direction and was wound back to the top again where it left the oven. Over this main heater was built a 1/8 in. thickness of sauereisen. A strip of mica, 4.75 in. long and 3/8 in. wide, on which had been wound about 100 turns of 0.008 in. constantan wire and silver plated in the usual way to form a heatmeter, was then bent over the sauereisen. The constantan leads from this heatmeter left the oven near the top. Over this oven heatmeter was built a further 1/8 in. thickness of sauereisen, and on top of this was wound the oven bucking heater in the same manner as for the main heater, except that the spacing was about 0.17 in. Over this bucking heater was built roughly another 1/8 in. of sauereisen.

The oven lid was then constructed. This lid consisted of an annular piece of 3/16 in. thick transite of 5 in. outside diameter having a tapered hole to suit the profile of the model. Over this was placed two annular pieces of transite of 5 in. outside diameter and 3 in. inside diameter, the inside of which was built up with sauereisen as shown in Figure 4. In the sauereisen were embedded first an annular heatmeter formed on a ring of

mica in the same manner as the strip heatmeter in the main oven, and an annular bucking heater, consisting of a ring of transite wound with 20 gage nichrome wire. The lid heatmeter was 1.8 in. inside diameter and 2.3 in. outside diameter, and the lid bucking heater was 1.8 in. inside diameter and 2.6 in. outside diameter. The lid was then completed by placing on the top another annular piece of transite of 5 in. outside diameter and just over $1\frac{1}{2}$ in. inside diameter.

The lid was then attached to the main oven by woodscrews through the base of the lid which were built on to the main oven by sauereisen. (Not shown in Figure 4.) The whole assembly was then mounted on a piece of 1/4 in. thick transite, on which were mounted terminals for the six heater leads and the four heatmeter leads. When the model was lowered into the finished oven there was a 3/16 in. air gap between it and the inner surface of the oven, with the base of the model some 0.090 in. above the bottom of the oven lid: the surface area of the model exposed to the oven was therefore 5.70 in.^{2}. During calibration a trickle of nitrogen was allowed to flow through the model to ensure that the gap between it and the oven was dry: to enable the nitrogen to escape a 0.042 in. diameter hole was drilled in the oven lid, as shown in Figure 4.

APPENDIX 2

HEAT FLOW IN THE SKIN

Consider the problem of the steady two-dimensional flow of heat in a thin flat-plate or skin. Take rectangular coordinates, x parallel to the skin surfaces and y normal to them. Let one surface of the skin, called the "inner surface", correspond to $y = 0$, and the other surface of the skin, called the "wall", to $y = y_1$.

Consider the temperature function

$$T = T_i + (T_{w_o} - T_i)\frac{y}{y_1} + \frac{y_1^2}{6}\left(\frac{\partial^2 T}{\partial x^2}\right)_{w_o}\frac{y}{y_1}$$

$$+ y_1\left(\frac{\partial T}{\partial x}\right)_{w_o}\frac{xy}{y_1^2} + \frac{y_1^2}{6}\left(\frac{\partial^2 T}{\partial x^2}\right)_{w_o}\left(3\frac{x^2 y}{y_1^3} - \frac{y^3}{y_1^3}\right) .$$

This function is a harmonic function in x, y, and thus satisfies the equation of heat conduction, and it yields the following boundary properties:

on $y = 0$, $T = T_i$, constant,

and $$\frac{\partial T}{\partial y} = \frac{1}{y_1}(T_{w_o} - T_i) + \frac{y_1}{6}\left(\frac{\partial^2 T}{\partial x^2}\right)_{w_o}$$

$$+ \left(\frac{\partial T}{\partial x}\right)_{w_o}\frac{x}{y_1} + \frac{y_1}{2}\left(\frac{\partial^2 T}{\partial x^2}\right)_{w_o}\frac{x^2}{y_1^2} \quad ;$$

on $y = y_1$, $T = T_{w_o} + \left(\frac{\partial T}{\partial x}\right)_{w_o} x + \frac{1}{2}\left(\frac{\partial^2 T}{\partial x^2}\right)_{w_o} x^2$,

and $$\frac{\partial T}{\partial y} = \frac{1}{y_1}(T_{w_o} - T_i) - \frac{y_1}{3}\left(\frac{\partial^2 T}{\partial x^2}\right)_{w_o}$$

$$+ \left(\frac{\partial T}{\partial x}\right)_{w_o}\frac{x}{y_1} + \frac{y_1}{2}\left(\frac{\partial^2 T}{\partial x^2}\right)_{w_o}\frac{x^2}{y_1^2} \quad .$$

We note that T_{w_o} , $\left(\frac{\partial T}{\partial x}\right)_{w_o}$, $\left(\frac{\partial^2 T}{\partial x^2}\right)_{w_o}$ are the values of T, $\frac{\partial T}{\partial x}$, $\frac{\partial^2 T}{\partial x^2}$ on the wall $y = y_1$ at the point $x = 0$. At the point $x = 0$, the flux of heat across the wall is given by

$$\frac{\dot{q}_w}{k} = \left(\frac{\partial T}{\partial y}\right)_{w_o} = \frac{1}{y_1}(T_{w_o} - T_i) - \frac{y_1}{3}\left(\frac{\partial^2 T}{\partial x^2}\right)_{w_o} ,$$

and the flux of heat across the inner surface is given by

$$\frac{\dot{q}_i}{k} = \left(\frac{\partial T}{\partial y}\right)_{i_o} = \frac{1}{y_1}(T_{w_o} - T_i) + \frac{y_1}{6}\left(\frac{\partial^2 T}{\partial x^2}\right)_{w_o} .$$

We note that these two fluxes of heat differ from the simple result

$$\frac{\dot{q}}{k} = \frac{1}{y_1}(T_{w_o} - T_i)$$

by a term depending on the derivative of the longitudinal temperature gradient and on the thickness of the skin. Moreover, for a given heat flux, $\dot{q}$, and a given skin thickness, y_1, the temperature difference across the skin, $(T_{w_o} - T_i)$, will be greater the lower the thermal conductivity, k.

For the case in which

$T_{w_o} = 120^\circ F$, $T_i = 80^\circ F$, $y_1 = 0.02$ in., $\left(\frac{\partial^2 T}{\partial x^2}\right)_{w_o} = 3000^\circ F/in.^2$

which values are typical of the present experiments,

$$\frac{1}{y_1}(T_{w_o} - T_i) = 2000^\circ F/in. ,$$

whereas

$$\frac{y_1}{3}\left(\frac{\partial^2 T}{\partial x^2}\right) = 20^\circ F/in. ,$$

which is negligible in comparison.

TABLE 1

MODEL ORDINATES, AND LOCATION OF PRESSURE ORIFICES, THERMOCOUPLES AND HEATMETERS

Station	Distance aft of the Nose x (in.)	Distance laterally from the Axis y (in.)	Distance from the Nose along a Meridian s (in.)	Angle of the Surface Profile to the Axis θ (deg.)	s/D
nose	0	0	0	90	0
	0.0015	0.05	0.050	86.4	0.033
	0.006	0.1	0.1005	82.8	0.067
	0.014	0.15	0.151	79.1	0.101
1	0.019	0.1735	0.175	77.2	0.117
	0.0255	0.2	0.202	75.1	0.135
	0.041	0.25	0.2545	70.8	0.170
2	0.0445	0.260	0.265	69.9	0.177
	0.0605	0.3	0.308	66.1	0.205
3	0.0815	0.342	0.355	61.3	0.237
	0.0855	0.35	0.364	60.7	0.243
	0.1175	0.4	0.4235	54.1	0.282
4	0.1305	0.417	0.445	51.6	0.297
	0.1595	0.45	0.4885	45.9	0.326
5	0.1935	0.4815	0.535	39.0	0.357
	0.2185	0.5	0.5665	33.9	0.378
6	0.2705	0.528	0.625	23.1	0.417
shoulder	0.330	0.546	0.688	10	0.459
7	0.357	0.551	0.715	10	0.477
8	0.7015	0.6115	1.065	10	0.710
9	1.046	0.6725	1.415	10	0.943
base	1.487	0.75	1.8625	10	1.242

The equation of the elliptic forebody is $\left(\frac{x - 0.375}{0.375}\right)^2 + \left(\frac{y}{0.550}\right)^2 = 1$.

The profile is straight from x = 0.330 to the base (10 degree cone).

The shoulder is the junction of the elliptic forebody to the conical afterbody.

TABLE 2

PERTINENT DATA ON TUNNEL AND MODEL

Tunnel stagnation pressure	6 atm. $\pm$ 0.02
Tunnel stagnation temperature	
with pressure model, nominal	250°F
with heat-flux model, nominal	325°F
with heat-flux model, measured	316°F $\pm$ 3
Tunnel Mach number, nominal	5.8
mean in vicinity of model	5.85 $\pm$ 0.04
$\frac{\text{Stagnation pressure behind a normal shock}}{\text{Tunnel stagnation pressure}}$	0.033 $\pm$ 0.001
$\frac{\text{Tunnel static pressure}}{\text{Tunnel stagnation pressure}}$	0.00074 $\pm$ 0.00003
$\frac{\text{Tunnel kinetic pressure } (\frac{1}{2} \rho_{\infty} V_{\infty}^{2})}{\text{Tunnel stagnation pressure}}$	0.0177 $\pm$ 0.0005
$\frac{\text{Tunnel static temperature}}{\text{Tunnel stagnation temperature}}$	0.1275 $\pm$ 0.0015
$\rho_{\infty} V_{\infty} \pi (D/2)^2$, with pressure model	0.00202 slug./sec.
with heat-flux model	0.00193 slug./sec.
Model base diameter	1.5 in.
Model ejection orifice area	0.0000358 ft.^{2}
Model surface area	0.0427 ft.^{2}
$\frac{\text{Model nose radius}}{\text{Model base diameter}}$	0.538

TABLE 3

GAS PROPERTIES

Gas	Air	N_2	He
Molecular weight	29.0	28.0	4.0
Ratio of the specific heats, γ	1.40	1.40	1.67
Prandtl number, $\mu c_p/k$	0.71	0.71	0.66
Specific heat at constant pressure, c_p			
in Btu/slug. degR	7.7	8.0	40
in $ft.^2/sec.^2$ degR	6000	6200	31000
Dynamic viscosity at 59°F, μ			
in lb. sec./$ft.^2$	3.75×10^{-7}	3.6×10^{-7}	4.1×10^{-7}
Thermal conductivity, k			
in Btu/ft. sec. degR	41×10^{-7}	41×10^{-7}	250×10^{-7}

TABLE 4

SILVER-CONSTANTAN THERMOCOUPLE CALIBRATION
(FROM REFERENCE 2, FIGURE 5)
REFERENCE JUNCTION 70°F

millivolts

°F	0	1	2	3	4	5	6	7	8	9
70	0	0.02	0.04	0.06	0.08	0.10	0.12	0.14	0.17	0.19
80	0.21	0.23	0.25	0.27	0.29	0.31	0.33	0.36	0.38	0.40
90	0.42	0.44	0.46	0.48	0.50	0.52	0.55	0.57	0.59	0.61
100	0.63	0.65	0.67	0.70	0.72	0.74	0.77	0.79	0.81	0.83
110	0.85	0.88	0.90	0.92	0.95	0.97	0.99	1.02	1.04	1.06
120	1.08	1.11	1.13	1.15	1.17	1.20	1.22	1.24	1.26	1.28
130	1.31	1.33	1.36	1.38	1.40	1.42	1.45	1.47	1.49	1.51
140	1.53	1.56	1.58	1.60	1.62	1.65	1.67	1.70	1.72	1.74
150	1.77	1.79	1.82	1.84	1.86	1.88	1.91	1.93	1.96	1.98
160	2.01	2.03	2.06	2.08	2.11	2.13	2.16	2.18	2.21	2.24
170	2.27	2.29	2.31	2.34	2.37	2.39	2.41	2.43	2.46	2.48
180	2.51	2.53	2.55	2.58	2.61	2.63	2.66	2.68	2.71	2.73
190	2.76	2.78	2.81	2.83	2.86	2.88	2.91	2.93	2.96	2.99
200	3.02	3.04	3.07	3.10	3.12	3.15	3.18	3.20	3.23	3.26
210	3.28	3.30	3.33	3.36	3.38	3.41	3.43	3.46	3.49	3.52
220	3.54	3.57	3.59	3.62	3.64	3.67	3.70	3.72	3.75	3.78
230	3.80	3.83	3.86	3.88	3.91	3.94	3.97	4.00	4.02	4.05
240	4.07	4.10	4.12	4.15	4.17	4.20	4.23	4.26	4.28	4.31
250	4.33	4.37	4.39	4.42	4.45	4.47	4.50	4.52	4.55	4.57
260	4.60	4.63	4.66	4.68	4.71	4.74	4.77	4.79	4.82	4.84
270	4.87									

TABLE 5

PLENUM CHAMBER PRESSURE AND TEMPERATURE
PRESSURE MODEL

Gas	Nitrogen				Helium	
Angle of Incidence deg.	0	4	8	-	0	
	$C_{P_{plen}}/C_{P_o}$			T_{plen} °F (Average for all Incidences) *	$C_{P_{plen}}/C_{P_o}$	T_{plen} °F
$C_{\dot{m}}$ = 0	1.00	0.99	0.99	180	1.00	180
0.0004					1.14	178
0.0010	1.06			179	1.34	167
0.0016					1.63	147
0.0020	1.14	1.11	1.11	177	1.88	131
0.0026					2.59	119
0.0030	1.32			174		
0.0040	1.52	1.48	1.50	169	3.93	110
0.0050	1.75			162		
0.0060	2.04	2.02	2.07	154	5.75	100
0.0080	2.73	2.75	2.77	135		

* These are average values: the individual measurements were fairly scattered, by about $\pm$ 5°F.

TABLE 6

PLENUM CHAMBER PRESSURE AND TEMPERATURE
HEAT-FLUX MODEL
SWIRLER AT 45°

Gas	Nitrogen			Helium		
Angle of Incidence deg.	0	4	8	0	4	8
	$C_{P_{plen}}/C_{P_o}$					
$C_{\dot{m}}$ = 0	0.98	0.99	0.98	0.98	0.99	0.98
0.0021	1.11	1.09	1.08	1.85	1.81	1.88
0.0032				2.86	2.85	2.94
0.0042	1.46	1.41	1.42	4.10	4.15	4.13
0.0049				4.56	4.58	4.78
0.0063	1.94	2.00	1.96			
0.0084	2.58	2.69	2.65			

Note: With the swirler at 45° the plenum chamber temperature was 79°F, with a maximum deviation of ± 2°, throughout.

TABLE 7

PLENUM CHAMBER PRESSURE AND TEMPERATURE
HEAT-FLUX MODEL
SWIRLER AT 90°

Gas	Nitrogen			Helium		
Angle of Incidence deg.	0	4	8	0	4	8
	$C_{P_{plen}}/C_{P_o}$					
$C_{\dot{m}}$ = 0	0.99	1.01	1.01	0.99	1.01	1.01
0.0020	1.10	1.08	1.08	1.72	1.69	1.72
0.0030				2.66	2.65	2.67
0.0040	1.43	1.36	1.35	3.50	3.61	3.64
0.0050				4.35	4.38	4.41
0.0060	1.84	1.80	1.83			
0.0080	2.47	2.44	2.45			

Note: With the swirler at 90° the plenum chamber temperature was 80°F, with a maximum deviation of ± 2°, throughout.

TABLE 8

PLENUM CHAMBER PRESSURE AND TEMPERATURE
HEAT-FLUX MODEL
SWIRLER REMOVED

Gas	Nitrogen			Helium		
Angle of Incidence deg.	0	4	8	0	4	8
	$C_{P_{plen}}/C_{P_o}$					
$C_{\dot{m}}$ = 0	1.01	1.03	1.00	1.01	1.03	1.00
0.0010				0.90	1.06	1.03
0.0020	0.97	1.01	1.01	0.92	1.05	1.23
0.0040	0.97	1.11	1.10	2.14	2.13	2.16
0.0050				2.72	2.74	2.72
0.0060	1.12	1.19	1.38			
0.0080	1.52	1.53	1.62			

Note: With the swirler removed the plenum chamber temperature was $80^{\circ}F$, with a maximum deviation of $\pm 2^{\circ}$, throughout.

TABLE 9

PRESSURE
NO EJECTION
$C_{\dot{m}} = 0$

Angle of Incidence deg.	0	4					8				
Meridian	--	windward	*	side	*	leeward	windward	*	side	*	leeward
	pressure coefficient ratio, C_P/C_{P_o}										
s/D = 0.117	0.95	0.97	0.97	0.95	0.93	0.91	0.99	0.99	0.93	0.90	0.87
0.177	0.88	0.93	0.91	0.87	0.84	0.83	0.97	0.93	0.86	0.80	0.77
0.237	0.75	0.82	0.79	0.74	0.70	0.68	0.87	0.82	0.74	0.65	0.62
0.297	0.57	0.64	0.61	0.57	0.52	0.50	0.69	0.66	0.56	0.47	0.45
0.357	0.37	0.43	0.42	0.37	0.33	0.32	0.51	0.45	0.37	0.29	0.28
0.417	0.17	0.22	0.20	0.17	0.15	0.14	0.26	0.23	0.17	0.13	0.11
0.477	0.09	0.12	0.10	0.09	0.07	0.06	0.15	0.12	0.09	0.06	0.04
0.710	0.08	0.10	0.09	0.07	0.06	0.06	0.13	0.11	0.07	0.05	0.05
0.943	0.07	0.09	0.08	0.06	0.05	0.05	0.11	0.08	0.06	0.04	0.03

* These meridians are at 45^{o} to the ones on either side.

TABLE 10

PRESSURE
NITROGEN EJECTED WITH SWIRL
$C_{\dot{m}} = 0.002$

Angle of Incidence deg.	0	4					8				
Meridian	--	windward	*	side	*	leeward	windward	*	side	*	leeward
	pressure coefficient ratio, C_P/C_{P_o}										
s/D = 0.117	0.95	0.97	0.97	0.94	0.91	0.89	0.98	0.99	0.93	0.88	0.86
0.177	0.88	0.92	0.92	0.87	0.83	0.83	0.97	0.93	0.86	0.80	0.77
0.237	0.75	0.82	0.78	0.74	0.70	0.67	0.87	0.82	0.74	0.65	0.60
0.297	0.57	0.64	0.61	0.56	0.52	0.51	0.69	0.66	0.56	0.47	0.45
0.357	0.37		0.42	0.37	0.33	0.32	0.51	0.45	0.37	0.29	0.27
0.417	0.17	0.22	0.20	0.17	0.15	0.14	0.26	0.23	0.17	0.13	0.11
0.477	0.09	0.12	0.10	0.09	0.07	0.07	0.15	0.12	0.09	0.06	0.04
0.710	0.08	0.10	0.09	0.07	0.06	0.05	0.13	0.11	0.07	0.05	0.05
0.943	0.07	0.09	0.08	0.06	0.05	0.05	0.11	0.08	0.06	0.04	0.03

* These meridians are at 45^o to the ones on either side.

TABLE 11

PRESSURE
NITROGEN EJECTED WITH SWIRL
$C_{\dot{m}} = 0.004$

Angle of Incidence deg.	0	4					8				
Meridian	--	windward	*	side	*	leeward	windward	*	side	*	leeward
	pressure coefficient ratio, C_P/C_{P_o}										
s/D = 0.117	0.94	1.01	0.99	0.88	0.86	0.87	0.98	0.99	0.95	0.81	0.86
0.177	0.89	0.92	0.93	0.90	0.83	0.83	0.96	0.93	0.88	0.77	0.77
0.237	0.74	0.82	0.81	0.73	0.71	0.68	0.87	0.82	0.73	0.65	0.58
0.297	0.57	0.64	0.61	0.57	0.52	0.52	0.69	0.66	0.56	0.47	0.41
0.357	0.37	0.43	0.42	0.37	0.33	0.32	0.51	0.45	0.37	0.29	0.27
0.417	0.17	0.22	0.20	0.17	0.15	0.14	0.26	0.23	0.17	0.13	0.12
0.477	0.09	0.12	0.10	0.09	0.07	0.06	0.15	0.12	0.09	0.06	0.04
0.710	0.08	0.10	0.09	0.07	0.06	0.05	0.13	0.11	0.07	0.05	0.05
0.943	0.07	0.09	0.08	0.06	0.05	0.05	0.11	0.08	0.06	0.04	0.03

* These meridians are at 45° to the ones on either side.

TABLE 12

PRESSURE
NITROGEN EJECTED WITH SWIRL
$C_{\dot{m}} = 0.006$

Angle of Incidence deg.	0	4					8				
Meridian	--	windward	*	side	*	leeward	windward	*	side	*	leeward
	pressure coefficient ratio, C_P/C_{P_o}										
s/D = 0.117	0.90	0.94	0.86	0.74	0.81	0.86	1.05	1.04	0.90	0.73	0.67
0.177	0.91	1.00	1.05	0.88	0.84	0.83	0.96	0.93	0.88	0.69	0.77
0.237	0.73	0.85	0.81	0.74	0.71	0.69	0.86	0.83	0.73	0.64	0.58
0.297	0.58	0.67	0.62	0.57	0.53	0.52	0.68	0.66	0.55	0.48	0.41
0.357	0.37	0.43	0.42	0.37	0.33	0.32	0.50	0.45	0.37	0.29	0.26
0.417	0.17	0.22	0.20	0.17	0.15	0.14	0.25	0.23	0.17	0.13	0.11
0.477	0.09	0.11	0.10	0.09	0.07	0.05	0.15	0.12	0.08	0.05	0.04
0.710	0.08	0.10	0.09	0.07	0.06	0.05	0.13	0.11	0.07	0.04	0.05
0.943	0.07	0.09	0.08	0.06	0.05	0.05	0.11	0.08	0.06	0.04	0.03

* These meridians are at 45° to the ones on either side.

TABLE 13

PRESSURE
NITROGEN EJECTED WITH SWIRL
$C_{\dot{m}} = 0.008$

Angle of Incidence deg.	0	4					8				
Meridian	--	windward	*	side	*	leeward	windward	*	side	*	leeward
	pressure coefficient ratio, C_P/C_{P_o}										
s/D = 0.117	0.82	0.77	0.78	0.72	0.79	0.76	1.14	1.08	0.83	0.64	0.52
0.177	0.93	0.99	1.02	0.85	0.83	0.81	0.98	1.01	0.83	0.59	0.75
0.237	0.76	0.92	0.87	0.77	0.71	0.70	0.86	0.93	0.72	0.62	0.54
0.297	0.56	0.70	0.64	0.57	0.52	0.50	0.68	0.69	0.56	0.45	0.37
0.357	0.37	0.44	0.42	0.37	0.33	0.32	0.50	0.45	0.37	0.29	0.25
0.417	0.16	0.21	0.20	0.17	0.15	0.14	0.25	0.23	0.16	0.13	0.11
0.477	0.08	0.11	0.10	0.09	0.07	0.05	0.15	0.12	0.08	0.05	0.04
0.710	0.08	0.10	0.09	0.07	0.06	0.05	0.13	0.11	0.07	0.04	0.04
0.943	0.07	0.09	0.08	0.06	0.05	0.05	0.11	0.08	0.06	0.04	0.03

* These meridians are at 45° to the ones on either side.

TABLE 14

PRESSURE
HELIUM EJECTED WITH SWIRL
ZERO INCIDENCE

$C_{\dot{m}}$	0.0004	0.001	0.0016	0.002	0.0026	0.004	0.006
	pressure coefficient ratio, C_P/C_{P_o}						
s/D = 0.117	0.94	0.95	0.94	0.92	0.88	0.79	0.64
0.177	0.88	0.88	0.90	0.94	0.97	0.93	0.88
0.237	0.74	0.73	0.72	0.69	0.70	0.69	0.69
0.297	0.57	0.56	0.57	0.57	0.56	0.52	0.48
0.357	0.37	0.37	0.37	0.37	0.37	0.37	0.37
0.417	0.17	0.17	0.17	0.17	0.16	0.16	0.16
0.477	0.09	0.09	0.09	0.09	0.09	0.08	0.08
0.710	0.08	0.08	0.08	0.08	0.08	0.08	0.08
0.943	0.07	0.07	0.07	0.07	0.07	0.07	0.07

TABLE 15

TEMPERATURE AND HEAT FLUX
NO EJECTION
$C_{\dot{m}} = 0$

Angle of Incidence deg.	0	4			8		
Meridian	--	windward	side	leeward	windward	side	leeward
	temperature, T - degF						
s/D = 0.117	129	129	129	126	127	129	124
0.177	127	127	127	123	127	127	121
0.237	126	127	126	122	127	125	120
0.297	119	122	120	116	122	119	112
0.357	112	114	113	108	115	112	105
0.417	103	104	103	101	105	103	96
0.477	97	98	97	94	99	97	91
0.710	94	95	94	93	95	93	89
0.943	93	94	93	92	94	92	89
	heat-flux ratio, $\dot{q}/\dot{q}_o$						
s/D = 0.117	0.91	0.95	0.91	0.88	1.05	0.93	0.86
0.177	0.81	0.82	0.79	0.79	0.88	0.81	0.73
0.237	0.72	0.76	0.71	0.70	0.80	0.71	0.72
0.297	0.59	0.63	0.59	0.56	0.68	0.58	0.54
0.357	0.48	0.52	0.48	0.41	0.58	0.48	0.38
0.417	0.33	0.38	0.33	0.29	0.42	0.32	0.27
0.477	0.22	0.25	0.20	0.18	0.29	0.20	0.16
0.710	0.18	0.22	0.18	0.14	0.27	0.18	0.12
0.943	0.17	0.21	0.18	0.14	0.25	0.16	0.12

TABLE 16

TEMPERATURE AND HEAT FLUX
NITROGEN EJECTED WITH SWIRLER AT 45°
$C_{\dot{m}} = 0.0021$

Angle of Incidence deg.	0	4			8		
Meridian	--	windward	side	leeward	windward	side	leeward
	temperature, T - degF						
s/D = 0.117	135		134	132		132	126
0.177	130		132	128		130	123
0.237	127		126	123		125	119
0.297	122		121	119		121	114
0.357	113		114	109		116	108
0.417	104		104	100		104	99
0.477	98		98	95		98	95
0.710	96		94	94		94	94
0.943	96		94	94		95	95
	heat-flux ratio, $\dot{q}/\dot{q}_o$						
s/D = 0.117	0.91	1.01	0.89		0.97	0.92	
0.177	1.00	0.98	1.02		1.00	1.00	
0.237	0.81		0.86	0.71		0.85	0.80
0.297							
0.357	0.53	0.66	0.52		0.65	0.53	
0.417	0.41		0.34	0.26		0.34	0.34
0.477	0.19	0.24	0.20		0.28	0.18	
0.710	0.19	0.21	0.17		0.26	0.17	
0.943	0.19		0.27	0.16		0.17	0.12

TABLE 17

TEMPERATURE AND HEAT FLUX
NITROGEN EJECTED WITH SWIRLER AT 45°
$C_{\dot{m}} = 0.0042$

Angle of Incidence deg.	0	4			8		
Meridian	--	windward	side	leeward	windward	side	leeward
	temperature, T - degF						
s/D = 0.117	137		143	135		142	131
0.177	135		142	131		134	126
0.237	129		131	125		127	123
0.297	123		125	120		121	116
0.357	115		115	110		116	108
0.417	104		103	100		104	99
0.477	98		98	95		98	97
0.710	96		93	93		94	96
0.943	96		94	93		95	95
	heat-flux ratio, $\dot{q}/\dot{q}_o$						
s/D = 0.117	0.96	1.08	0.91		1.04	0.93	
0.177	0.98	0.99	1.09		0.99	1.08	
0.237	0.84		0.84	0.68		0.86	0.81
0.297							
0.357	0.53	0.59	0.51		0.65	0.51	
0.417	0.39		0.30	0.19		0.33	0.29
0.477	0.19	0.24	0.19		0.28	0.21	
0.710	0.17	0.22	0.16		0.25	0.17	
0.943	0.18		0.24	0.15		0.16	0.10

TABLE 18

TEMPERATURE AND HEAT FLUX
NITROGEN EJECTED WITH SWIRLER AT 45°
$C_{\dot{m}} = 0.0063$

Angle of Incidence deg.	0	4			8		
Meridian	--	windward	side	leeward	windward	side	leeward
		temperature, T - degF					
s/D = 0.117	146		145	137		149	133
0.177	144		151	138		152	131
0.237	134		138	130		137	125
0.297	126		129	122		127	118
0.357	115		116	111		115	110
0.417	104		105	99		103	99
0.477	98		99	94		97	95
0.710	96		93	91		93	93
0.943	96		94	91		94	93
		heat-flux ratio, $\dot{q}/\dot{q}_o$					
s/D = 0.117	0.98	1.05	0.90		1.17	0.98	
0.177	1.09	1.02	1.04		0.98	1.16	
0.237	0.89		0.84	0.70		0.87	0.74
0.297							
0.357	0.51	0.59	0.47		0.64	0.52	
0.417	0.36		0.28	0.14		0.32	0.22
0.477	0.17	0.22	0.18		0.28	0.20	
0.710	0.16	0.21	0.12		0.25	0.16	
0.943	0.17		0.22	0.14		0.16	0.08

TABLE 19

TEMPERATURE AND HEAT FLUX
NITROGEN EJECTED WITH SWIRLER AT 45°
$C_{\dot{m}} = 0.0084$

Angle of Incidence deg.	0	4			8		
Meridian	--	windward	side	leeward	windward	side	leeward
	temperature, T - degF						
s/D = 0.117	150		145	139		137	130
0.177	147		151	142		155	128
0.237	136		141	133		145	122
0.297	128		131	124		133	117
0.357	116		116	111		115	108
0.417	104		104	101		102	98
0.477	98		99	95		98	93
0.710	96		95	92		94	92
0.943	96		96	93		96	91
	heat-flux ratio, $\dot{q}/\dot{q}_o$						
s/D = 0.117	0.87	0.89	0.83		1.30	0.81	
0.177	1.10	1.18	1.00		1.14	1.31	
0.237	0.88		0.96	0.70			0.67
0.297							
0.357	0.50	0.58	0.44		0.64	0.49	
0.417	0.31		0.28	0.13			0.18
0.477	0.12	0.18	0.14		0.29	0.17	
0.710	0.15	0.20	0.10		0.24	0.16	
0.943	0.14		0.25	0.13			0.05

TABLE 20

TEMPERATURE AND HEAT FLUX
HELIUM EJECTED WITH SWIRLER AT 45°
$C_{\dot{m}} = 0.0021$

Angle of Incidence deg.	0	4			8		
Meridian	--	windward	side	leeward	windward	side	leeward
	temperature, T - degF						
s/D = 0.117	143		141	138		146	139
0.177	143		148	137		152	133
0.237	134		136	131		137	130
0.297	126		126	123		126	118
0.357	115		115	111		115	108
0.417	108		103	100		103	96
0.477	97		96	94		97	90
0.710	96		93	91		93	86
0.943	95		94	90		94	88
	heat-flux ratio, $\dot{q}/\dot{q}_o$						
s/D = 0.117	0.95	0.80	0.85		1.13	0.93	
0.177	1.01	0.99	1.03		1.04	1.14	
0.237	0.91		0.77	0.71		0.82	0.53
0.297							
0.357	0.51		0.44		0.65	0.50	
0.417	0.26		0.15	0.17		0.36	0.08
0.477	0.13	0.17	0.12		0.27	0.20	
0.710	0.17		0.11		0.25	0.16	
0.943	0.12		0.11	0.07		0.17	-0.02

TABLE 21

TEMPERATURE AND HEAT FLUX
HELIUM EJECTED WITH SWIRLER AT 45°
$C_{\dot{m}} = 0.0032$

Angle of Incidence deg.	0	4			8		
Meridian	--	windward	side	leeward	windward	side	leeward
	temperature, T - degF						
s/D = 0.117	152		146	143		144	143
0.177	148		152	144		156	138
0.237	136		140	134		143	132
0.297	126		130	124		130	120
0.357	115		115	110		115	109
0.417	102		102	99		102	96
0.477	96		96	93		97	91
0.710	94		93	91		92	87
0.943	93		94	91		94	88
	heat-flux ratio, $\dot{q}/\dot{q}_o$						
s/D = 0.117	0.83	0.65	0.86		1.19	0.84	
0.177	1.07	1.10	0.94		1.05	0.98	
0.237	0.81		0.85	0.68		0.83	0.59
0.297							
0.357	0.48		0.38		0.65	0.42	
0.417	0.20		0.17	0.12		0.32	0.07
0.477	0.06	0.10	0.08		0.26	0.14	
0.710	0.15		0.07		0.25	0.10	
0.943	0.09		0.13	0.04		0.17	-0.03

TABLE 22

TEMPERATURE AND HEAT FLUX
HELIUM EJECTED WITH SWIRLER AT 45°
$C_{\dot{m}} = 0.0042$

Angle of Incidence deg.	0	4			8		
Meridian	--	windward	side	leeward	windward	side	leeward
	temperature, T - degF						
s/D = 0.117	156		154	149		138	142
0.177	150		157	147		152	139
0.237	142		143	135		142	129
0.297	126		131	124		129	118
0.357	115		115	111		111	107
0.417	103		102	99		99	94
0.477	96		97	93		94	89
0.710	95		94	91		91	85
0.943	95		95	92		93	87
	heat-flux ratio, $\dot{q}/\dot{q}_o$						
s/D = 0.117	0.72	0.51	0.75		0.62	0.83	
0.177	1.11	1.12	0.97		1.29	0.61	
0.237	0.66		0.75	0.62		0.84	0.58
0.297							
0.357	0.46		0.37		0.64	0.27	
0.417	0.11		0.11	0.08		0.28	0.04
0.477	-0.03	0.02	-0.01		0.14	0.08	
0.710	0.14		0.05		0.24	-0.01	
0.943	0.03		0.08	0.00		0.17	-0.04

TABLE 23

TEMPERATURE AND HEAT FLUX
HELIUM EJECTED WITH SWIRLER AT 45°
$C_{\dot{m}} = 0.0049$

Angle of Incidence deg.	0	4			8		
Meridian	--	windward	side	leeward	windward	side	leeward
	temperature, T - degF						
s/D = 0.117	154		156	151		138	140
0.177	148		159	147		150	141
0.237	134		142	135		141	127
0.297	125		131	124		130	116
0.357	114		115	110		111	104
0.417	102		102	99		98	94
0.477	99		98	93		94	89
0.710	95		94	91		90	84
0.943	95		95	92		93	85
	heat-flux ratio, $\dot{q}/\dot{q}_o$						
s/D = 0.117	0.69	0.49	0.73		0.50	0.84	
0.177	1.10	1.11	0.97		1.27	0.57	
0.237	0.64		0.70	0.56		0.80	0.59
0.297							
0.357	0.43		0.36		0.64	0.24	
0.417	0.09		0.09	0.06		0.26	0.04
0.477	-0.05	0.00	-0.03		0.09	0.06	
0.710	0.14		0.05		0.24	-0.03	
0.943	0.01		0.07	-0.01		0.17	-0.04

TABLE 24

TEMPERATURE AND HEAT FLUX
NITROGEN EJECTED WITH SWIRLER AT 90°
$C_{\dot{m}} = 0.002$

Angle of Incidence deg.	0	4			8		
Meridian	--	windward	side	leeward	windward	side	leeward
	temperature, T - degF						
s/D = 0.117	128	130	129	127	131	127	127
0.177	126	128	125	123	132	124	121
0.237	124	126	125	124	131	123	123
0.297	118	121	118	114	125	117	113
0.357	110	114	110	106	118	110	105
0.417	101	104	102	97	108	101	95
0.477	96	98	96	92	103	95	89
0.710	93	95	93	91	98	92	89
0.943	93	94	92	91	96	92	
	heat-flux ratio, $\dot{q}/\dot{q}_o$						
s/D = 0.117	0.94	1.00	0.89	0.66	1.10	0.90	0.66
0.177	0.80	0.85	0.80	0.77	0.95	0.80	0.61
0.237	0.73	0.73	0.72	0.62	0.79	0.72	0.69
0.297	0.58	0.64	0.58	0.49	0.73	0.59	0.49
0.357	0.46	0.53	0.48	0.38	0.61	0.48	0.30
0.417	0.33	0.37	0.31	0.26	0.42	0.33	0.26
0.477	0.21	0.25	0.19	0.16	0.30	0.21	0.15
0.710	0.17	0.24	0.18	0.15	0.29	0.18	0.10
0.943	0.17	0.22	0.18	0.13	0.26	0.18	0.12

TABLE 25

TEMPERATURE AND HEAT FLUX
NITROGEN EJECTED WITH SWIRLER AT 90°
$C_{\dot{m}} = 0.004$

Angle of Incidence deg.	0	4			8		
Meridian	--	windward	side	leeward	windward	side	leeward
	temperature, T - degF						
s/D = 0.117	128	141	133	126	132	128	125
0.177	127	136	127	123	130	124	121
0.237	126	133	127	122	129	124	120
0.297	119	124	120	114	124	118	112
0.357	111	116	111	105	117	111	103
0.417	102	105	102	96	108	101	94
0.477	96	99	96	91	102	96	89
0.710	93	96	93	89	97	92	88
0.943	92	94	92	90	96	92	88
	heat-flux ratio, $\dot{q}/\dot{q}_o$						
s/D = 0.117	0.96	1.01	1.00	0.81		0.96	0.75
0.177	0.82	0.95	0.84	0.78	0.95	0.81	0.71
0.237	0.74	0.73	0.79	0.68	0.79	0.73	0.74
0.297	0.57	0.64	0.61	0.50	0.74	0.59	0.43
0.357	0.46	0.53	0.48	0.38	0.62	0.48	0.33
0.417	0.33	0.37	0.32	0.28	0.42	0.32	0.27
0.477	0.20	0.25	0.20	0.15	0.31	0.20	0.12
0.710	0.17	0.23	0.18	0.13	0.29	0.18	0.10
0.943	0.17	0.22	0.17	0.14	0.26	0.18	0.12

TABLE 26

TEMPERATURE AND HEAT FLUX
NITROGEN EJECTED WITH SWIRLER AT 90°
$C_{\dot{m}} = 0.006$

Angle of Incidence deg.	0	4			8		
Meridian	--	windward	side	leeward	windward	side	leeward
	temperature, T - degF						
s/D = 0.117	129	147	137	123	148	132	124
0.177	127	147	135	122	138	127	119
0.237	127	143	135	121	136	127	117
0.297	119	128	123	115	127	119	110
0.357	110	117	112	104	119	110	101
0.417	100	105	101	95	108	101	93
0.477	94	98	95	91	102	95	88
0.710	91	94	92	88	96	91	86
0.943	91	93	91	90	95	91	87
	heat-flux ratio, $\dot{q}/\dot{q}_o$						
s/D = 0.117	0.95	1.24	0.97	0.88	1.11	1.16	0.89
0.177	0.82	1.04	0.97	0.83	0.94	0.82	0.72
0.237	0.77	0.84	0.91	0.74	0.79	0.85	0.71
0.297	0.58	0.66	0.63	0.57	0.72	0.61	0.48
0.357	0.45	0.54	0.49	0.38	0.60	0.48	0.30
0.417	0.33	0.38	0.32	0.27	0.42	0.32	0.25
0.477	0.20	0.25	0.17	0.14	0.29	0.19	0.11
0.710	0.15	0.23	0.17	0.11	0.29	0.18	0.06
0.943	0.17	0.22	0.18	0.13	0.25	0.18	0.10

TABLE 27

TEMPERATURE AND HEAT FLUX
NITROGEN EJECTED WITH SWIRLER AT 90°
$C_{\dot{m}} = 0.008$

Angle of Incidence deg.	0	4			8		
Meridian	--	windward	side	leeward	windward	side	leeward
		temperature, T - degF					
s/D = 0.117	128	135	135	123	162	137	123
0.177	128	144	133	123	146	135	119
0.237	126	144	133	123	143	133	117
0.297	119	130	123	115	131	124	111
0.357	108	117	112	104	121	112	101
0.417	98	104	100	95	110	101	93
0.477	92	98	94	89	103	95	90
0.710	90	93	91	87	97	92	85
0.943	90	93	91	89	95	92	88
		heat-flux ratio, $\dot{q}/\dot{q}_o$					
s/D = 0.117	1.04	1.10	0.95	0.98	1.61	1.08	0.80
0.177	0.82	1.11	0.87	0.85	0.98	1.06	0.69
0.237	0.84	0.94	0.89	0.75	0.81	0.95	0.66
0.297	0.61	0.67	0.62	0.58	0.72	0.66	0.48
0.357	0.43	0.52	0.47	0.37	0.60	0.49	0.29
0.417	0.32	0.38	0.29	0.28	0.42	0.30	0.17
0.477	0.18	0.24	0.15	0.15	0.29	0.17	0.08
0.710	0.12	0.21	0.16	0.08	0.28	0.18	0.03
0.943	0.16	0.23	0.17	0.13	0.26	0.21	0.06

TABLE 28

TEMPERATURE AND HEAT FLUX
HELIUM EJECTED WITH SWIRLER AT 90°
$C_{\dot{m}} = 0.002$

Angle of Incidence deg.	0	4			8		
Meridian	--	windward	side	leeward	windward	side	leeward
	temperature, T - degF						
s/D = 0.117	136	133	139	129	149	136	126
0.177	133	141	134	127	141	132	121
0.237	132	142	132	126	137	132	118
0.297	124	129	123	120	127	127	114
0.357	113	117	113	110	119	118	104
0.417	102	104	102	101	108	103	96
0.477	97	98	97	96	102	98	93
0.710	93	94	93	93	96	96	90
0.943	92	93	92	91	95	94	88
	heat-flux ratio, $\dot{q}/\dot{q}_o$						
s/D = 0.117	1.04	1.11	0.97	0.98	1.07	1.14	0.81
0.177	0.77	0.92	0.86	0.82	0.87	0.83	0.62
0.237	0.77	0.84	0.82	0.81	0.85	0.84	0.72
0.297	0.60	0.66	0.58	0.57	0.69	0.59	0.39
0.357	0.36	0.49	0.44	0.33	0.55	0.46	0.21
0.417	0.30	0.39	0.26	0.29	0.43	0.30	0.17
0.477	0.18	0.24	0.14	0.12	0.28	0.18	-0.02
0.710	0.08	0.19	0.14	0.07	0.26	0.18	0.00
0.943	0.16	0.23	0.15	0.14	0.27	0.18	0.06

TABLE 29

TEMPERATURE AND HEAT FLUX
HELIUM EJECTED WITH SWIRLER AT 90°
$C_{\dot{m}} = 0.003$

Angle of Incidence deg.	0	4			8		
Meridian	--	windward	side	leeward	windward	side	leeward
	temperature, T - degF						
s/D = 0.117	129	121	133	126	165	139	121
0.177	127	129	130	126	151	133	119
0.237	125	133	128	123	145	131	116
0.297	118	128	120	118	130	121	111
0.357	107	113	109	107	120	111	101
0.417	97	100	99	98	108	100	93
0.477	92	94	93	93	101	95	89
0.710	89	91	90	90	95	92	86
0.943	89	91	90	88	93	93	84
	heat-flux ratio, $\dot{q}/\dot{q}_o$						
s/D = 0.117	1.06	1.17	1.03	1.13	1.39	0.84	0.77
0.177	0.75	0.78	0.80	0.75	0.95	0.97	0.61
0.237	0.82	0.91	0.85	0.78	0.87	0.98	0.64
0.297	0.59	0.68	0.58	0.59	0.69	0.66	0.45
0.357	0.34	0.44	0.38	0.30	0.58	0.47	0.22
0.417	0.28	0.38	0.24	0.24	0.43	0.26	0.14
0.477	0.16	0.24	0.11	0.14	0.27	0.12	0.01
0.710	0.05	0.13	0.10	0.03	0.25	0.16	-0.02
0.943	0.15	0.23	0.14	0.12	0.27	0.20	0.04

TABLE 30

TEMPERATURE AND HEAT FLUX
HELIUM EJECTED WITH SWIRLER AT 90°
$C_{\dot{m}} = 0.004$

Angle of Incidence deg.	0	4			8		
Meridian	--	windward	side	leeward	windward	side	leeward
	temperature, T - degF						
s/D = 0.117	126	115	131	124	125	136	117
0.177	125	119	127	122	143	135	117
0.237	123	121	125	119	149	134	115
0.297	117	120	118	114	136	124	112
0.357	106	108	107	103	117	111	100
0.417	95	95	97	94	103	99	92
0.477	92	89	91	91	96	94	88
0.710	88	86	89	88	93	92	84
0.943	89	88	90	87	93	92	84
	heat-flux ratio, $\dot{q}/\dot{q}_o$						
s/D = 0.117	1.07	1.06	1.08	1.13	1.07	0.83	0.88
0.177	0.69	0.67	0.74	0.69	0.94	0.78	0.67
0.237	0.79	0.94	0.82	0.71	0.98	0.79	0.66
0.297	0.57	0.70	0.58	0.57	0.73	0.52	0.49
0.357	0.29	0.40	0.34	0.26	0.52	0.41	0.25
0.417	0.24	0.35	0.21	0.21	0.41	0.19	0.15
0.477	0.13	0.22	0.10	0.11	0.25	0.06	0.04
0.710	0.01	0.08	0.07	0.00	0.22	0.11	-0.01
0.943	0.13	0.22	0.13	0.10	0.27	0.14	0.05

TABLE 31

TEMPERATURE AND HEAT FLUX
HELIUM EJECTED WITH SWIRLER AT 90°
$C_{\dot{m}} = 0.005$

Angle of Incidence deg.	0	4			8		
Meridian	--	windward	side	leeward	windward	side	leeward
	temperature, T - degF						
s/D = 0.117	125	114	129	123	113	132	116
0.177	122	116	125	119	125	129	116
0.237	120	116	123	115	132	128	114
0.297	115	116	117	112	133	121	111
0.357	104	104	106	100	117	110	100
0.417	93	92	95	91	100	98	91
0.477	89	85	90	88	93	93	88
0.710	86	83	88	85	90	91	85
0.943	87	85	89	84	92	92	83
	heat-flux ratio, $\dot{q}/\dot{q}_o$						
s/D = 0.117	1.10	1.07	1.12	1.12	0.94	0.85	1.04
0.177	0.65	0.65	0.71	0.65	0.80	0.75	0.65
0.237	0.76	0.92	0.79	0.72	1.06	0.77	0.66
0.297	0.56	0.67	0.57	0.54	0.74	0.52	0.53
0.357	0.26	0.35	0.32	0.23	0.51	0.39	0.22
0.417	0.20	0.31	0.20	0.18	0.41	0.17	0.14
0.477	0.10	0.18	0.09	0.09	0.23	0.05	0.07
0.710	-0.02	0.06	0.05	-0.02	0.19	0.10	-0.02
0.943	0.11	0.20	0.12	0.08	0.28	0.12	0.04

TABLE 32

TEMPERATURE AND HEAT FLUX
NITROGEN EJECTED STRAIGHT OUT
$C_{\dot{m}} = 0.002$

Angle of Incidence deg.	0	4			8		
Meridian	--	windward	side	leeward	windward	side	leeward
	temperature, T - degF						
s/D = 0.117	119	126	133		128	127	114
0.177	120	125	130	114	127	123	110
0.237	119	124	128	112	126	121	108
0.297	113	118	122	107	122	115	103
0.357	106	110	115	100	113	107	96
0.417	98	101	106	94	104	98	90
0.477	92	95	100	89	97	92	86
0.710	89	91	96	87	93	88	84
0.943	89	90	95	88	92	88	84
	heat-flux ratio, $\dot{q}/\dot{q}_o$						
s/D = 0.117	0.80	0.84	0.95	0.82	0.90	0.94	0.75
0.177	0.78	0.80	0.77	0.61	0.84	0.79	0.64
0.237	0.65	0.73	0.72	0.53	0.77	0.71	0.31
0.297	0.55	0.59	0.58	0.51	0.66	0.58	0.47
0.357	0.44	0.52	0.46	0.34	0.56	0.48	0.34
0.417	0.30	0.36	0.33	0.19	0.41	0.33	0.10
0.477	0.19	0.23	0.20	0.16	0.29	0.20	0.14
0.710	0.17	0.22	0.17	0.12	0.26	0.18	0.11
0.943	0.16	0.21	0.18	0.11	0.24	0.18	0.06

TABLE 33

TEMPERATURE AND HEAT FLUX
NITROGEN EJECTED STRAIGHT OUT
$C_{\dot{m}} = 0.004$

Angle of Incidence deg.	0	4			8		
Meridian	--	windward	side	leeward	windward	side	leeward
	temperature, T - degF						
s/D = 0.117	120	134	142		129	128	120
0.177	132	127	138	118	127	125	113
0.237	132	125	134	115	126	122	110
0.297	121	118	123	110	121	117	107
0.357	110	110	114	102	114	109	100
0.417	99	101	104	94	104	99	93
0.477	93	95	99	89	97	93	89
0.710	89	91	94	86	93	89	85
0.943	89	90	93	87	92	89	86
	heat-flux ratio, $\dot{q}/\dot{q}_o$						
s/D = 0.117	0.64	1.11	1.14	0.74	0.89	0.96	0.87
0.177	1.04	0.82	0.89	0.68	0.83	0.79	0.70
0.237	0.94	0.71	0.78	0.54	0.77	0.71	0.46
0.297	0.65	0.59	0.61	0.47	0.65	0.58	0.47
0.357	0.49	0.51	0.46	0.35	0.56	0.47	0.35
0.417	0.32	0.35	0.32	0.15	0.40	0.32	0.14
0.477	0.19	0.22	0.20	0.12	0.29	0.20	0.13
0.710	0.17	0.22	0.17	0.10	0.26	0.18	0.10
0.943	0.16	0.20	0.18	0.08	0.24	0.18	0.07

TABLE 34

TEMPERATURE AND HEAT FLUX
NITROGEN EJECTED STRAIGHT OUT
$C_{\dot{m}} = 0.006$

Angle of Incidence deg.	0	4			8		
Meridian	--	windward	side	leeward	windward	side	leeward
	temperature, T - degF						
s/D = 0.117	120	154	134		138	144	118
0.177	131	145	141	117	132	143	114
0.237	134	139	141	116	129	137	111
0.297	125	123	129	112	122	122	108
0.357	109	113	115	102	114	111	98
0.417	97	102	102	92	104	101	91
0.477	91	95	97	88	98	94	87
0.710	88	91	92	85	93	90	84
0.943	89	90	92	86	92	89	85
	heat-flux ratio, $\dot{q}/\dot{q}_o$						
s/D = 0.117	0.64	1.30	0.98	0.70	1.16	1.29	0.70
0.177	0.98	1.02	1.05	0.65	0.89	0.97	0.62
0.237	0.97	0.82	0.97	0.59	0.80	0.78	0.55
0.297	0.68	0.63	0.68	0.47	0.66	0.60	0.38
0.357	0.46	0.53	0.47	0.33	0.56	0.45	0.26
0.417	0.27	0.36	0.30	0.13	0.40	0.30	0.12
0.477	0.13		0.17	0.07	0.28	0.18	0.03
0.710	0.13	0.22	0.16	0.05	0.25	0.18	0.03
0.943	0.17	0.21	0.20	0.06	0.24	0.18	0.03

TABLE 35

TEMPERATURE AND HEAT FLUX
NITROGEN EJECTED STRAIGHT OUT
$C_{\dot{m}} = 0.008$

Angle of Incidence deg.	0	4			8		
Meridian	--	windward	side	leeward	windward	side	leeward
	temperature, T - degF						
s/D = 0.117	113	141	123	110	150	140	115
0.177	125	155	133	112	133	145	112
0.237	132	153	136	112	132	143	111
0.297	127	131	129	110	124	127	106
0.357	111	114	113	100	116	113	97
0.417	96	101	100	90	105	102	89
0.477	91	95	94	85	97	97	85
0.710	87	92	91	83	93	92	82
0.943	89	93	92	84	92	93	83
	heat-flux ratio, $\dot{q}/\dot{q}_o$						
s/D = 0.117	0.55	1.11	0.72	0.56	1.44	1.14	0.64
0.177	0.90	1.23	0.95	0.58	0.88	1.02	0.59
0.237	0.96	0.98	0.98	0.59	0.81	0.92	0.64
0.297	0.71	0.68	0.69	0.48	0.67	0.63	0.37
0.357	0.46	0.53	0.45	0.33	0.57	0.44	0.25
0.417	0.24	0.35	0.26	0.12	0.40	0.28	0.10
0.477	0.10	0.18	0.12	0.04	0.27	0.16	0.02
0.710	0.10	0.23	0.12	0.03	0.25	0.17	0.01
0.943	0.17	0.25	0.20	0.04	0.22	0.20	0.02

TABLE 36

TEMPERATURE AND HEAT FLUX
HELIUM EJECTED STRAIGHT OUT
$C_{\dot{m}} = 0.001$

Angle of Incidence deg.	0	4			8		
Meridian	--	windward	side	leeward	windward	side	leeward
		temperature, T - degF					
s/D = 0.117	127	133	142	123	124	134	107
0.177	131	127	139	118	124	131	99
0.237	130	126	136	116	123	129	94
0.297	122	121	124	110	119	122	94
0.357	110	112	115	101	113	114	84
0.417	99	102	105	93	103	104	78
0.477	94	96	98	90	97	98	77
0.710	91	93	94	89	93	93	80
0.943	90	92	94	89	91	93	81
		heat-flux ratio, $\dot{q}/\dot{q}_o$					
s/D = 0.117	0.91	1.10	1.11	0.84	1.06	0.93	0.86
0.177	1.01	0.81	0.86	0.76	0.84	0.78	0.58
0.237	0.84	0.78	0.75	0.57	0.79	0.71	0.45
0.297	0.62	0.59	0.60	0.49	0.67	0.57	0.48
0.357	0.47	0.49	0.46	0.36	0.56	0.47	0.20
0.417	0.29	0.37	0.30	0.13	0.42	0.31	0.04
0.477	0.16		0.18	0.10		0.20	0.12
0.710	0.16	0.20	0.17	0.08	0.25	0.18	0.01
0.943	0.15	0.21	0.17	0.05	0.25	0.17	-0.01

TABLE 37

TEMPERATURE AND HEAT FLUX
HELIUM EJECTED STRAIGHT OUT
$C_{\dot{m}} = 0.002$

Angle of Incidence deg.	0	4			8		
Meridian	--	windward	side	leeward	windward	side	leeward
	temperature, T - degF						
s/D = 0.117	120	148	138	118	133	148	115
0.177	131	141	143	114	128	142	110
0.237	136	137	142	112	127	137	105
0.297	127	125	128	108	119	124	102
0.357	111	115	114	98	112	113	93
0.417	98	103	102	89	101	103	86
0.477	92	98	95	86	94	97	84
0.710	90	95	92	84	91	93	83
0.943	90	94	92	84	90	92	83
	heat-flux ratio, $\dot{q}/\dot{q}_o$						
s/D = 0.117	0.60	1.31	0.96	0.68	1.25	1.15	0.68
0.177	0.91	0.96	1.00	0.61	0.86	0.93	0.57
0.237	0.93	0.82	0.88	0.53	0.79	0.75	0.47
0.297	0.66	0.62	0.63	0.39	0.67	0.58	0.30
0.357	0.42	0.49	0.45	0.24	0.54	0.45	0.15
0.417	0.23	0.36	0.27	0.06	0.40	0.28	0.02
0.477	0.09		0.13	-0.02		0.16	-0.04
0.710	0.10	0.20	0.15	0.00	0.24	0.17	-0.03
0.943	0.13	0.21	0.17	0.01	0.24	0.17	-0.02

TABLE 38

TEMPERATURE AND HEAT FLUX
HELIUM EJECTED STRAIGHT OUT
$C_{\dot{m}} = 0.004$

Angle of Incidence deg.	0	4			8		
Meridian	--	windward	side	leeward	windward	side	leeward
	temperature, T - degF						
s/D = 0.117	103	114	107	98	153	143	108
0.177	113	133	118	101	141	152	107
0.237	118	147	124	100	140	148	101
0.297	125	144	127	101	128	130	97
0.357	113	117	113	94	119	113	89
0.417	97	98	98	85	108	102	83
0.477	89	92	91	80	101	96	81
0.710	86	91	87	80	97	93	81
0.943	87	94	89	79	95	94	80
	heat-flux ratio, $\dot{q}/\dot{q}_o$						
s/D = 0.117	0.36	0.58	0.38	0.34	1.80	1.02	0.45
0.177	0.61	1.00	0.60	0.36	0.88	1.02	0.44
0.237	0.80	1.21	0.76	0.40	0.81	0.95	0.40
0.297	0.69	0.87	0.68	0.40	0.70	0.65	0.21
0.357	0.51	0.45	0.50	0.28	0.57	0.44	0.07
0.417	0.23	0.23	0.23	0.08	0.40	0.22	-0.05
0.477	0.05		0.04	-0.04		0.11	-0.09
0.710	0.04	0.15	0.05	-0.02	0.24	0.16	-0.08
0.943	0.10	0.28	0.10	0.00	0.24	0.21	-0.06

TABLE 39

TEMPERATURE AND HEAT FLUX
HELIUM EJECTED STRAIGHT OUT
$C_{\dot{m}} = 0.005$

Angle of Incidence deg.	0	4			8		
Meridian	--	windward	side	leeward	windward	side	leeward
	temperature, T - degF						
s/D = 0.117	97	110	101	99	173	125	103
0.177	103	128	108	101	151	138	104
0.237	107	138	111	100	143	138	99
0.297	115	145	118	103	129	133	95
0.357	109	124	110	98	121	115	88
0.417	96	102	96	91	109	101	83
0.477	88	94	88	86	102	94	81
0.710	85	90	85	85	97	92	81
0.943	85	92	86	84	96	94	80
	heat-flux ratio, $\dot{q}/\dot{q}_o$						
s/D = 0.117	0.24	0.49	0.27	0.26	1.51	0.72	0.39
0.177	0.45	0.84	0.48	0.29	0.91	1.03	0.37
0.237	0.65	1.12	0.63	0.41	0.80	1.01	0.34
0.297	0.60	0.93	0.59	0.34	0.63	0.71	0.16
0.357	0.51	0.56	0.50	0.24	0.55	0.43	0.04
0.417	0.28	0.25	0.25	0.09	0.39	0.21	-0.06
0.477	0.06	0.10	0.05	-0.04		0.08	-0.12
0.710	0.04	0.11	0.04	-0.03	0.25	0.13	-0.09
0.943	0.09	0.25	0.08	0.00	0.26	0.22	-0.06

TABLE 40

TEMPERATURE AND HEAT FLUX
WITH NO COOLANT WATER FLOW
NITROGEN EJECTED STRAIGHT OUT
ZERO INCIDENCE

$C_{\dot{m}}$	0.008	0.006	0.004	0.002	0
	temperature, T - degF				
Plenum Chamber	202	203	221	237	241
s/D = 0.117	205	215	225	249	253
0.177	209	218	228	248	251
0.237	212	219	230	248	251
0.297	208	213	224	244	247
0.357	200	207	219	240	244
0.417	195	205	217	237	241
0.477	195	205	215	236	240
0.710	195	206	213	234	237
0.943	197	208	211	232	235
	heat-flux ratio, $\dot{q}/\dot{q}_o$				
s/D = 0.117	0.11	0.07	0.08	0.24	0.29
0.177	0.34	0.33	0.40	0.25	0.22
0.237	0.38	0.30	0.32	0.20	0.17
0.297	0.18	0.07	0.15	0.11	0.09
0.357	-0.05	-0.08	0.04	0.08	0.00
0.417	-0.14	-0.14	-0.05	-0.05	-0.06
0.477	-0.15	-0.15	-0.07	-0.07	-0.07
0.710	-0.10	-0.09	-0.02	-0.03	-0.04
0.943	-0.05	-0.06	-0.02	-0.03	-0.03

TABLE 41

TEMPERATURE AND HEAT FLUX
WITH NO COOLANT WATER FLOW
HELIUM EJECTED STRAIGHT OUT
ZERO INCIDENCE

$C_{\dot{m}}$	0.005	0.004	0.003	0.002	0.001	0
	temperature, T - degF					
Plenum Chamber	172	183	192	198	212	241
s/D = 0.117	169	183	192	202	225	253
0.177	171	185	195	206	226	251
0.237	175	189	200	209	227	251
0.297	177	190	198	202	222	247
0.357	172	183	188	194	217	244
0.417	165	174	180	190	214	241
0.477	162	172	179	189	214	240
0.710	161	171	178	189	215	237
0.943	162	172	179	190	215	235
	heat-flux ratio, $\dot{q}/\dot{q}_o$					
s/D = 0.117	0.00	0.05	0.08	0.08	0.22	0.29
0.177	0.12	0.18	0.32	0.39	0.41	0.22
0.237	0.31	0.36	0.42	0.38	0.28	0.17
0.297	0.26	0.30	0.28	0.16	0.13	0.09
0.357	0.15	0.12	0.01	-0.04	0.02	0.00
0.417	0.03	-0.07	-0.14	-0.14	-0.09	-0.06
0.477	-0.15	-0.17	-0.19	-0.17	-0.10	-0.07
0.710	-0.09	-0.11	-0.12	-0.10	-0.04	-0.04
0.943	-0.05	-0.06	-0.07	-0.07	-0.05	-0.03

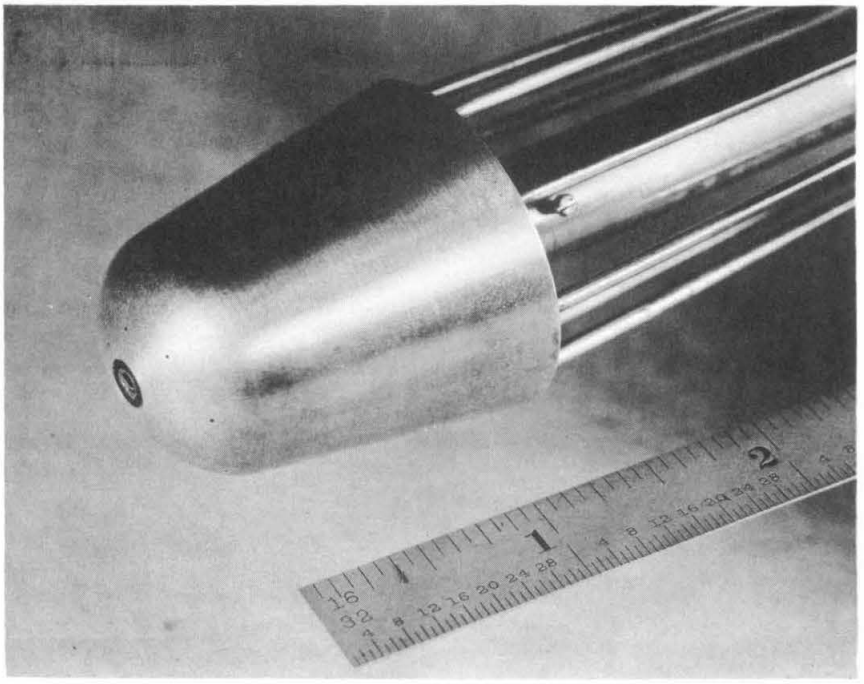

(a) PRESSURE MODEL

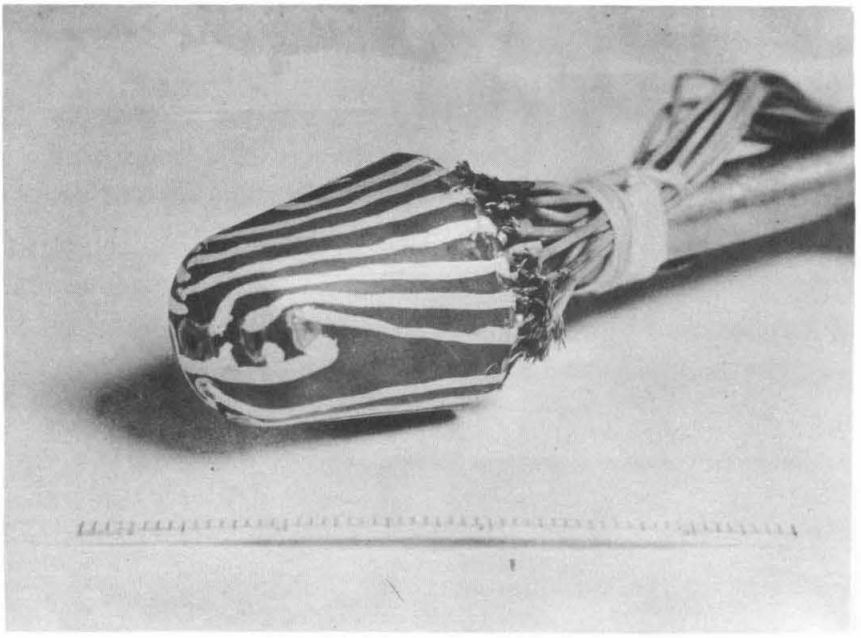

(b) HEAT-FLUX MODEL

FIG. 1 PHOTOGRAPHS OF THE MODELS

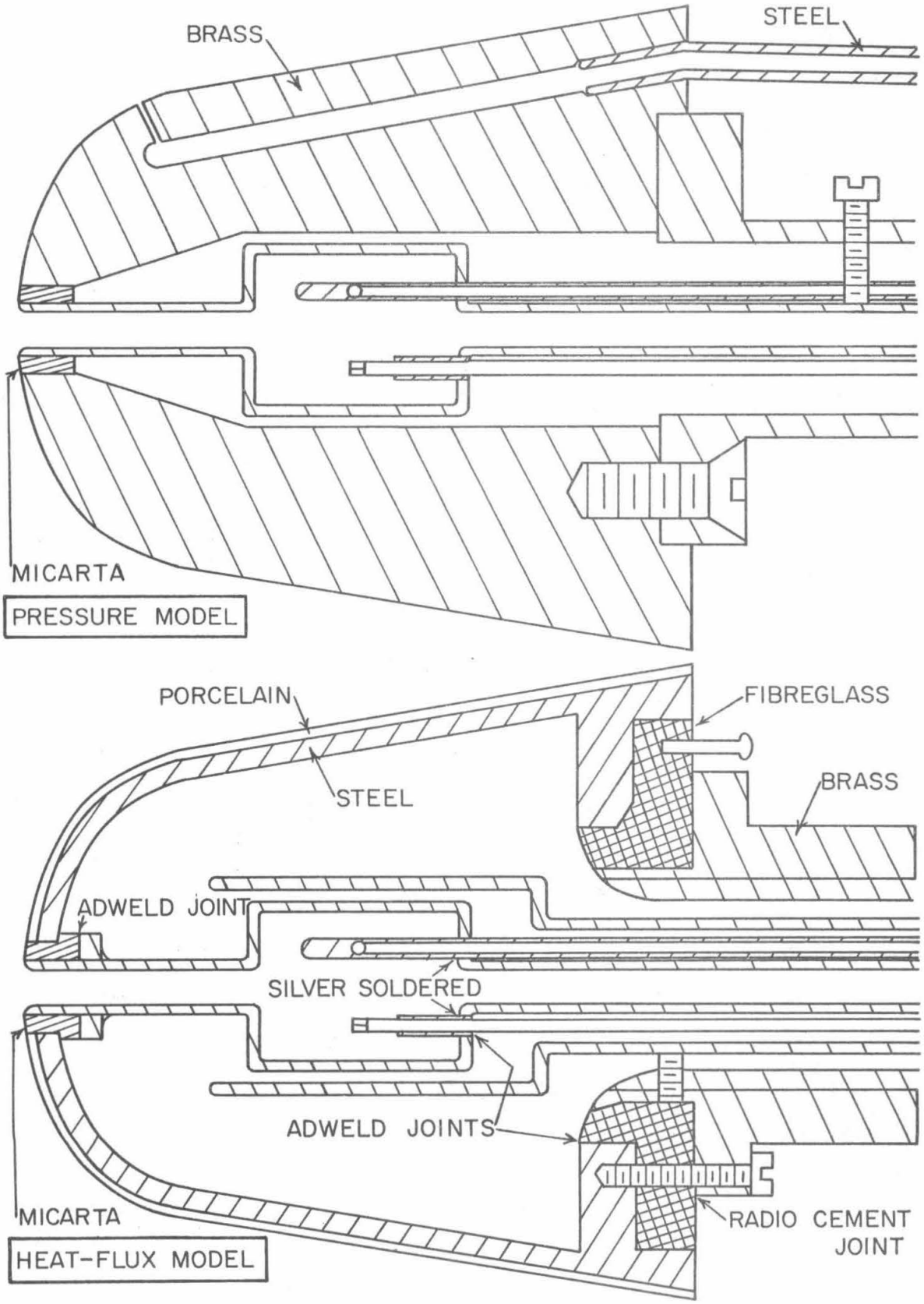

FIG. 2 CONSTRUCTION OF MODELS

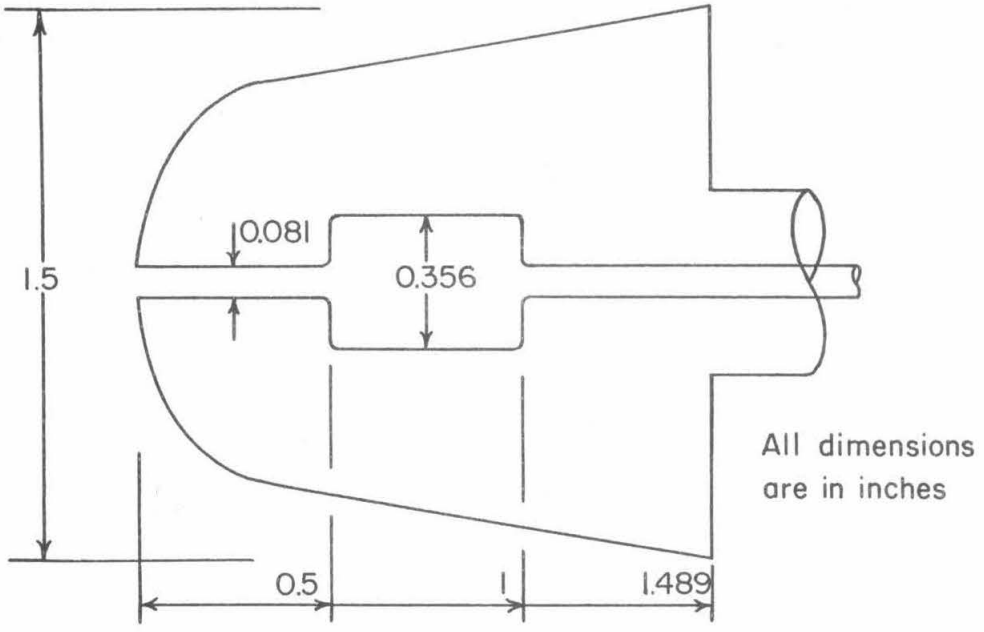

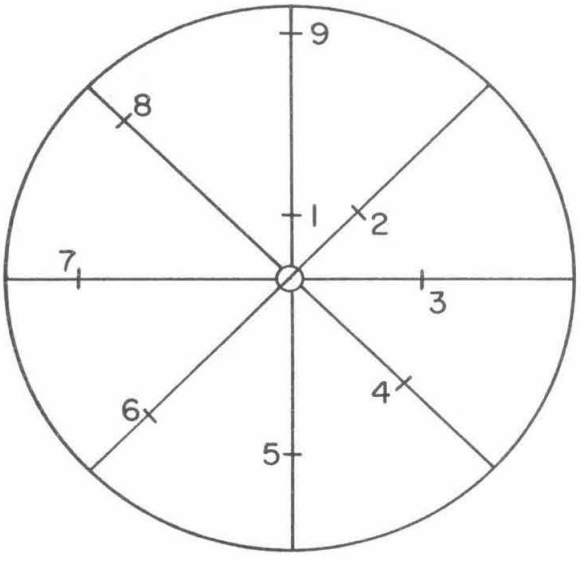

RELATIVE LOCATION OF PRESSURE ORIFICES

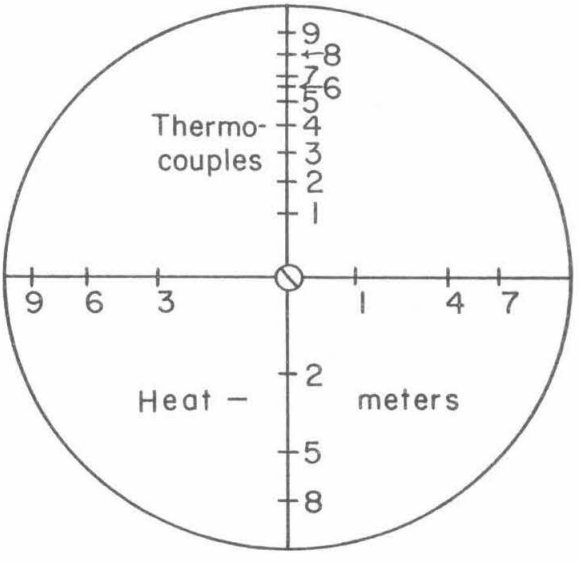

RELATIVE LOCATION OF THERMO-COUPLES AND HEATMETERS

FIG. 3 GEOMETRY OF MODELS

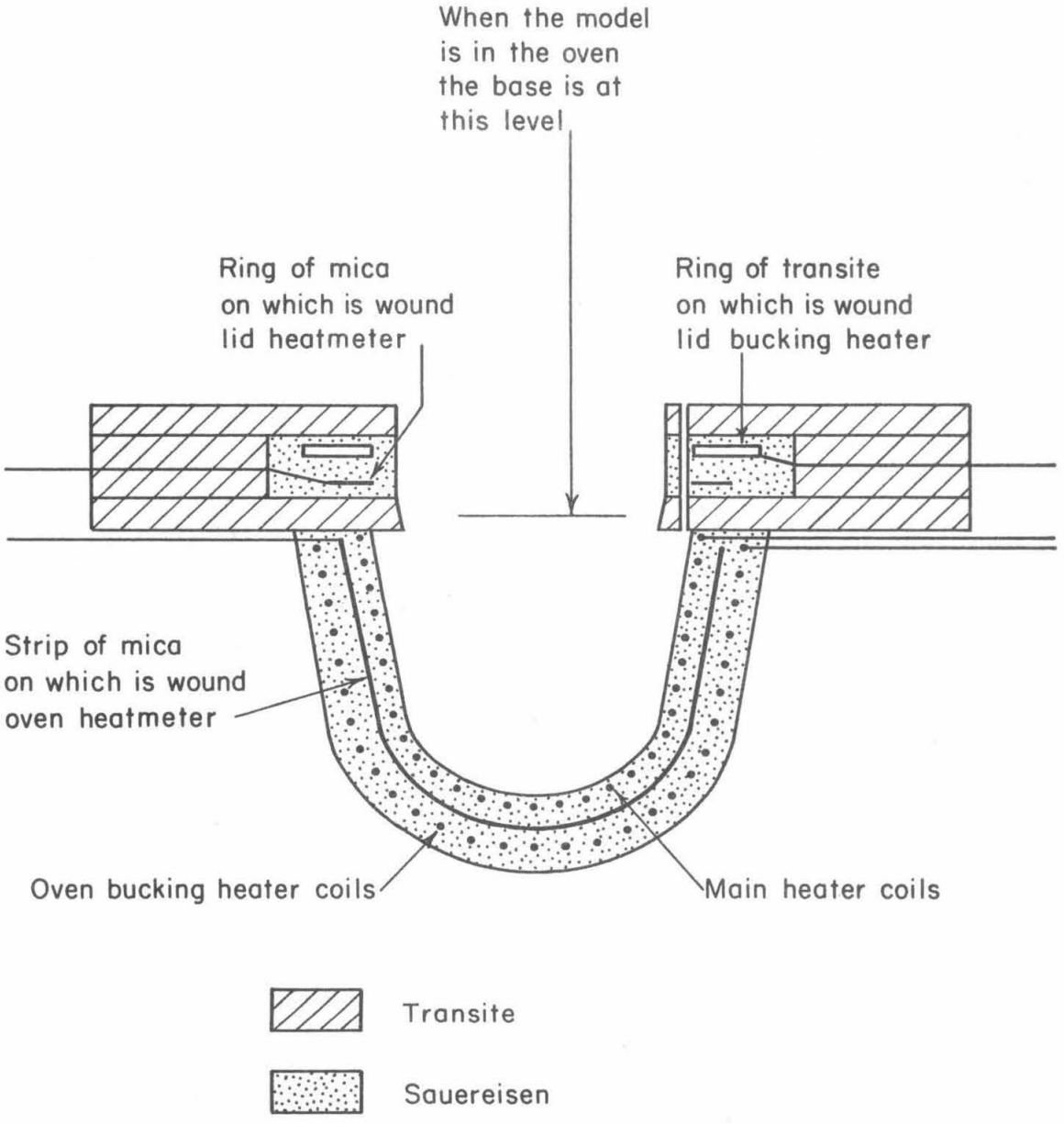

FIG. 4 DIAGRAM OF CALIBRATION OVEN

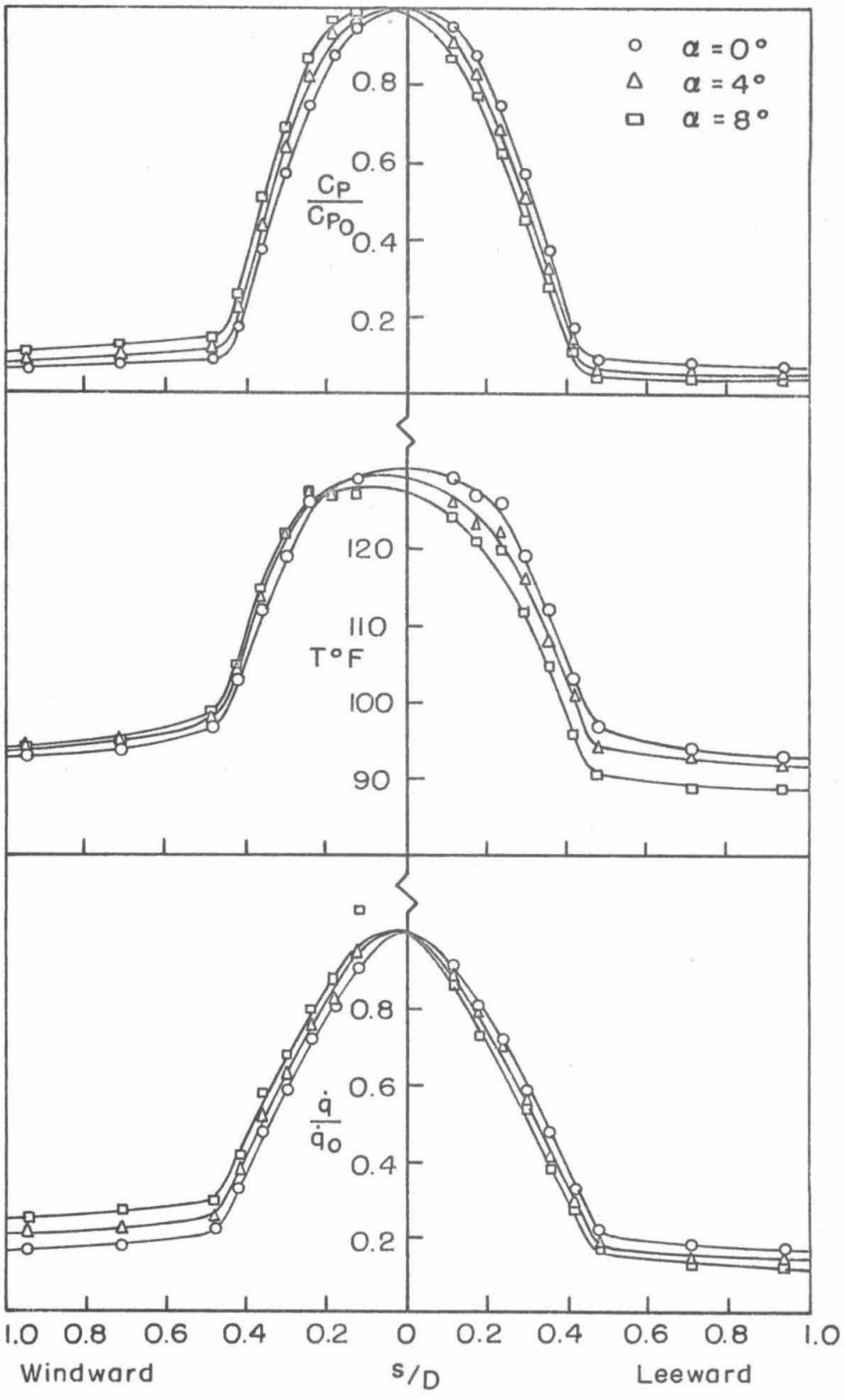

FIG. 5 DISTRIBUTIONS OF PRESSURE, TEMPERATURE AND HEAT FLUX IN THE PLANE OF INCIDENCE WITH NO EJECTION ($C_{\dot{m}} = 0$)

THE CURVES ARE DEDUCED FROM THE MEASUREMENTS OF RICHARDS (REF. 4)

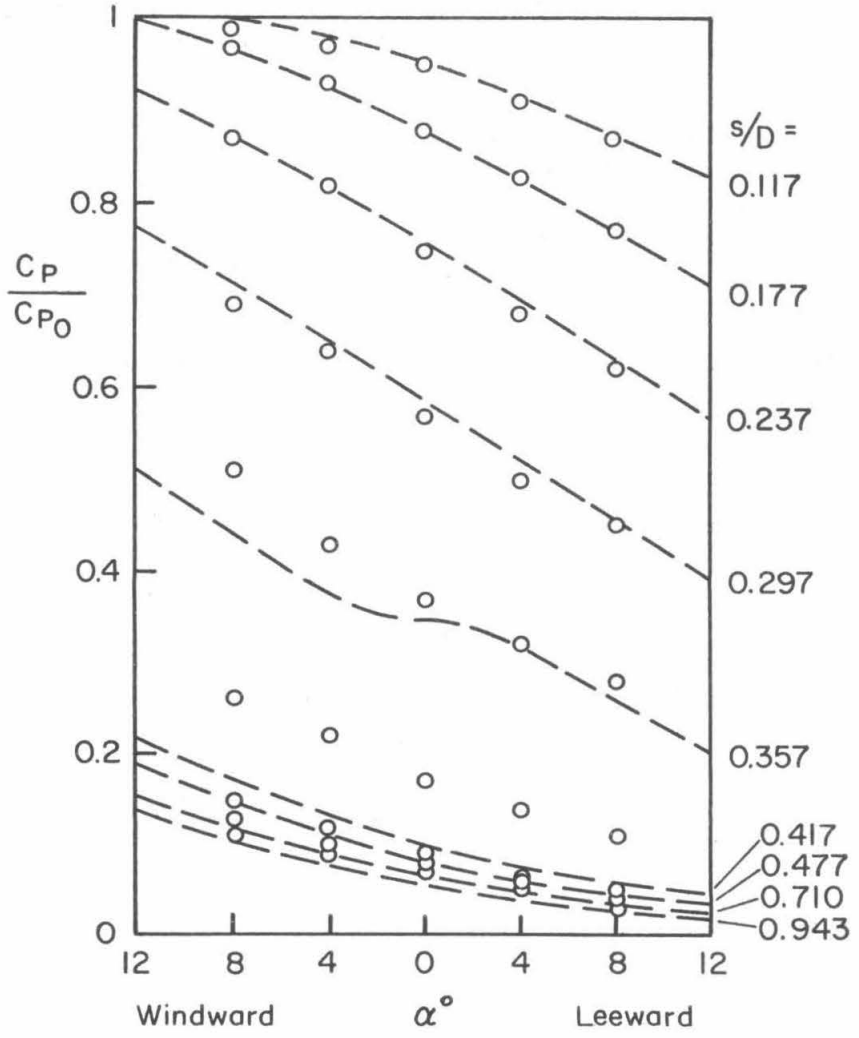

FIG. 6 EFFECT OF INCIDENCE ON PRESSURE IN THE PLANE OF INCIDENCE WITH NO EJECTION ($C_{\dot{m}} = 0$)

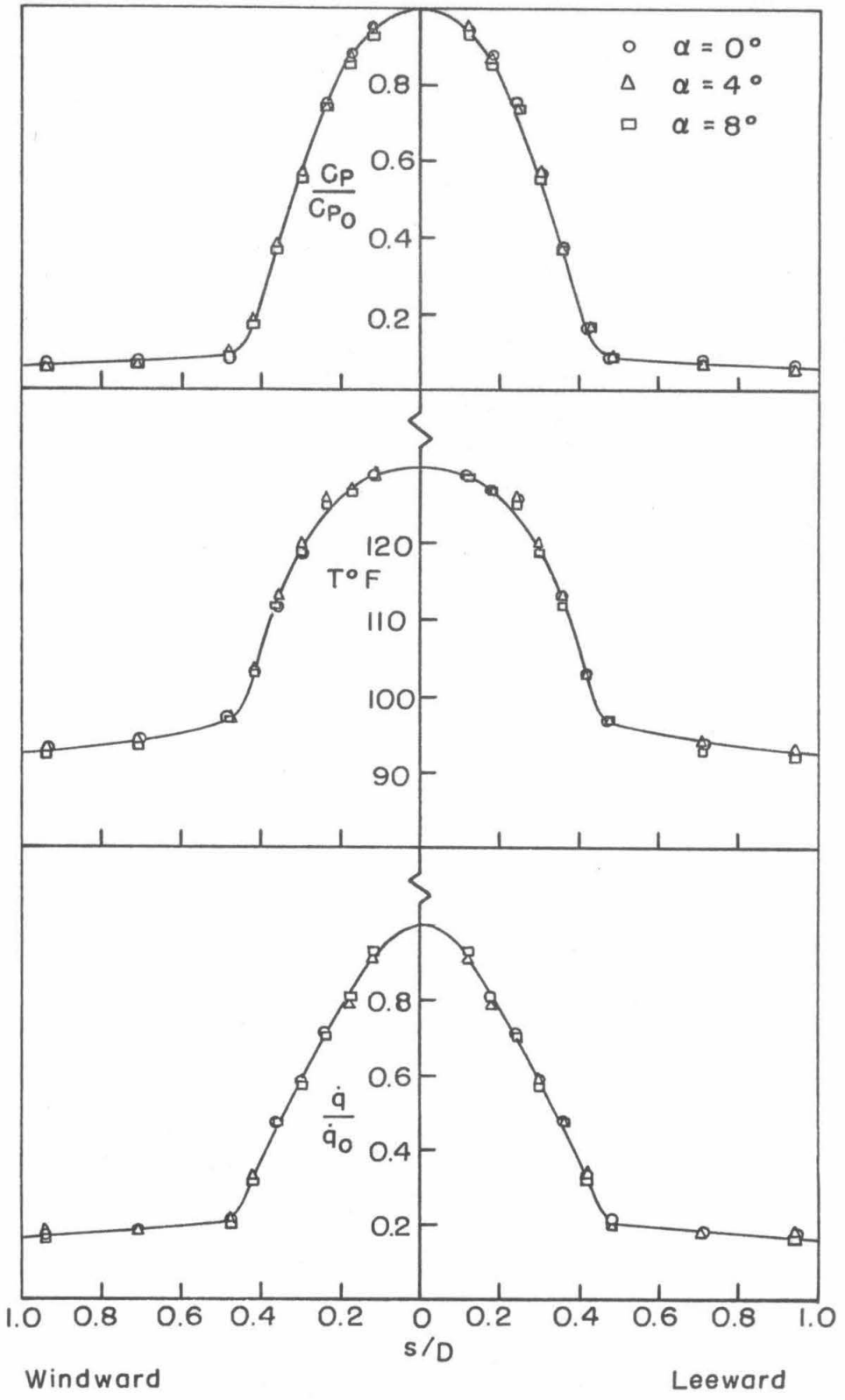

FIG. 7 DISTRIBUTIONS OF PRESSURE, TEMPERATURE AND HEAT FLUX IN THE MERIDIAN PLANE NORMAL TO THE PLANE OF INCIDENCE WITH NO EJECTION ($C_{\dot{m}}=0$)

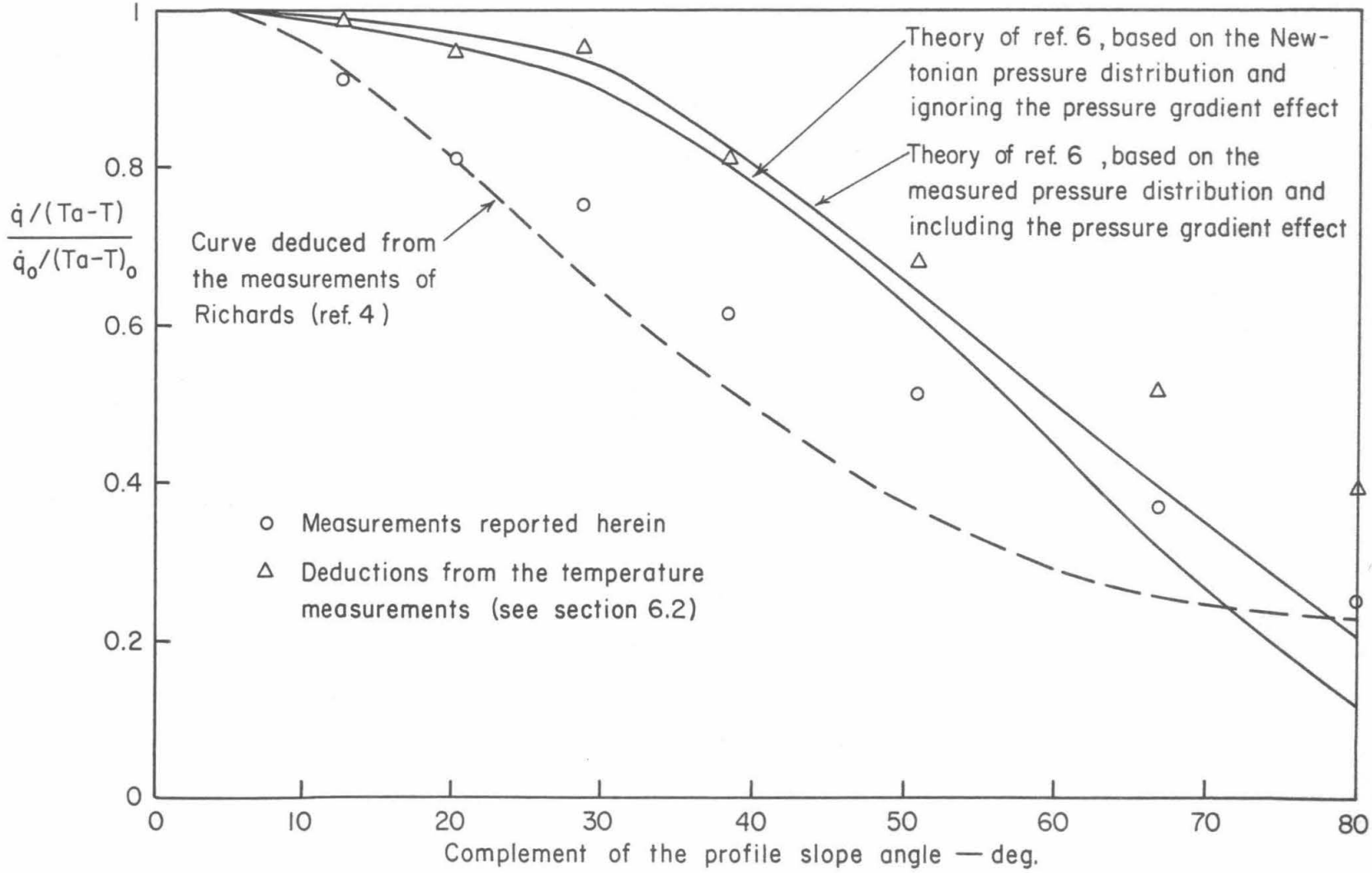

FIG. 8 COMPARISON OF MEASUREMENTS OF HEAT FLUX WITH THEORY, NO EJECTION ($C_{\dot{m}} = 0$), ZERO INCIDENCE ($\alpha = 0°$)

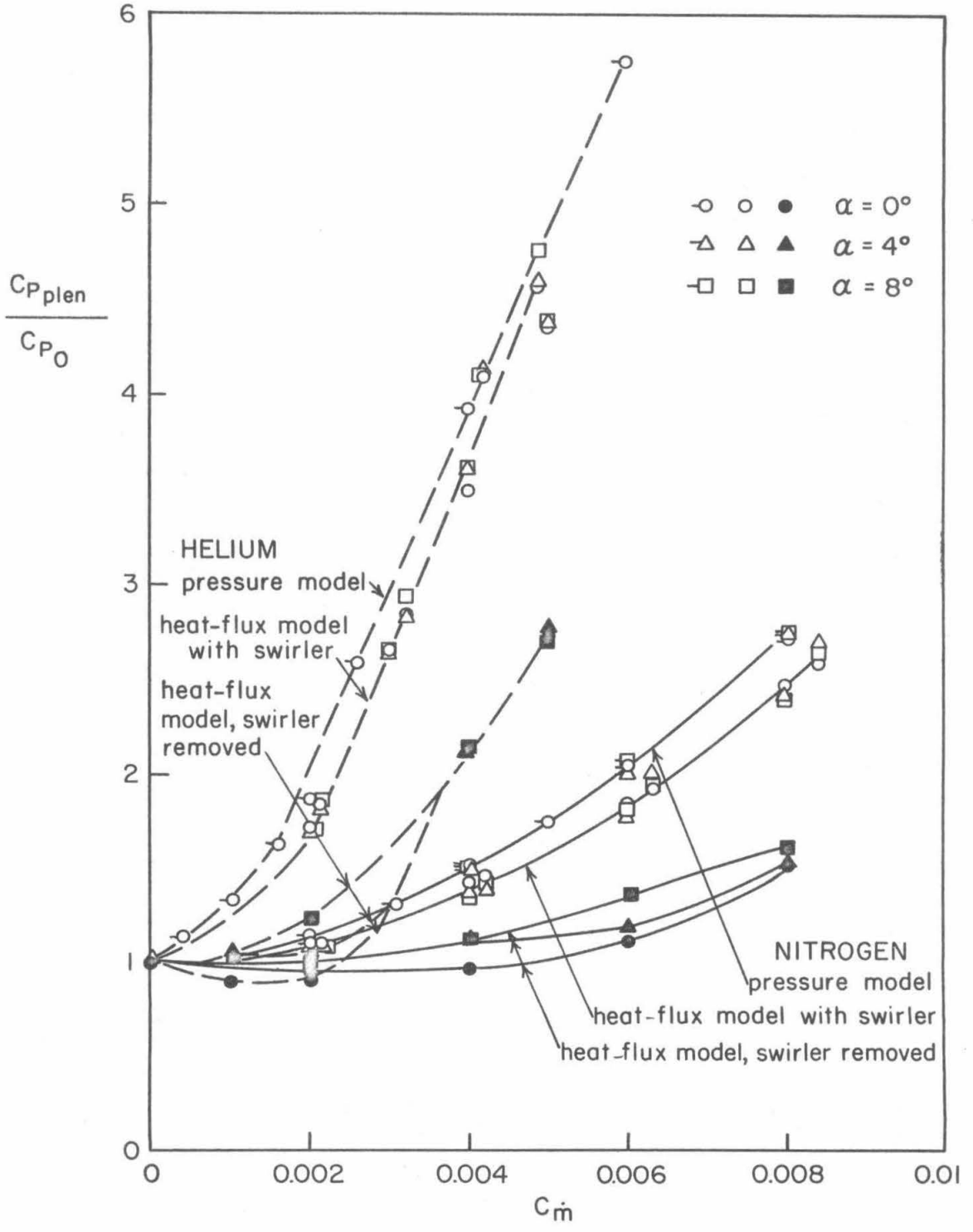

FIG. 9 EFFECT OF EJECTION ON PLENUM CHAMBER PRESSURE

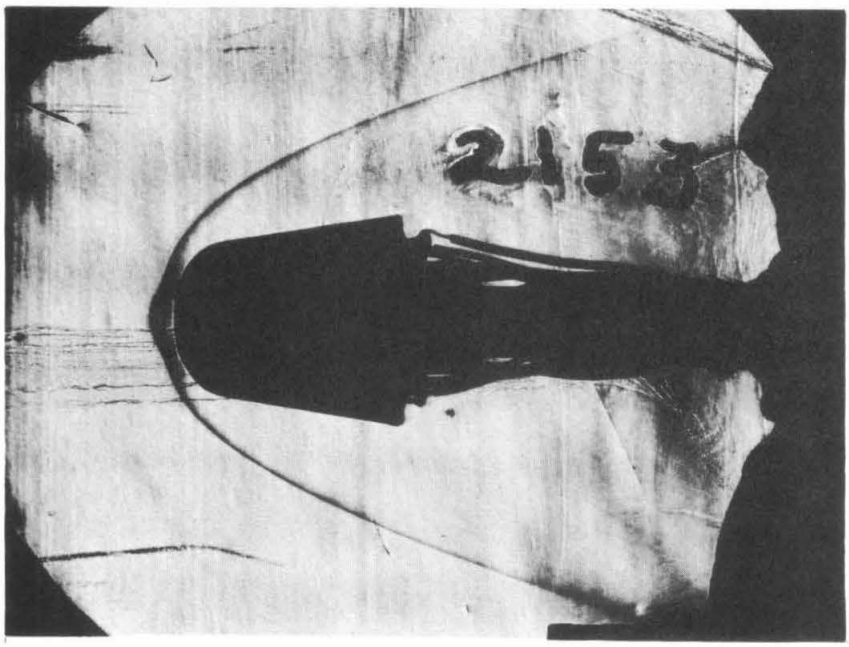

(a) NITROGEN EJECTED STRAIGHT OUT, $C_{\dot{m}} = 0.004$; $\alpha = 0^{\circ}$

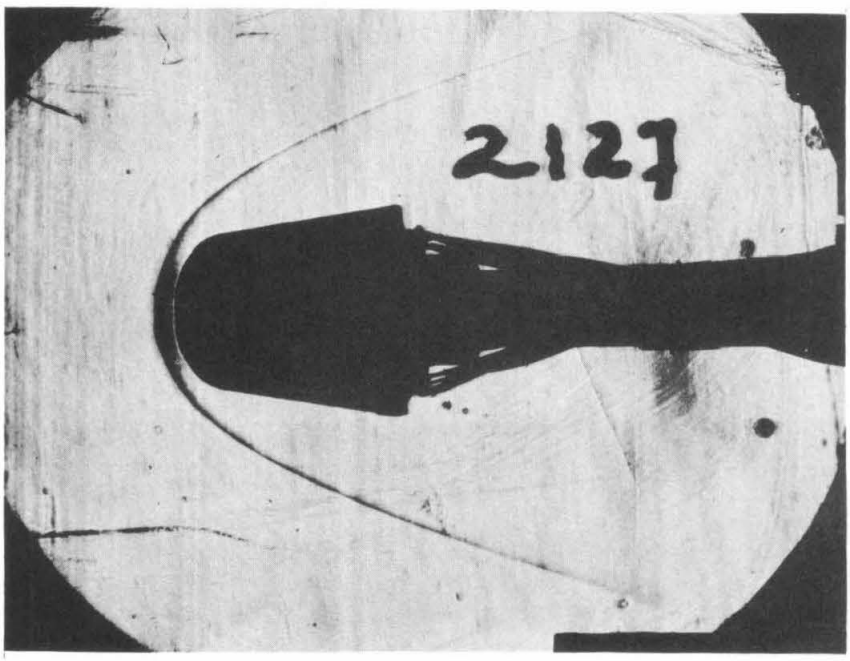

(b) NITROGEN EJECTED WITH SWIRL, $C_{\dot{m}} = 0.006$; $\alpha = 0^{\circ}$

FIG. 10 SCHLIEREN PHOTOGRAPHS

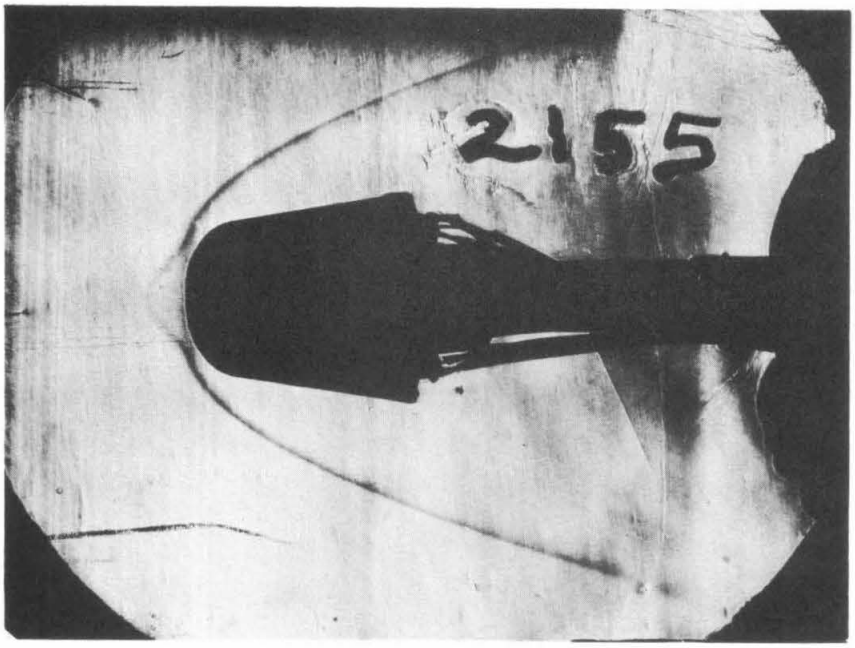

(c) HELIUM EJECTED STRAIGHT OUT, $C_{\dot{m}} = 0.002$; $a = 0^{\circ}$

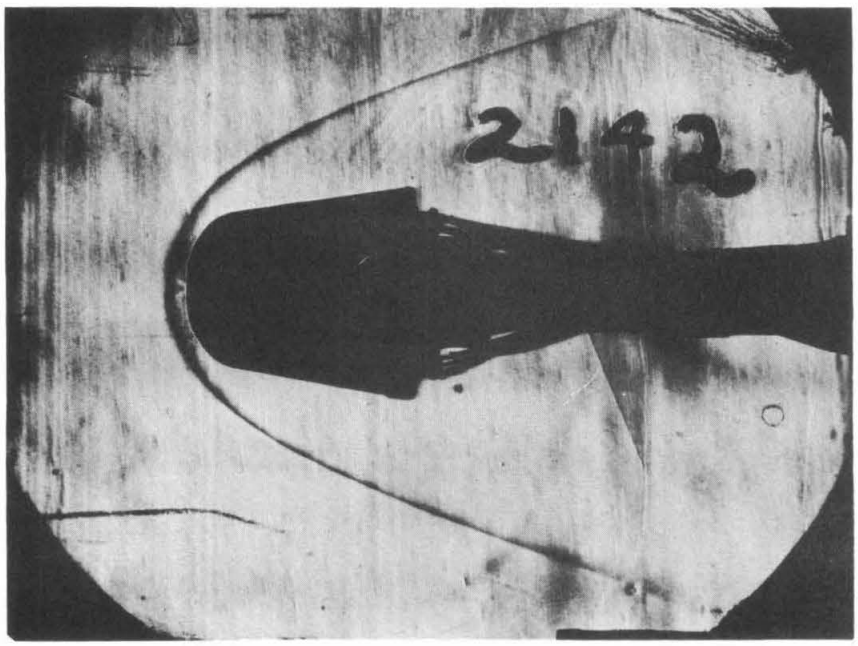

(d) HELIUM EJECTED WITH SWIRL, $C_{\dot{m}} = 0.002$; $a = 0^{\circ}$

FIG. 10 (continued) SCHLIEREN PHOTOGRAPHS

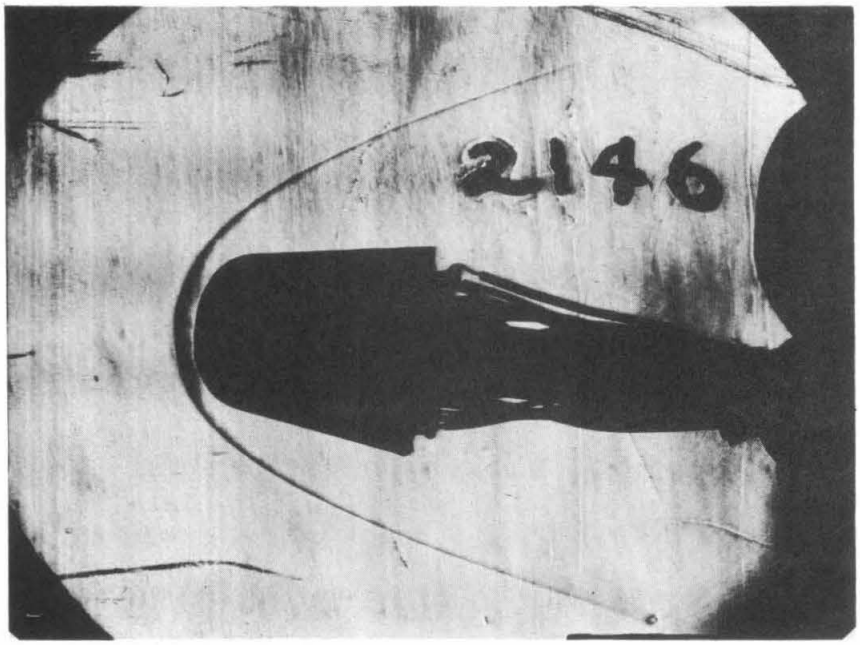

(e) NITROGEN EJECTED STRAIGHT OUT, $C_{\dot{m}} = 0.004$; $\alpha = 8^{\circ}$

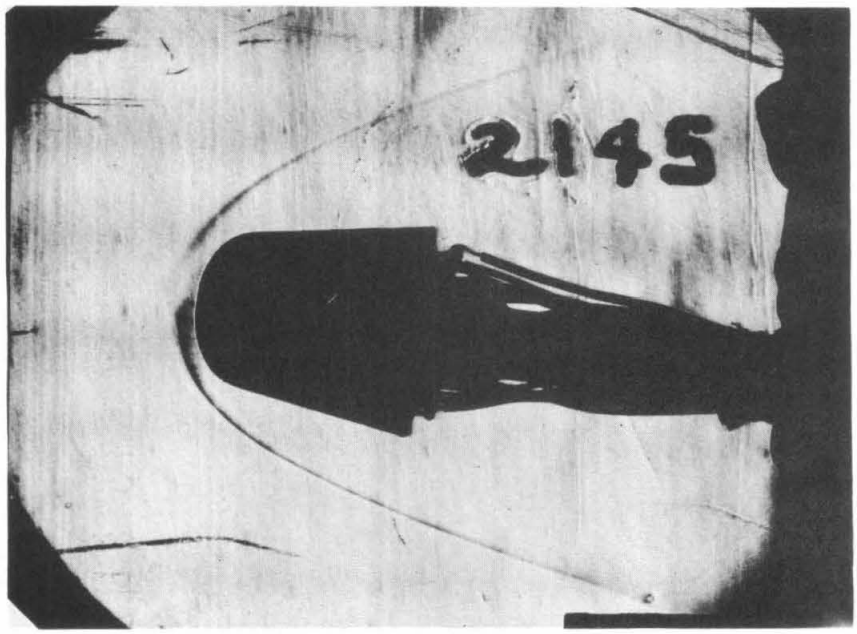

(f) NITROGEN EJECTED STRAIGHT OUT, $C_{\dot{m}} = 0.006$; $\alpha = 8^{\circ}$

FIG. 10 (continued) SCHLIEREN PHOTOGRAPHS

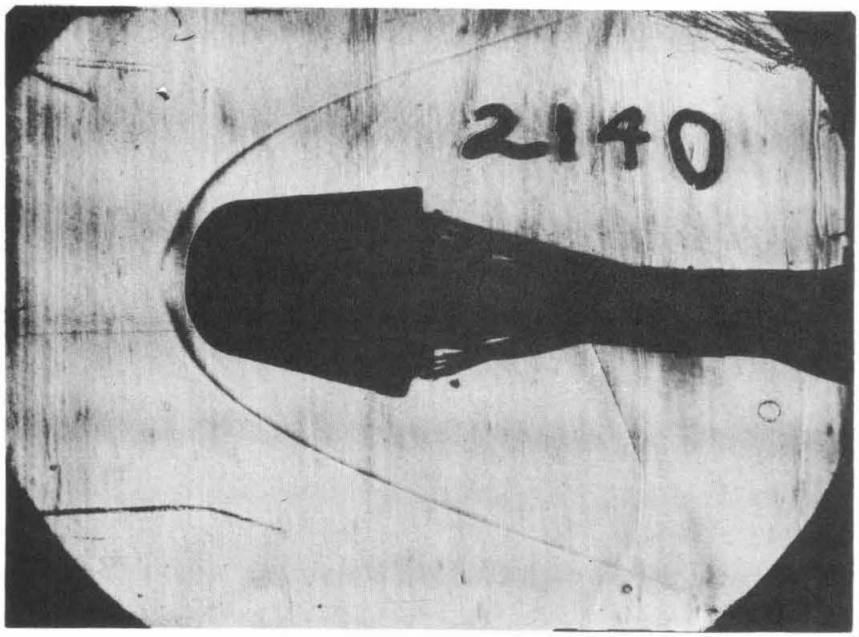

(g) HELIUM EJECTED WITH SWIRL, $C_{\dot{m}} = 0.002$; $\alpha = 4^{\circ}$

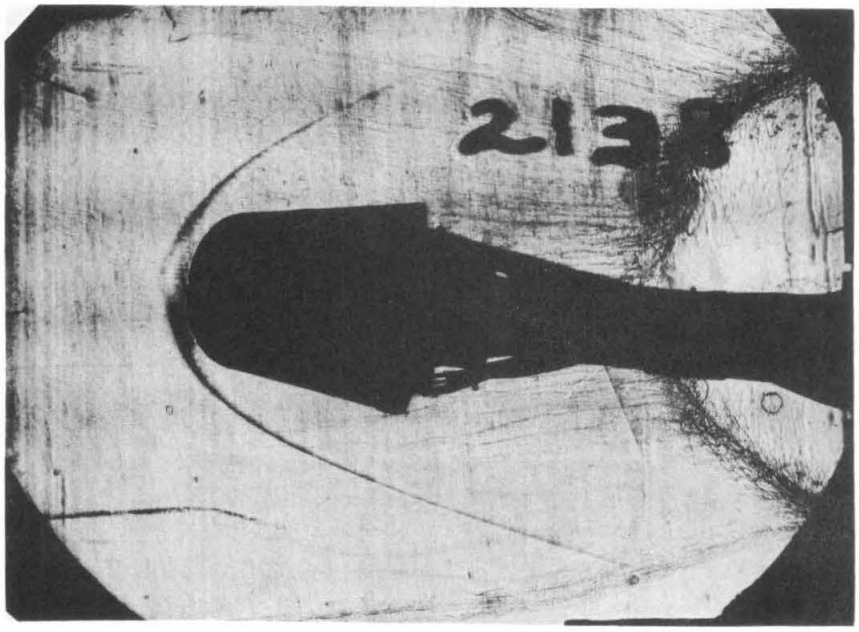

(h) HELIUM EJECTED WITH SWIRL, $C_{\dot{m}} = 0.002$; $\alpha = 8^{\circ}$

FIG. 10 (concluded) SCHLIEREN PHOTOGRAPHS

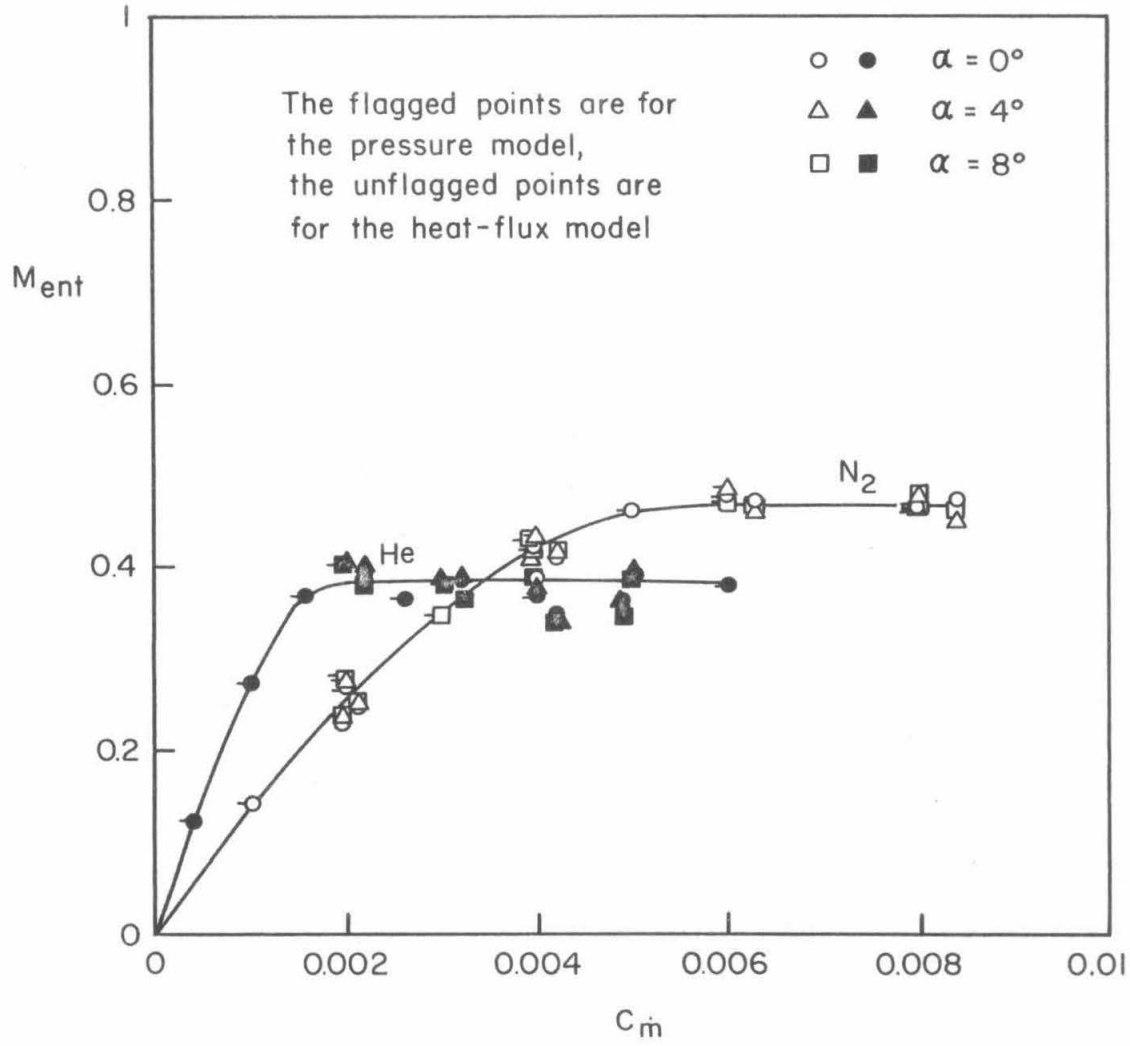

FIG. II MACH NUMBER OF COOLANT AT ENTRY TO THE FINAL SWIRL PIPE FOR EJECTION WITH SWIRL

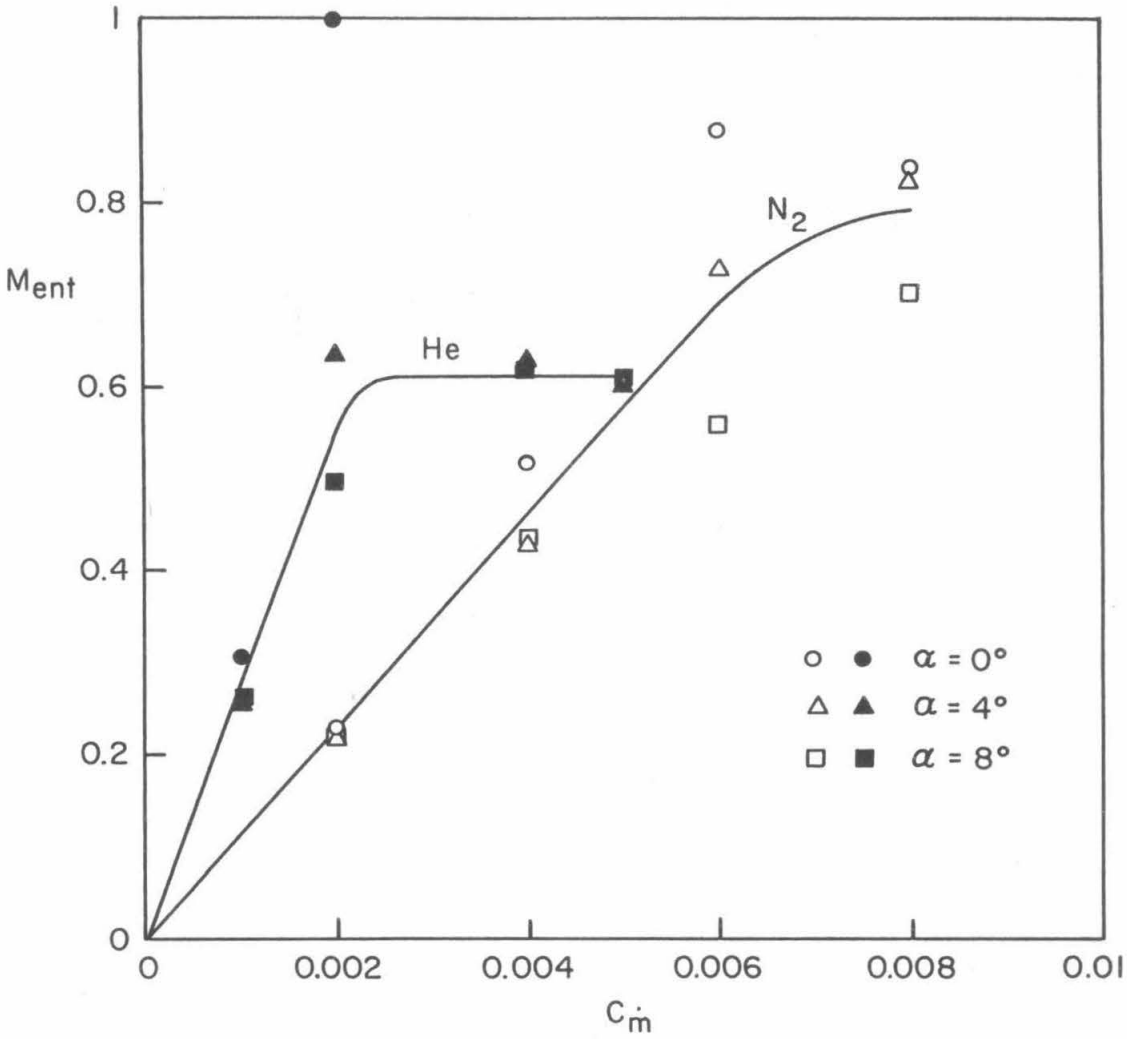

FIG. 12 MACH NUMBER OF COOLANT AT ENTRY TO THE FINAL EJECTION PIPE FOR STRAIGHT-OUT EJECTION

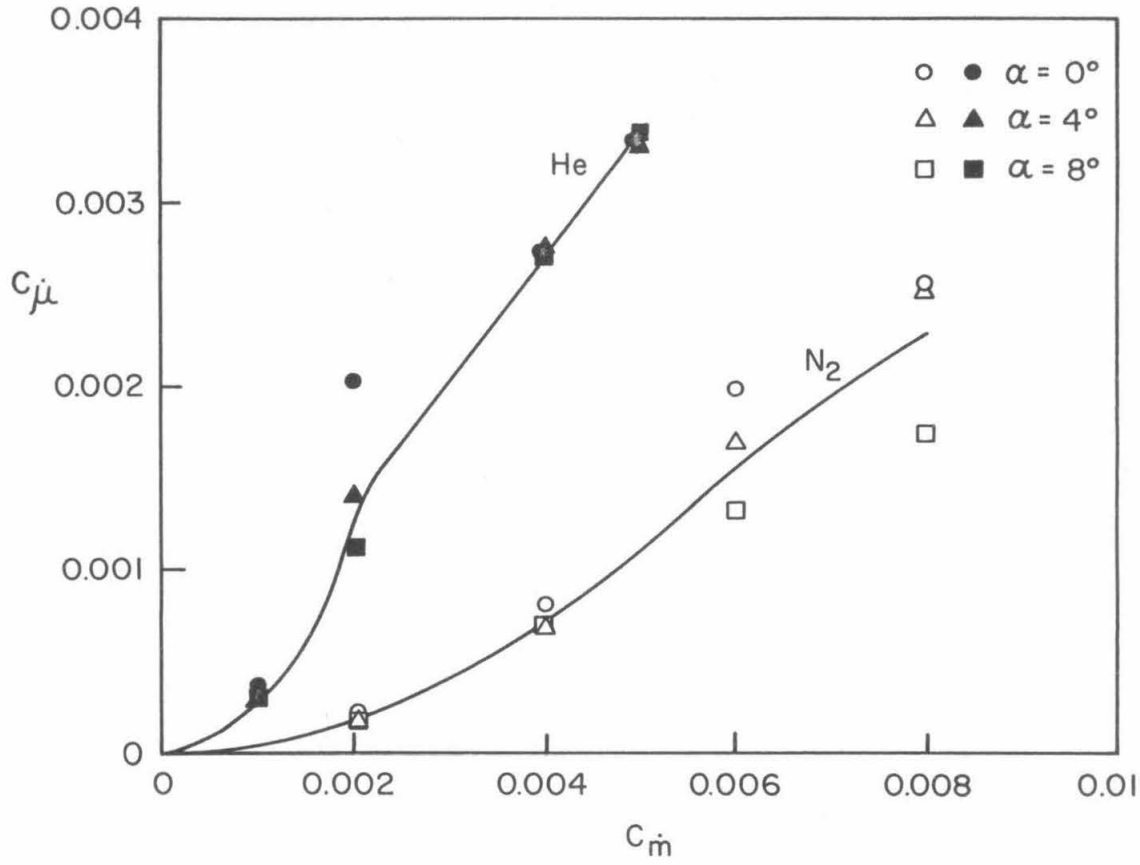

FIG.13 VARIATION OF COOLANT MOMENTUM FLOW WITH COOLANT MASS FLOW FOR STRAIGHT-OUT EJECTION

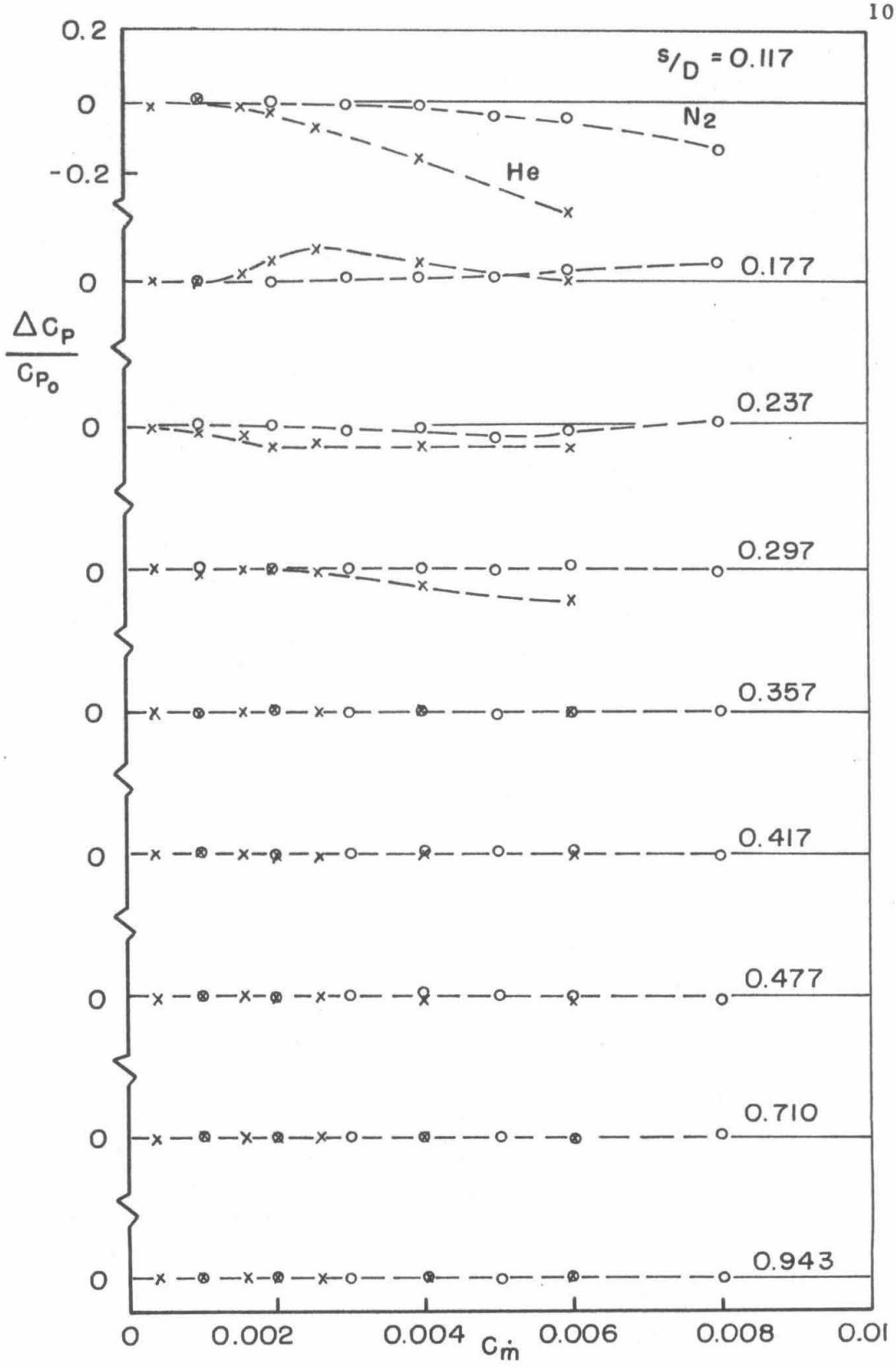

FIG. 14 EFFECT OF EJECTION WITH SWIRL ON PRESSURE, $\alpha = 0°$

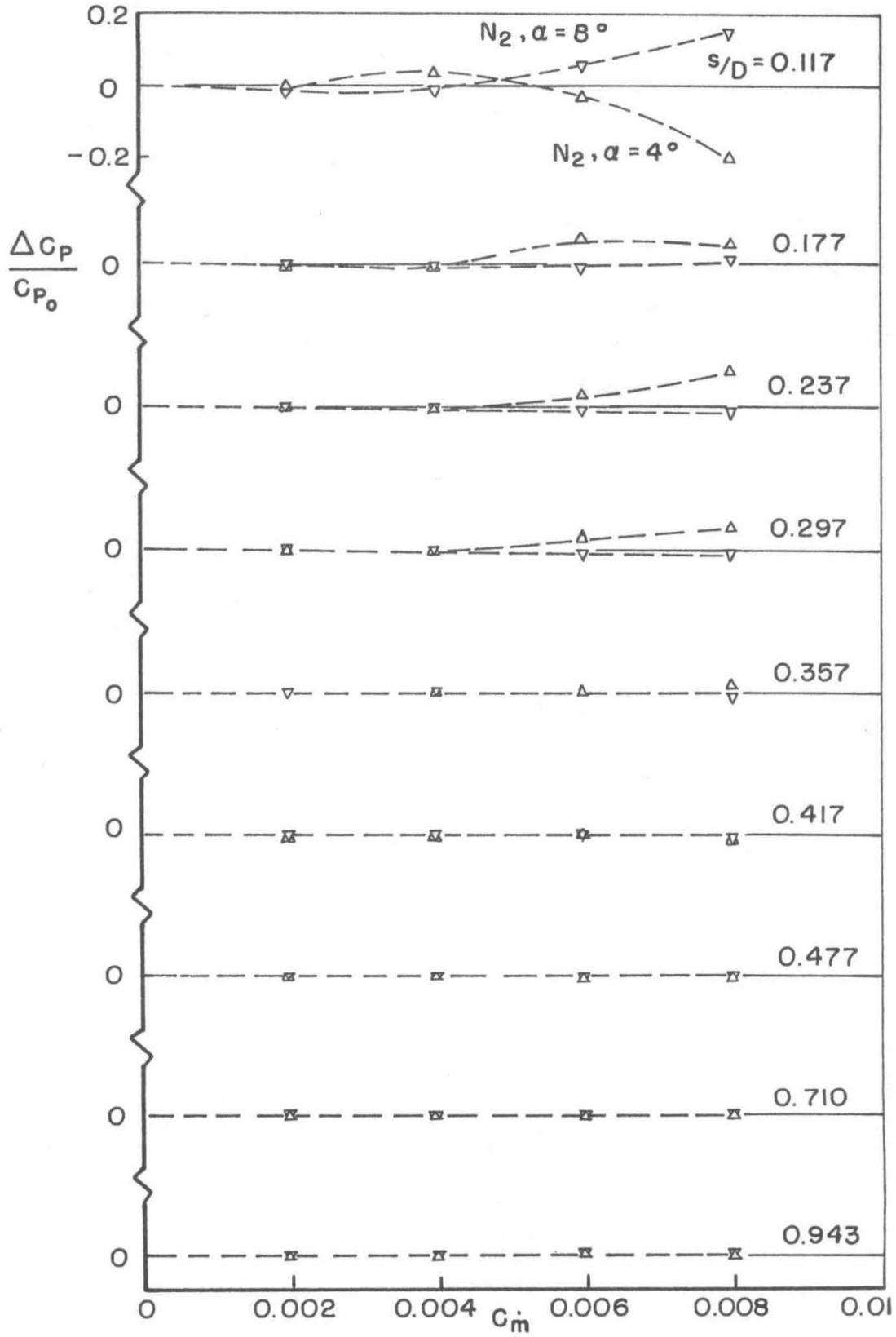

FIG. 15 EFFECT OF EJECTION WITH SWIRL ON PRESSURE
$\alpha = 4°$ & $8°$, WINDWARD MERIDIAN

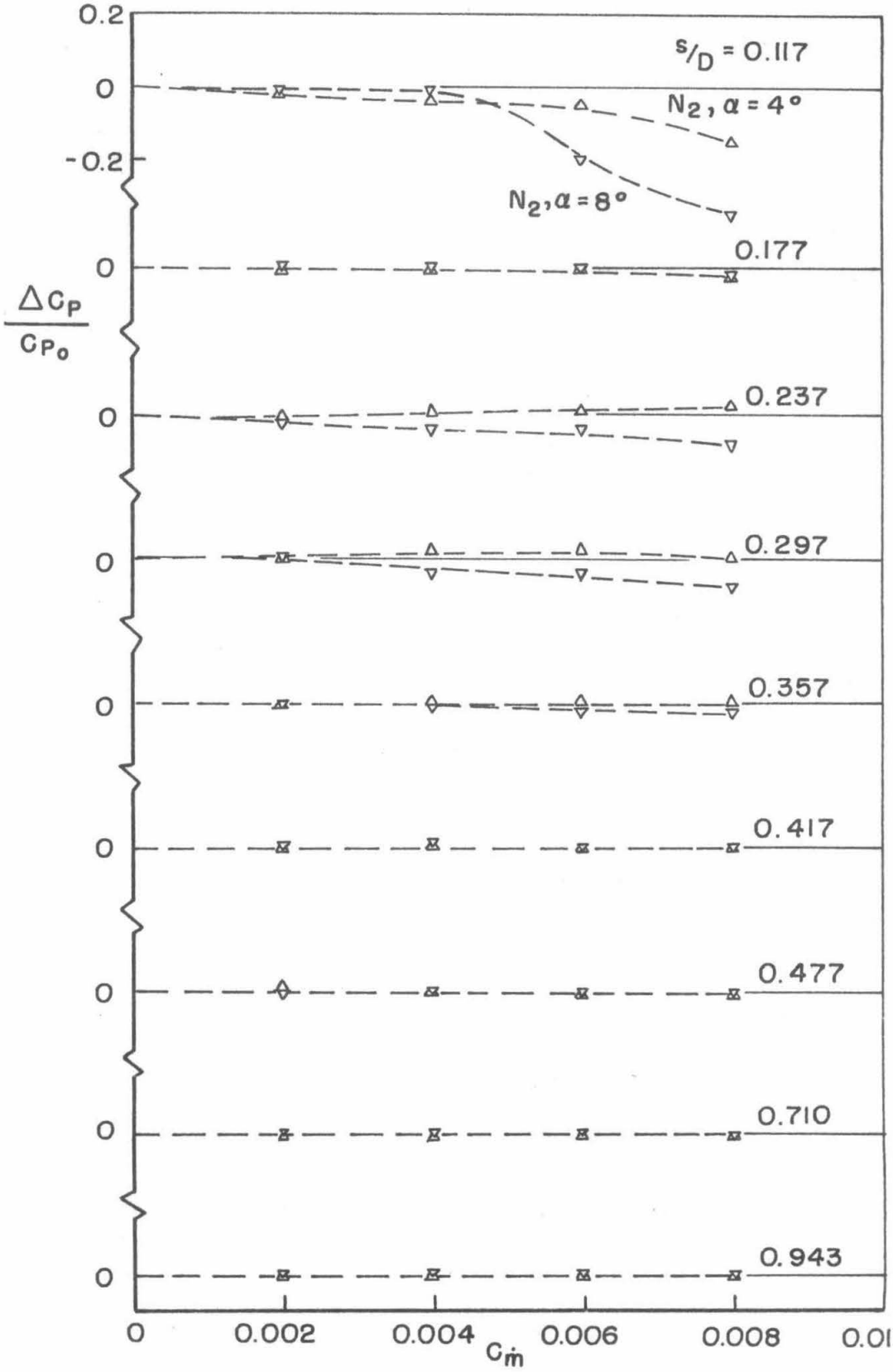

FIG. 16 EFFECT OF EJECTION WITH SWIRL ON PRESSURE
$\alpha = 4° \& 8°$, LEEWARD MERIDIAN

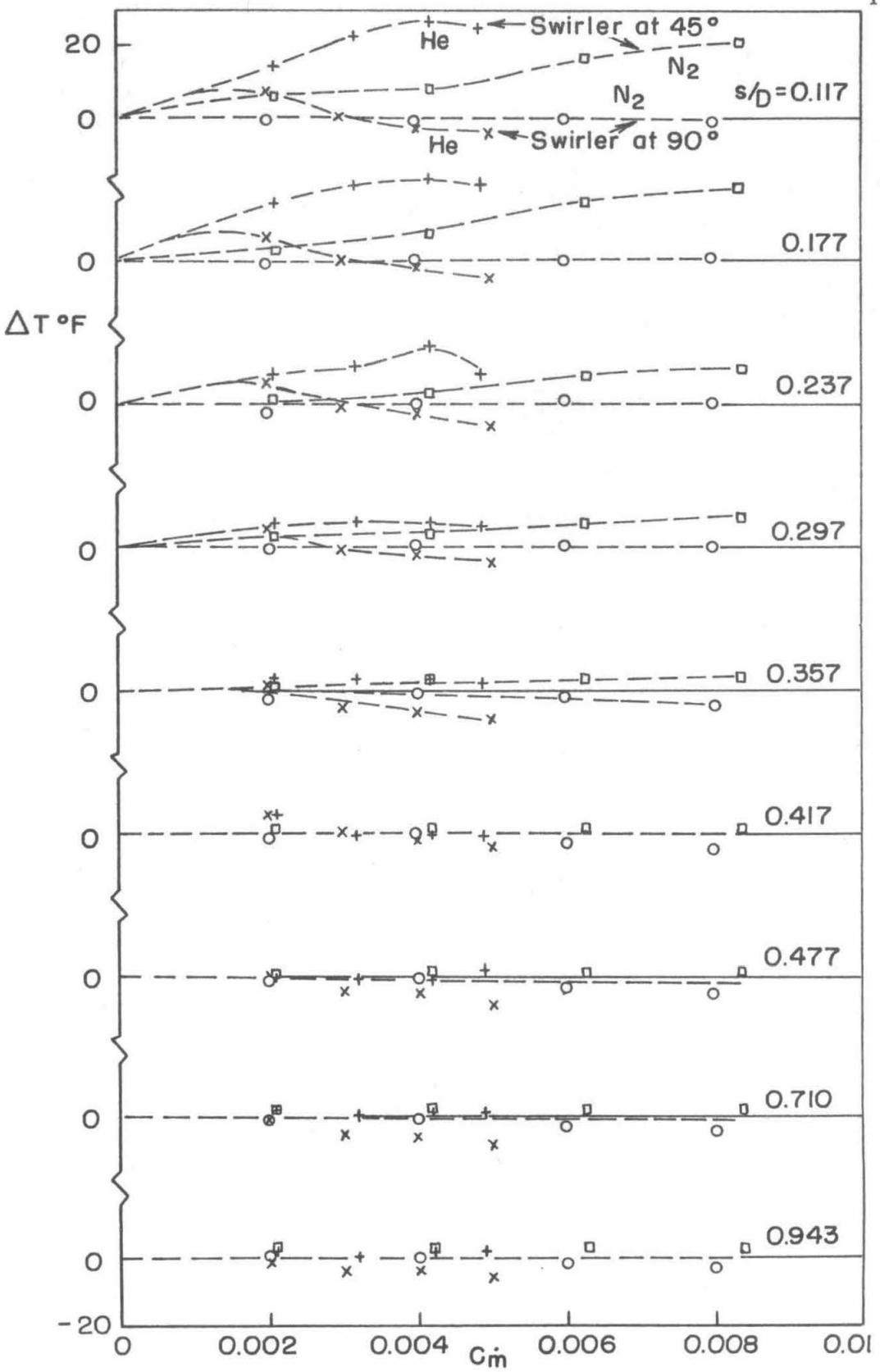

FIG. 17 EFFECT OF EJECTION WITH SWIRL ON TEMPERATURE, $\alpha = 0°$

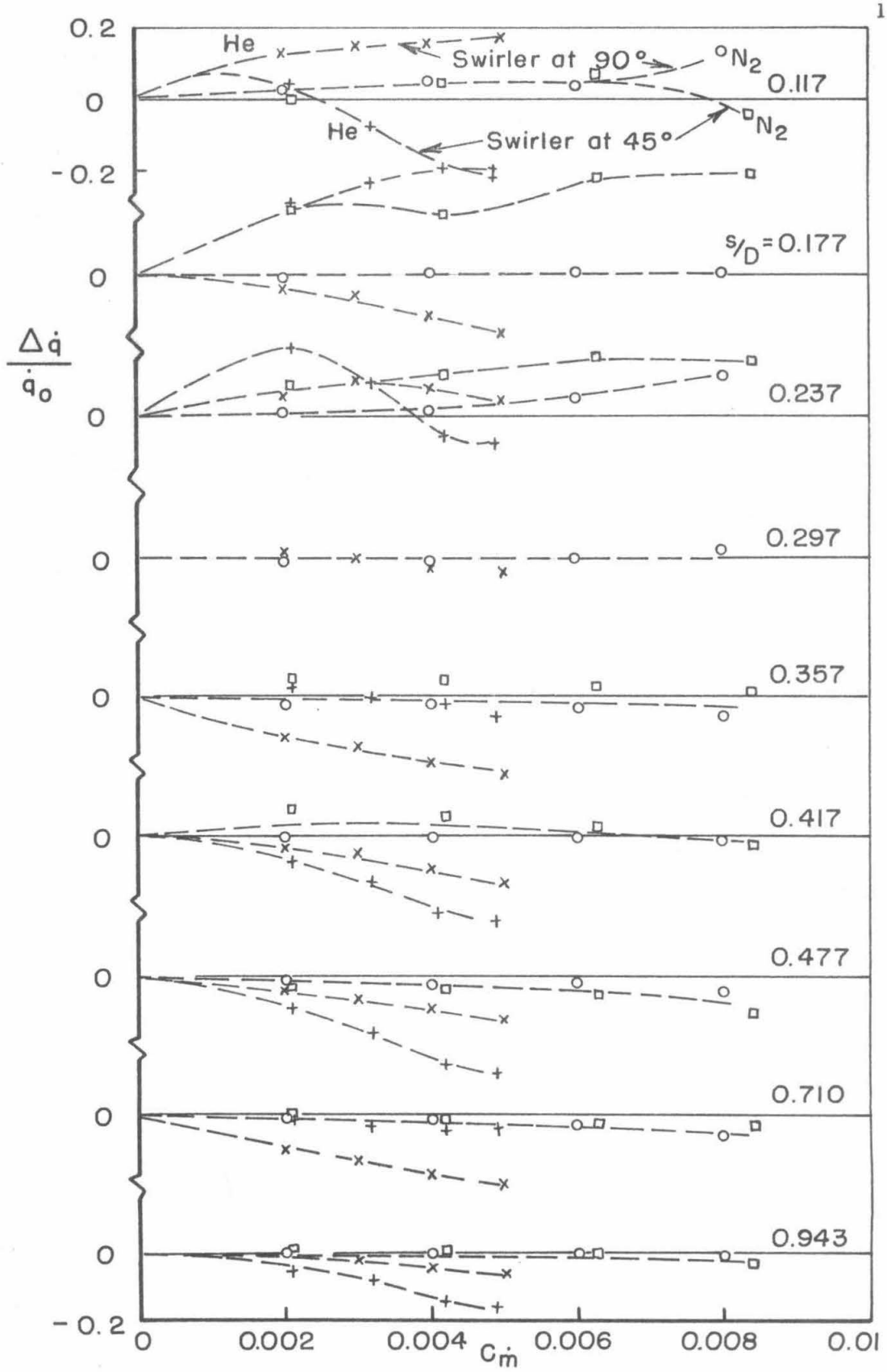

FIG. 18 EFFECT OF EJECTION WITH SWIRL ON HEAT FLUX, $\alpha = 0°$

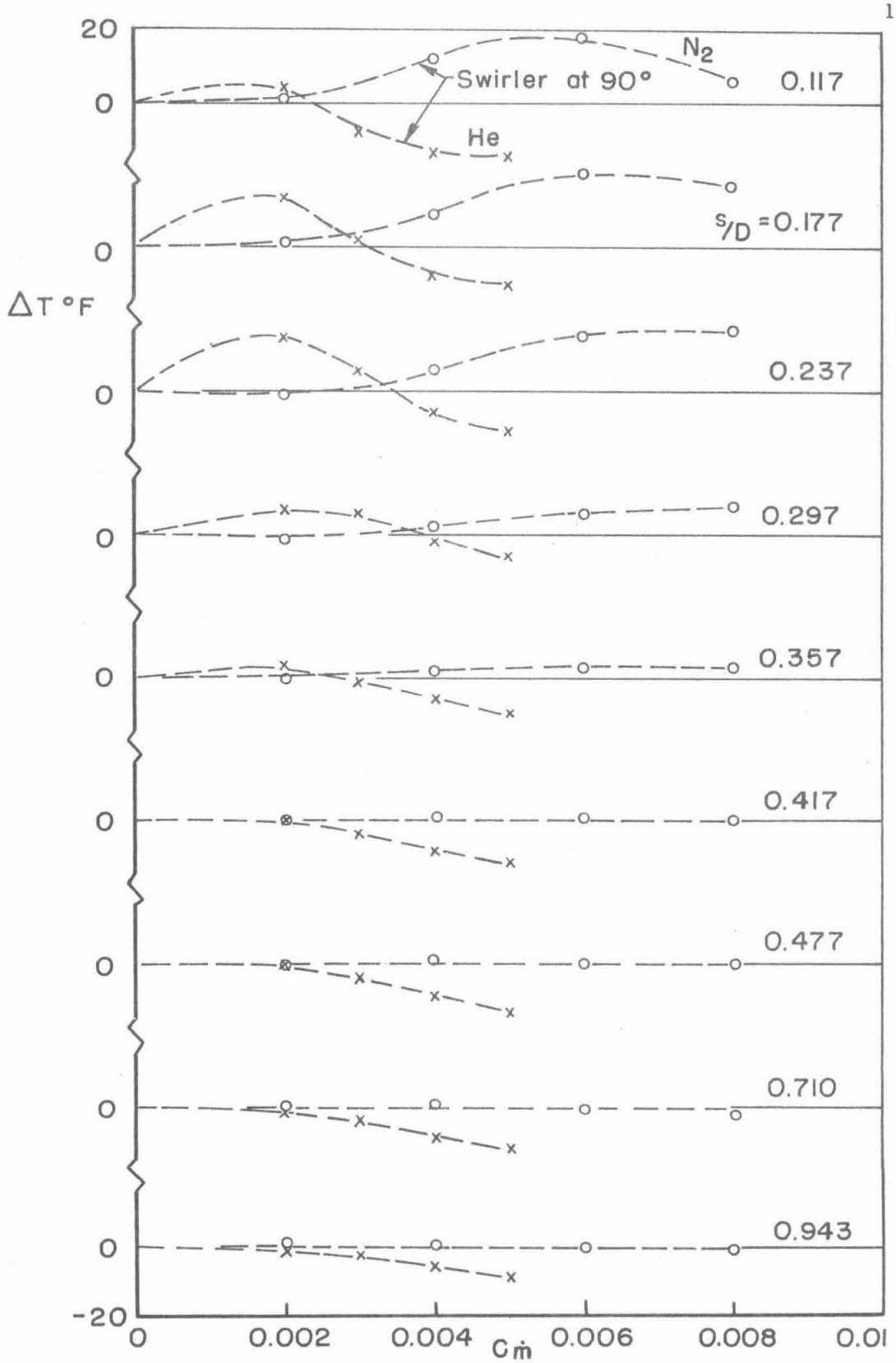

FIG.19 EFFECT OF EJECTION WITH SWIRL ON TEMPERATURE

$\alpha = 4°$, WINDWARD MERIDIAN

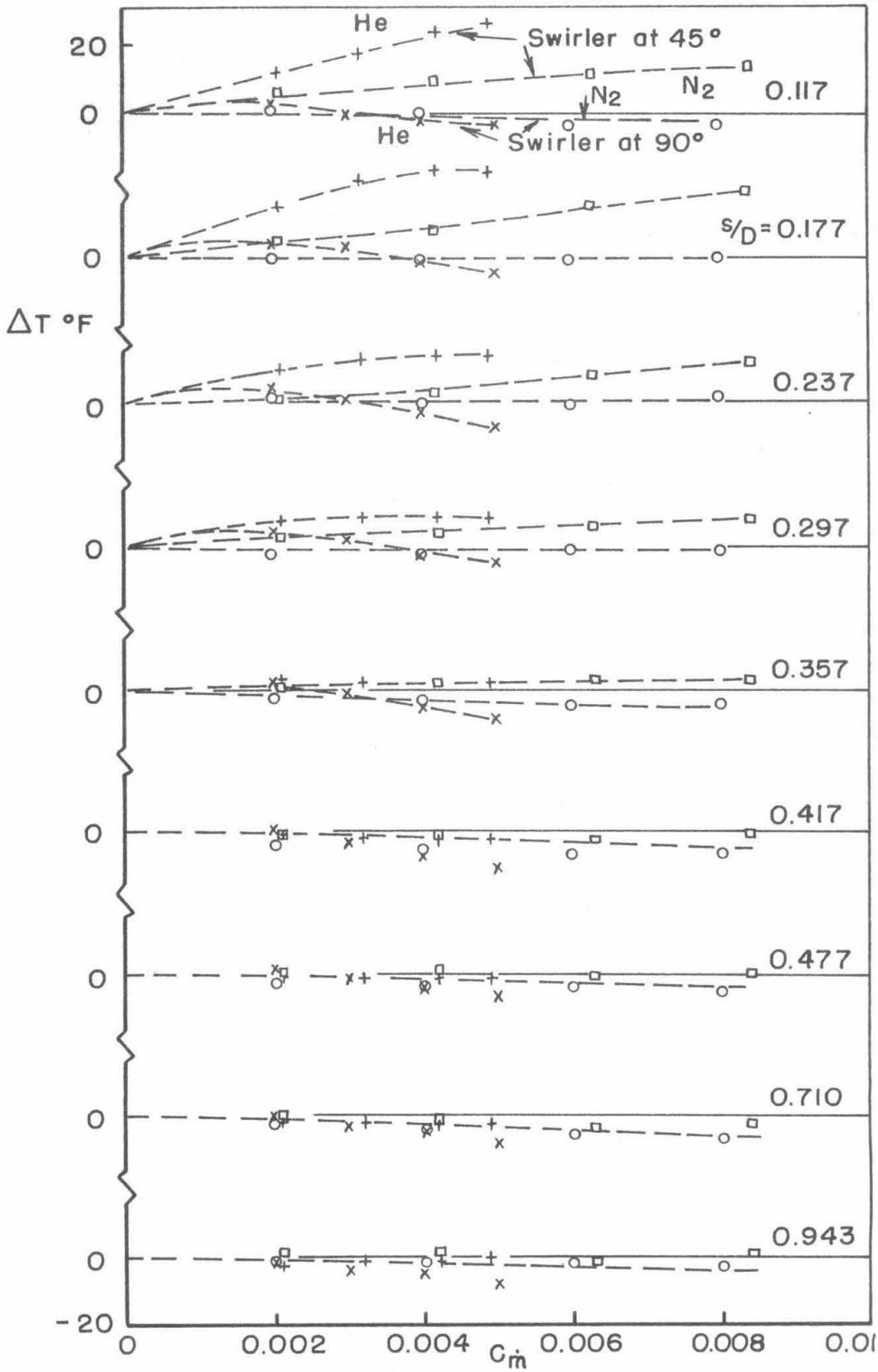

FIG.20 EFFECT OF EJECTION WITH SWIRL ON TEMPERATURE
$\alpha = 4°$, LEEWARD MERIDIAN

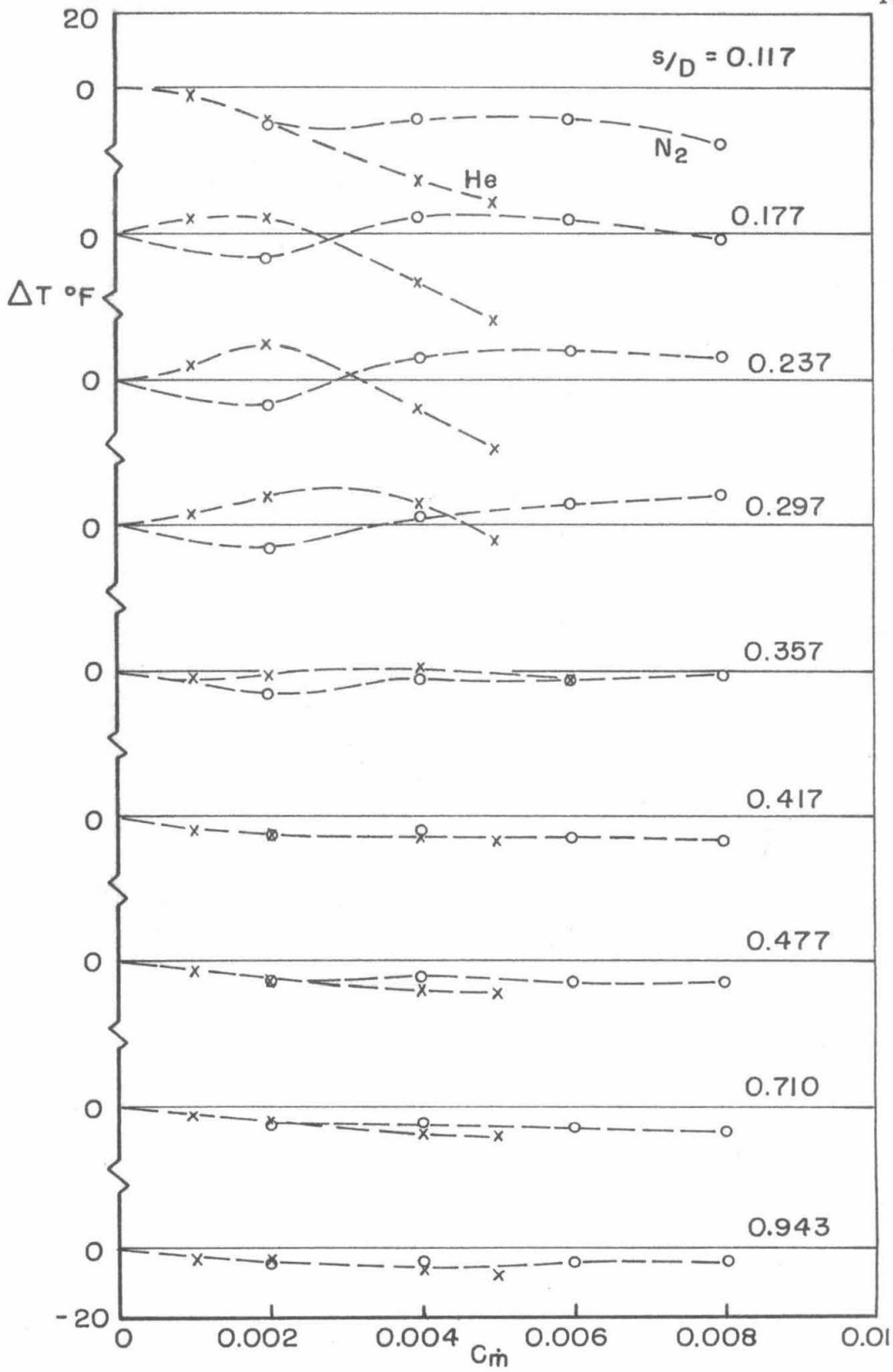

FIG. 21 EFFECT OF STRAIGHT-OUT EJECTION ON TEMPERATURE
$\alpha = 0°$

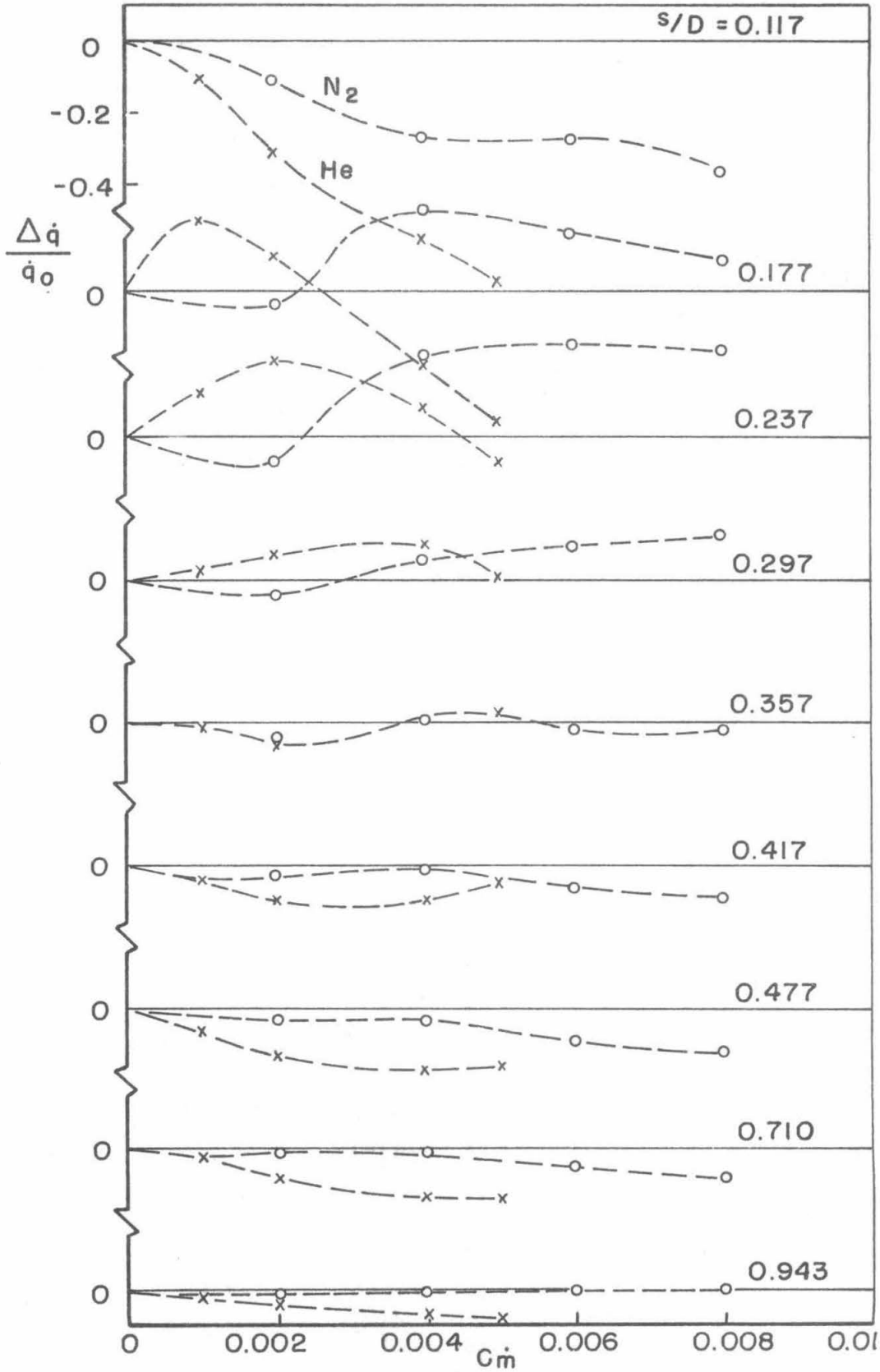

FIG.22 EFFECT OF STRAIGHT-OUT EJECTION ON HEAT FLUX
$\alpha = 0°$

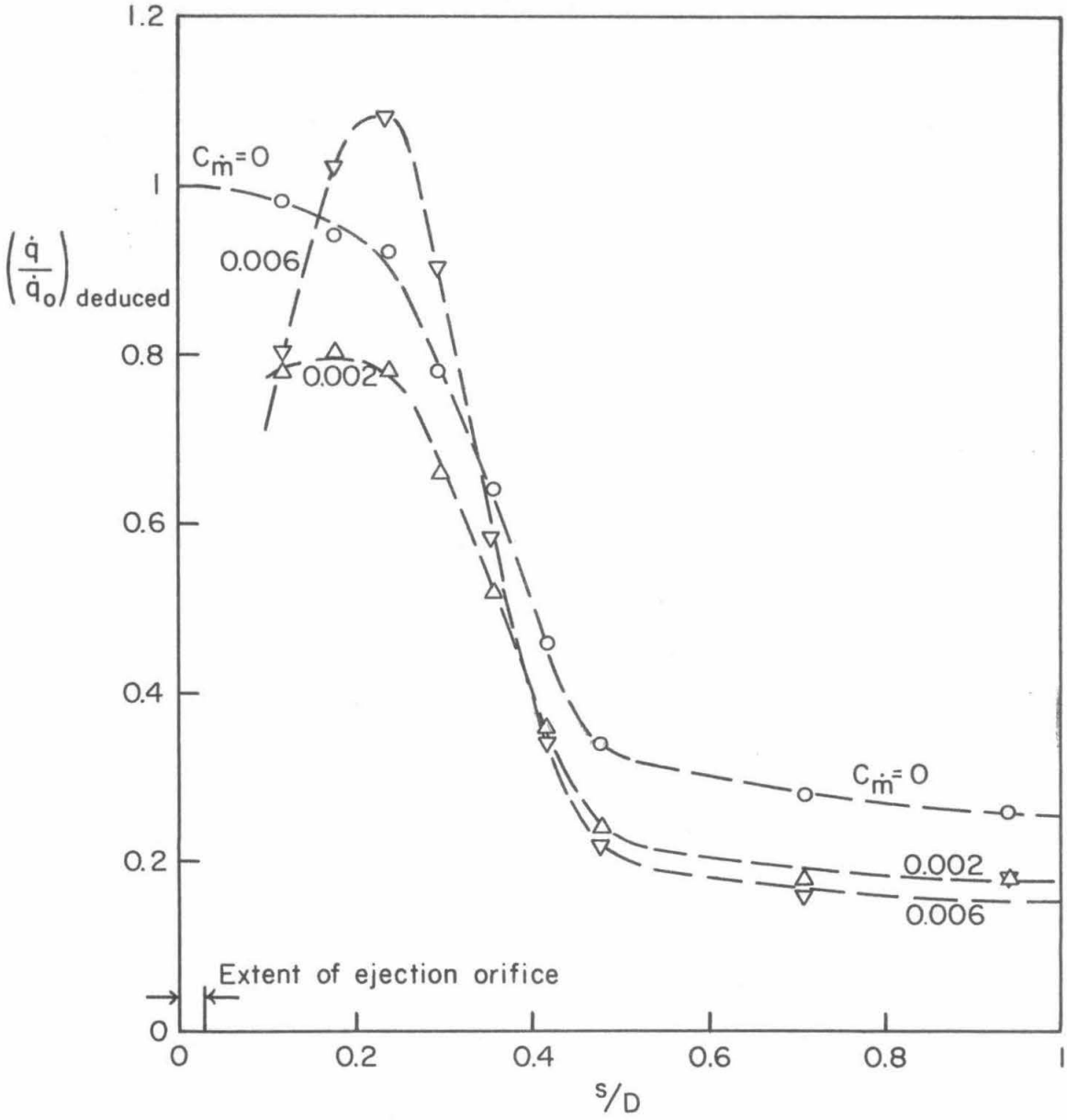

FIG. 23 DISTRIBUTIONS OF HEAT FLUX, DEDUCED FROM THE TEMPERATURE MEASUREMENTS, FOR THE STRAIGHT-OUT EJECTION OF NITROGEN

$\alpha = 0°$

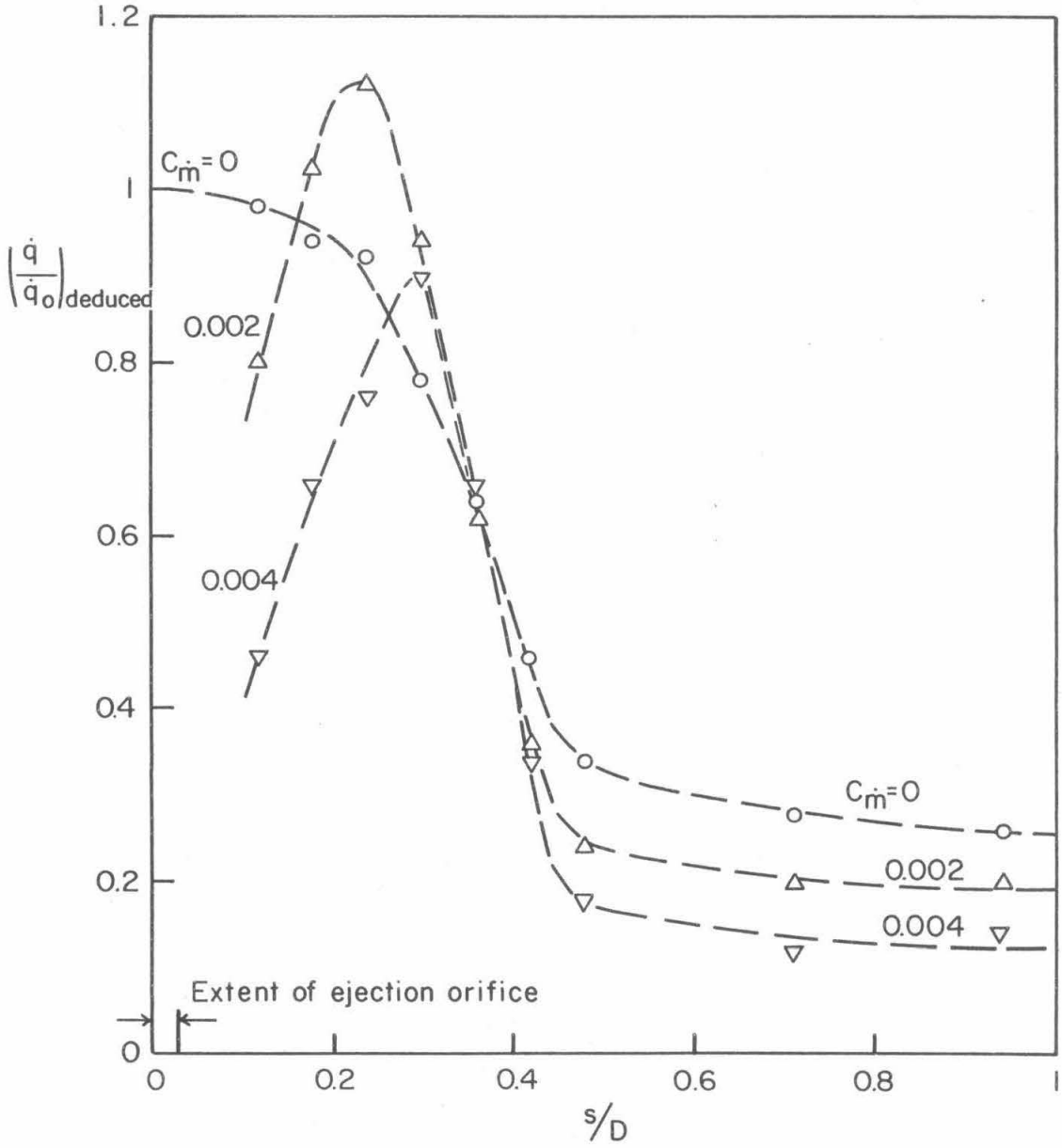

FIG. 24 DISTRIBUTIONS OF HEAT FLUX, DEDUCED FROM THE TEMPERATURE MEASUREMENTS, FOR THE STRAIGHT-OUT EJECTION OF HELIUM

$\alpha = 0°$

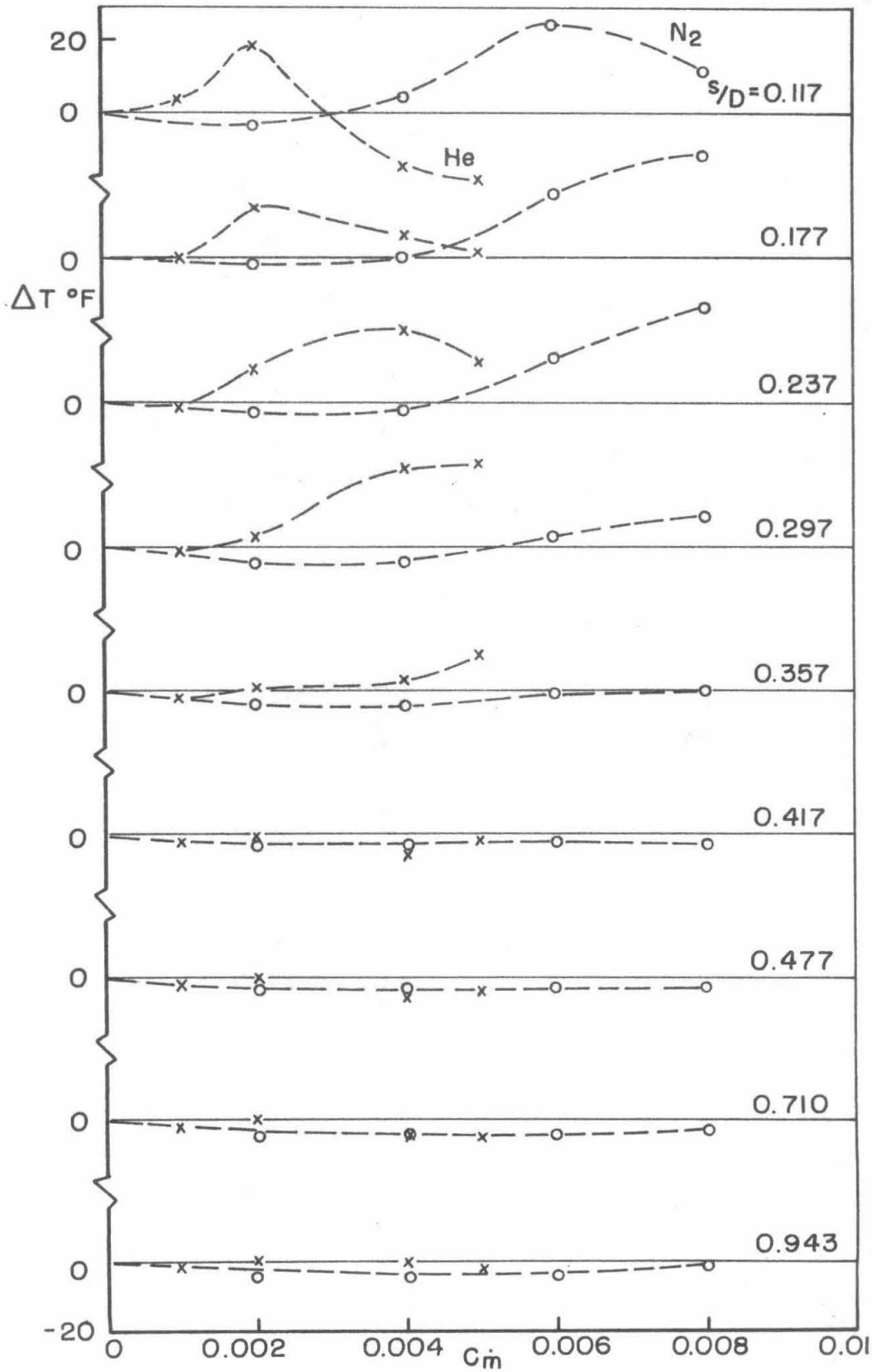

FIG. 25 EFFECT OF STRAIGHT-OUT EJECTION ON TEMPERATURE
$\alpha = 4°$, WINDWARD MERIDIAN

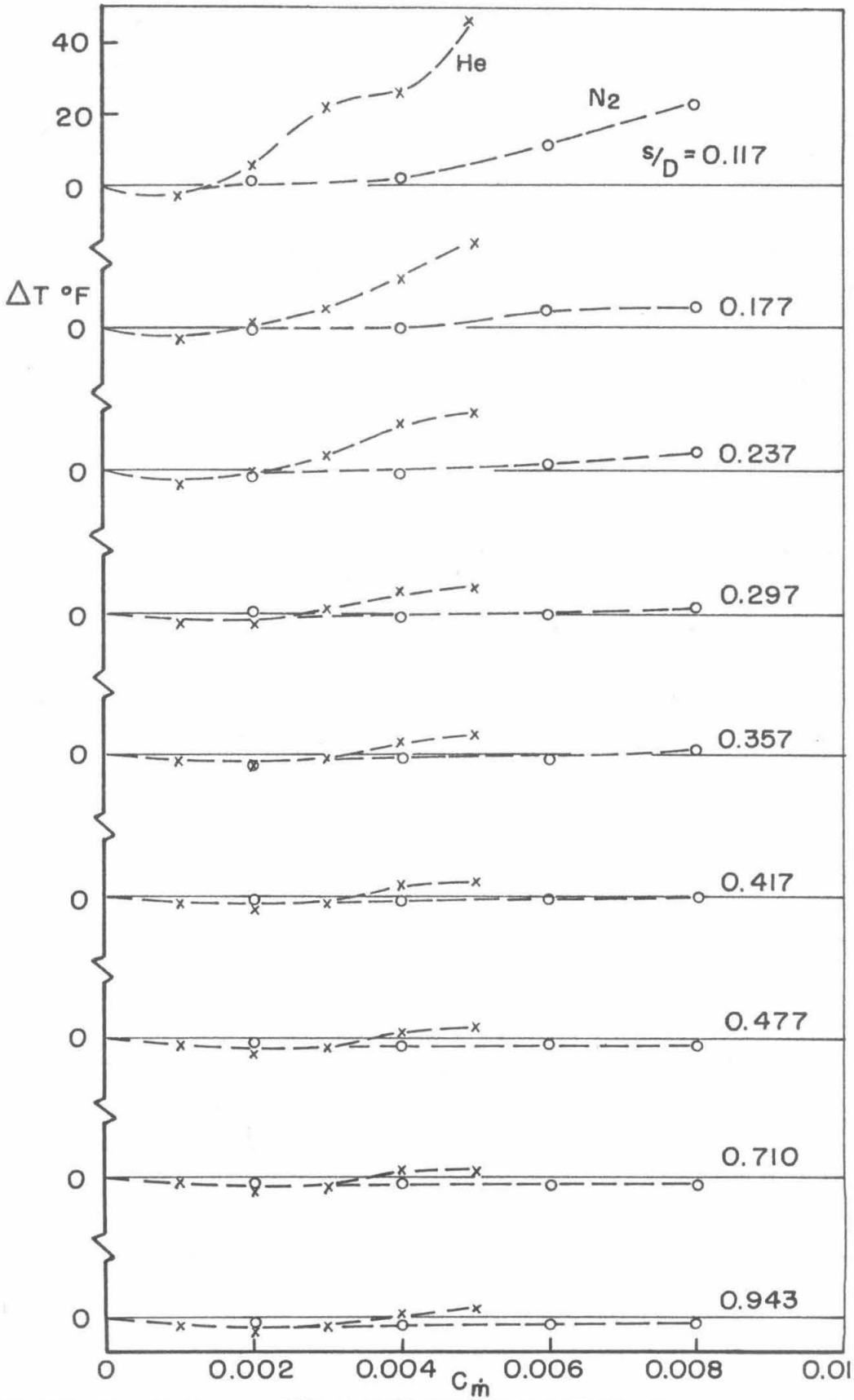

FIG. 26 EFFECT OF STRAIGHT-OUT EJECTION ON TEMPERATURE
$\alpha = 8°$, WINDWARD MERIDIAN

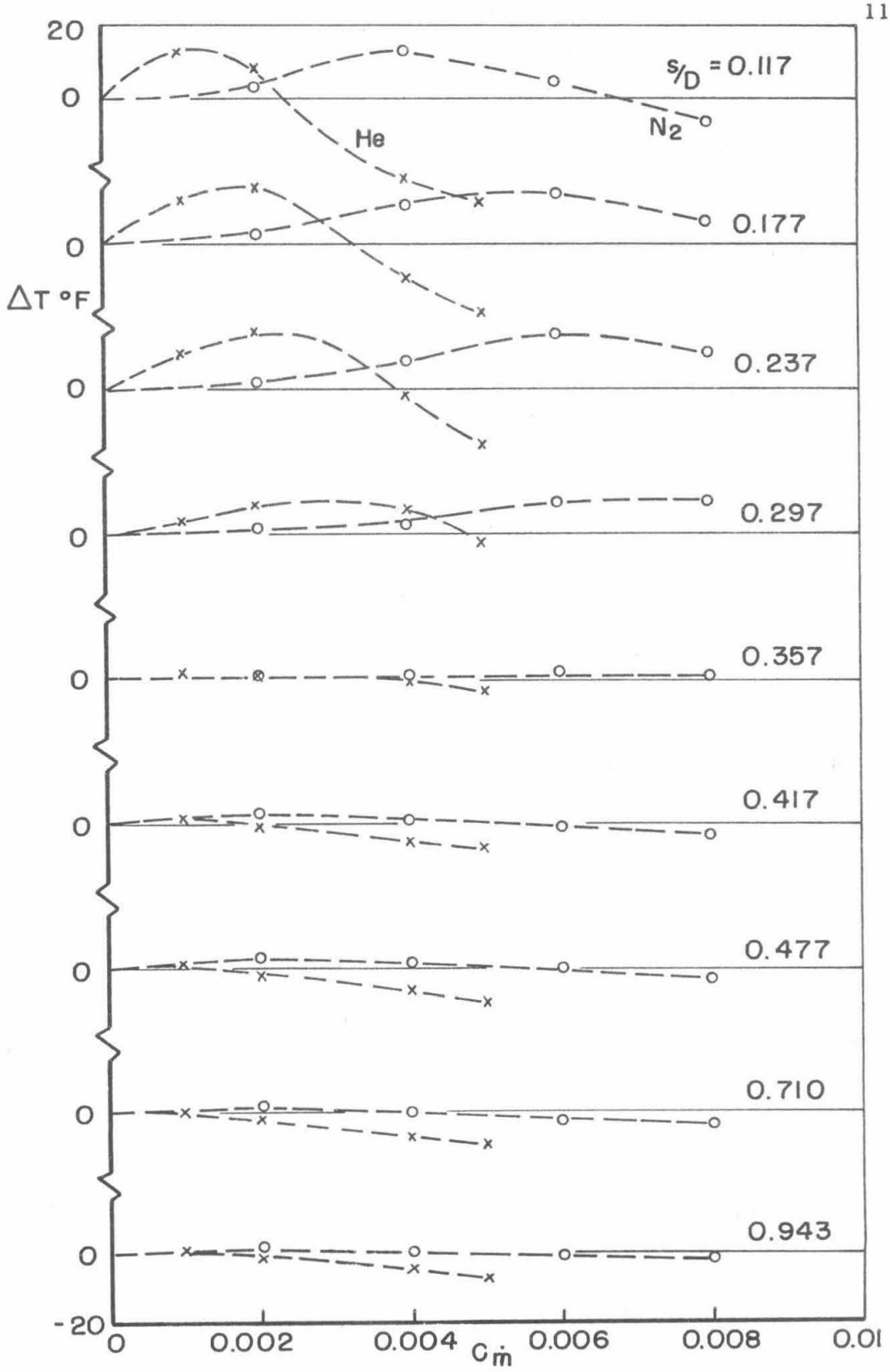

FIG. 27 EFFECT OF STRAIGHT-OUT EJECTION ON TEMPERATURE
$\alpha = 4°$, SIDE MERIDIAN

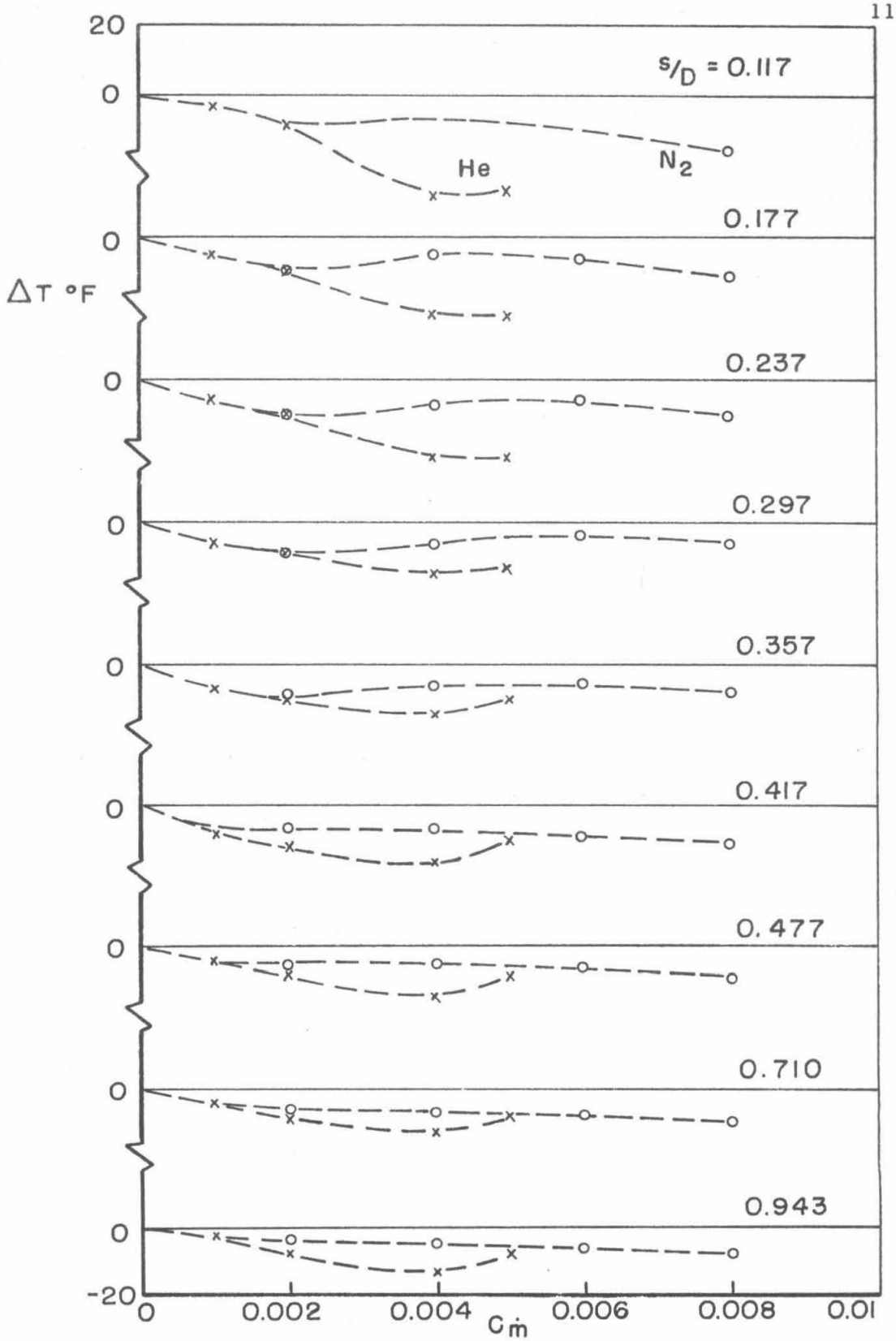

FIG. 28 EFFECT OF STRAIGHT-OUT EJECTION ON TEMPERATURE
$\alpha = 4°$, LEEWARD MERIDIAN

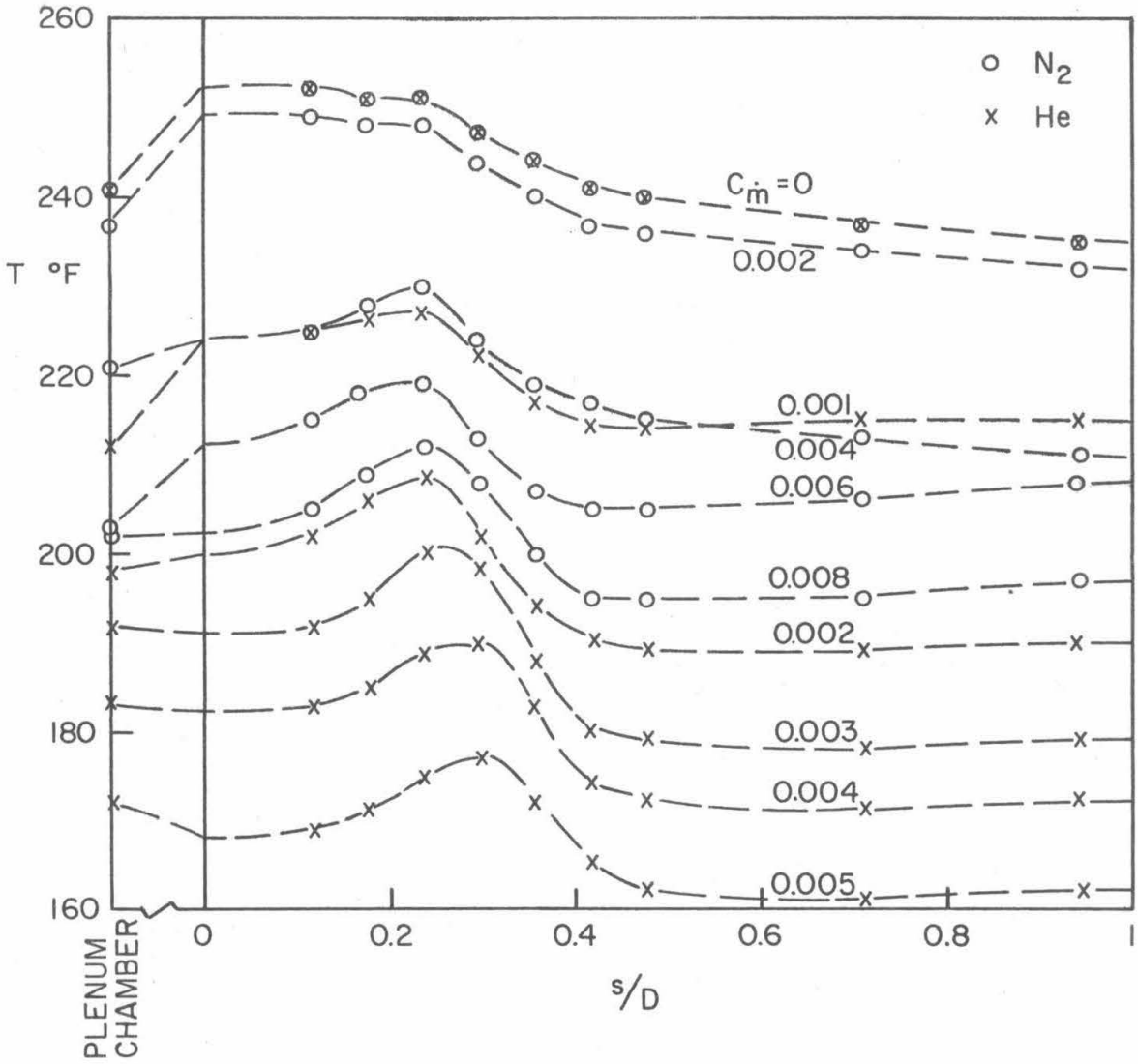

FIG. 29 EFFECT OF STRAIGHT-OUT EJECTION ON TEMPERATURE WITH NO COOLANT WATER FLOW

$\alpha = 0°$

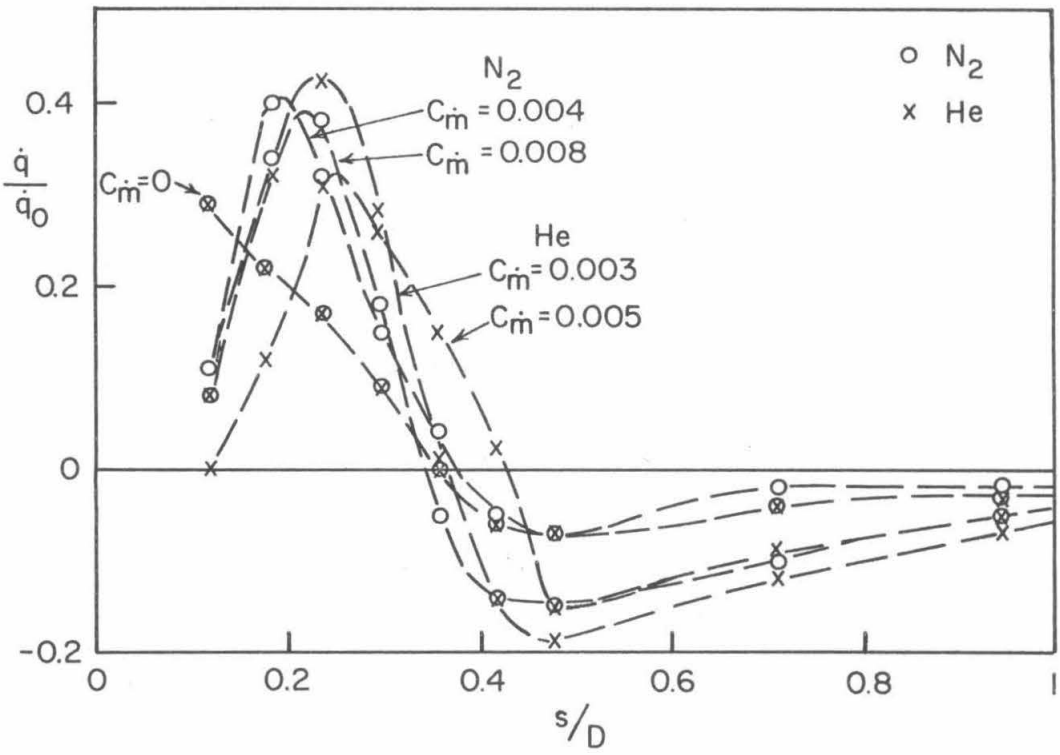

FIG. 30 EFFECT OF STRAIGHT-OUT EJECTION ON HEAT FLUX WITH NO COOLANT WATER FLOW

$\alpha = 0°$

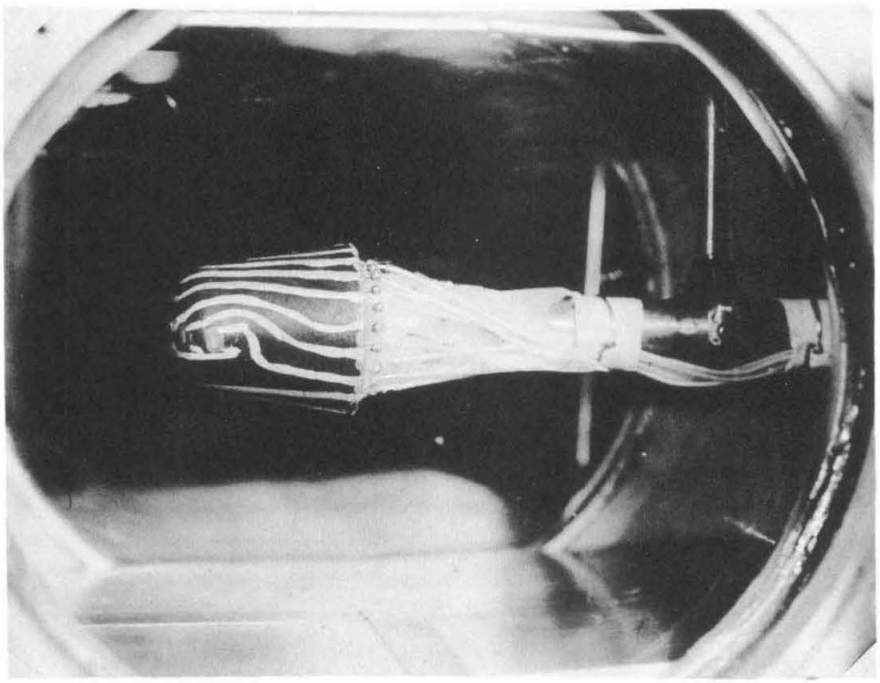

FIG. 31 PHOTOGRAPH OF THE HEAT-FLUX MODEL
INSTALLED IN THE TUNNEL,
AND SHOWING ICE FORMATION FOLLOWING A WATER LEAK
(See Section 6.7)

1 November 1958

GUGGENHEIM AERONAUTICAL LABORATORY
CALIFORNIA INSTITUTE OF TECHNOLOGY

HYPERSONIC RESEARCH PROJECT
Contract No. DA-04-495-Ord-19

DISTRIBUTION LIST

U. S. Government Agencies

Los Angeles Ordnance District
55 South Grand Avenue
Pasadena 2, California
Attention: Mr. E. L. Stone
2 copies

Los Angeles Ordnance District
55 South Grand Avenue
Pasadena 2, California
Attention: ORDEV-00-
Mr. Typaldos

Chief of Ordnance
Department of the Army
ORDTB - Ballistic Section
The Pentagon
Washington 25, D. C.
Attention: Mr. G. Stetson

Chief of Ordnance
Department of the Army
Washington 25, D. C.
Attention: ORDTB
For Transmittal To
Department of Commerce
Office of Technical Information

Office of Ordnance Research
Box CM, Duke Station
Durham, North Carolina
10 copies

Ordnance Aerophysics Laboratory
Daingerfield, Texas
Attention: Mr. R. J. Valluz

Commanding Officer
Diamond Ordnance Fuze Laboratories
Washington 25, D. C.
Attention: ORDTL 06.33

Commanding General
Army Ballistics Missile Agency
Huntsville, Alabama
Attention: ORDAB-1P
2 copies

Commanding General
Army Ballistics Missile Agency
Huntsville, Alabama
Attention: ORDAB-DA
Mr. T. G. Reed
3 copies

Commanding General
Redstone Arsenal
Huntsville, Alabama
Attention: Technical Library

Commanding General
Redstone Arsenal
Huntsville, Alabama
Attention: Dr. E. Geissler

Chief of Staff
United States Army
The Pentagon
Washington 25, D. C.
Attention: Director/Research

Exterior Ballistic Laboratories
Aberdeen Proving Ground
Maryland
Attention: Mr. C. L. Poor

Ballistic Research Laboratories
Aberdeen Proving Ground
Maryland
Attention: Dr. Joseph Sternberg

Commanding General
White Sands Proving Ground
Las Cruces, New Mexico

Directorate of Advanced Studies
Air Force Office of Scientific Research
P. O. Box 2035-D
Pasadena 2, California
Attention: Dr. M. Alperin

Commander
Air Force
Office of Scientific Research
Washington 25, D. C.
Attention: RDTRRF

Mechanics Division
Air Force
Office of Scientific Research
Washington 25, D. C.

Commander
Hq., Air Research and
Development Command
Bolling Air Force Base
Washington, D. C.
Attention: RDS-TIS-3

Air Force Armament Center
Air Research and Development
Command
Eglin Air Force Base
Florida
Attention: Technical Library

Commander
Wright Air Development Center
Wright-Patterson Air Force Base
Ohio
Attention: WCLSR

Commander
Wright Air Development Center
Wright-Patterson Air Force Base
Ohio
Attention: WCLSW

Commander
Wright Air Development Center
Wright-Patterson Air Force Base
Ohio
Attention: WCOSI-9-5 (Distribution)

Commander
Wright Air Development Center
Wright-Patterson Air Force Base
Ohio
Attention: WCLSW, Mr. P. Antonatos

Commander
Wright Air Development Center
Wright-Patterson Air Force Base
Ohio
Attention: Dr. H. K. Doetsch

Commander
Wright Air Development Center
Wright-Patterson Air Force Base
Ohio
Attention: Dr. G. Guderley

Commander
Wright Air Development Center
Wright-Patterson Air Force Base
Ohio
Attention: WCLJD, Lt. R. D. Stewart

Director of Research and Development
DCS/D
Headquarters
USAF
Washington 25, D. C.
Attention: AFDRD-RE

Commander
Western Development Division
P. O. Box 262
Inglewood, California

Commander
Western Development Division
5760 Arbor Vitae Street
Los Angeles, California
Attention: Maj. Gen. B. A. Schriever

Commander
Arnold Engineering Development Center
Tullahoma, Tennessee
Attention: AEORL

Commander
Arnold Engineering Development Center
Tullahoma, Tennessee
Attention: Col. F. H. Richardson

Air University Library
Maxwell Air Force Base
Alabama

Hollomann Air Force Base
Alamogordo, New Mexico
Attention: Dr. G. Eber

U. S. Naval Ordnance Laboratory
White Oak
Silver Spring, Maryland
Attention: Dr. H. Kurzweg

U. S. Naval Ordnance Laboratory
White Oak
Silver Spring 19, Maryland
Attention: Dr. R. K. Lobb

U. S. Naval Ordnance Laboratory
White Oak
Silver Spring 19, Maryland
Attention: Dr. Z. I. Slawsky

U. S. Naval Ordnance Laboratory
White Oak
Silver Spring 19, Maryland
Attention: Dr. R. Wilson

U. S. Naval Ordnance Test Station
China Lake
Inyokern, California
Attention: Mr. Howard R. Kelly, Head
Aerodynamics Branch,
Code 5032

Navy Department
Bureau of Ordnance
Technical Library
Washington 25, D. C.
Attention: Ad-3

Director
Naval Research Laboratory
Washington 25, D. C.

Office of Naval Research
Department of the Navy
Washington 25, D. C.
Attention: Mr. M. Tulin

Commander
U. S. Naval Proving Ground
Dahlgren, Virginia

Bureau of Aeronautics
Department of the Navy
Room 2 w 75
Washington 25, D. C.
Attention: Mr. F. A. Louden

Commander
Armed Services Technical
Information Agency
Attention: TIPDR
Arlington Hall Station
Arlington 12, Virginia
10 copies

National Bureau of Standards
Department of Commerce
Washington 25, D. C.
Attention: Dr. G. B. Schubauer

National Advisory Committee
for Aeronautics
1512 H Street, N. W.
Washington 25, D. C.
Attention: Dr. H. L. Dryden, Director
5 copies

National Advisory Committee
for Aeronautics
Ames Aeronautical Laboratory
Moffett Field, California
Attention: Mr. H. Julian Allen

National Advisory Committee
for Aeronautics
Ames Aeronautical Laboratory
Moffett Field, California
Attention: Dr. D. Chapman

National Advisory Committee
for Aeronautics
Ames Aeronautical Laboratory
Moffett Field, California
Attention: Dr. A. C. Charters

National Advisory Committee
for Aeronautics
Ames Aeronautical Laboratory
Moffett Field, California
Attention: Mr. A. J. Eggers

National Advisory Committee
for Aeronautics
Ames Aeronautical Laboratory
Moffett Field, California
Attention: Dr. M. K. Rubesin

National Advisory Committee
for Aeronautics
Ames Aeronautical Laboratory
Moffett Field, California
Attention: Mr. J. R. Stalder

National Advisory Committee
for Aeronautics
Langley Aeronautical Laboratory
Langley Field, Virginia
Attention: Mr. M. Bertram

National Advisory Committee
for Aeronautics
Langley Aeronautical Laboratory
Langley Field, Virginia
Attention: Dr. A. Busemann

National Advisory Committee
for Aeronautics
Langley Aeronautical Laboratory
Langley Field, Virginia
Attention: Mr. C. McLellan

National Advisory Committee
for Aeronautics
Langley Aeronautical Laboratory
Langley Field, Virginia
Attention: Mr. John Stack

National Advisory Committee
for Aeronautics
Lewis Flight Propulsion Laboratory
Cleveland Municipal Airport
Cleveland 11, Ohio

National Advisory Committee
for Aeronautics
Lewis Flight Propulsion Laboratory
Cleveland Municipal Airport
Cleveland 11, Ohio
Attention: Dr. J. C. Evvard

National Advisory Committee
for Aeronautics
Lewis Flight Propulsion Laboratory
Cleveland Municipal Airport
Cleveland 11, Ohio
Attention: Dr. A. Silverstein

Technical Information Service
P. O. Box 62
Oak Ridge, Tennessee

U. S. Government Agencies
For Transmittal to
Foreign Countries

Chief of Ordnance
Department of the Army
Washington 25, D. C.
Attention: ORDGU-SE
Foreign Relations Section
For Transmittal To
Australian Joint Services Mission

Chief of Ordnance
Department of the Army
Washington 25, D. C.
Attention: ORDGU-SE
Foreign Relations Section
For Transmittal To
Canadian Joint Staff

Chief of Ordnance
Department of the Army
Washington 25, D. C.
Attention: ORDGU-SE
Foreign Relations Section
For Transmittal To
Dr. Josef Rabinowicz
Department of Aeronautical Engineering
TECHNION
Israel Institute of Technology
Haifa, Israel

Chief of Ordnance
Department of the Army
Washington 25, D. C.
Attention: ORDGU-SE
Foreign Relations Section
For Transmittal To
Professor Itiro Tani
Aeronautical Research Institute
Tokyo University
Komaba, Meguro-ku
Tokyo, Japan

Chief of Ordnance
Department of the Army
Washington 25, D. C.
Attention: ORDGU-SE
Foreign Relations Section
For Transmittal To
Professor D. C. Pack
Royal Technical College
Glasgow, Scotland

Chief of Ordnance
Department of the Army
Washington 25, D. C.
Attention: ORDGU-SE
Foreign Relations Section
For Transmittal To
The Aeronautical Research
Institute of Sweden
Ulvsunda 1, Sweden
Attention: Mr. Georg Drougge

Air Research and Development
Command
European Office
Shell Building
60 Rue Rabenstein
Brussels, Belgium
Attention: Col. Lee Gossick, Chief
5 copies

Commanding Officer
Office of Naval Research
Branch Office
Navy, 100
FPO
New York, N. Y.
2 copies

Universities and Non-Profit Organizations

Brown University
Providence 12, R. I.
Attention: Professor R. Meyer

Brown University
Graduate Division of Applied Mathematics
Providence 12, Rhode Island
Attention: Dr. W. Prager

Brown University
Graduate Division of Applied Mathematics
Providence 12, Rhode Island
Attention: Dr. R. Probstein

University of California
Low Pressures Research
Institute of Engineering Research
Engineering Field Station
1301 South 46th Street
Richmond, California
Attention: Professor S. A. Schaaf

University of California at Los Angeles
Department of Engineering
Los Angeles 24, California
Attention: Dr. L. M. K. Boelter

University of California at Los Angeles
Department of Engineering
Los Angeles 24, California
Attention: Professor J. Miles

Case Institute of Technology
Cleveland, Ohio
Attention: Dr. G. Kuerti

Catholic University of America
Department of Physics
Washington 17, D. C.
Attention: Professor K. F. Herzfeld

Cornell University
Graduate School of Aeronautical Engineering
Ithaca, New York
Attention: Dr. E. L. Resler, Jr.

Cornell University
Graduate School of Aeronautical Engineering
Ithaca, New York
Attention: Dr. W. R. Sears

Harvard University
Department of Applied Physics and
Engineering Science
Cambridge 38, Massachusetts
Attention: Dr. A. Bryson

Harvard University
Department of Applied Physics and
Engineering Science
Cambridge 38, Massachusetts
Attention: Dr. H. W. Emmons

University of Illinois
Department of Aeronautical Engineering
Urbana, Illinois
Attention: Professor C. H. Fletcher

The Johns Hopkins University
Applied Physics Laboratory
8621 Georgia Avenue
Silver Spring, Maryland
Attention: Dr. E. A. Bonney

The Johns Hopkins University
Applied Physics Laboratory
8621 Georgia Avenue
Silver Spring, Maryland
Attention: Dr. F. N. Frenkiel

The Johns Hopkins University
Applied Physics Laboratory
8621 Georgia Avenue
Silver Spring, Maryland
Attention: Dr. F. K. Hill

The Johns Hopkins University
Department of Aeronautical Engineering
Baltimore 18, Maryland
Attention: Dr. F. H. Clauser

The Johns Hopkins University
Department of Aeronautical Engineering
Baltimore 18, Maryland
Attention: Dr. L. Kovasznay

The Johns Hopkins University
Department of Mechanical Engineering
Baltimore 18, Maryland
Attention: Dr. S. Corrsin

Lehigh University
Physics Department
Bethlehem, Pennsylvania
Attention: Dr. R. Emrich

University of Maryland
Department of Aeronautical Engineering
College Park, Maryland
Attention: Dr. S. F. Shen

University of Maryland
Institute of Fluid Dynamics and
Applied Mathematics
College Park, Maryland
Attention: Director

University of Maryland
Institute of Fluid Dynamics and
Applied Mathematics
College Park, Maryland
Attention: Professor J. M. Burgers

University of Maryland
Institute of Fluid Dynamics and
Applied Mathematics
College Park, Maryland
Attention: Professor F. R. Hama

University of Maryland
Institute of Fluid Dynamics and
Applied Mathematics
College Park, Maryland
Attention: Professor S. I. Pai

Massachusetts Institute of Technology
Cambridge 39, Massachusetts
Attention: Dr. A. H. Shapiro

Massachusetts Institute of Technology
Department of Aeronautical Engineering
Cambridge 39, Massachusetts
Attention: Professor M. Finston

Massachusetts Institute of Technology
Department of Aeronautical Engineering
Cambridge 39, Massachusetts
Attention: Professor E. Mollo-Christensen

Massachusetts Institute of Technology
Department of Aeronautical Engineering
Cambridge 39, Massachusetts
Attention: Dr. G. Stever

Massachusetts Institute of Technology
Department of Mathematics
Cambridge 39, Massachusetts
Attention: Professor C. C. Lin

University of Michigan
Ann Arbor, Michigan
Attention: Dr. H. P. Liepmann

University of Michigan
Department of Aeronautical Engineering
East Engineering Building
Ann Arbor, Michigan
Attention: Dr. Arnold Kuethe

University of Michigan
Department of Aeronautical Engineering
East Engineering Building
Ann Arbor,Michigan
Attention: Professor W. C. Nelson

University of Michigan
Department of Aeronautical Engineering
Aircraft Propulsion Laboratory
Ann Arbor, Michigan
Attention: Mr. J. A. Nicholls

University of Michigan
Department of Physics
Ann Arbor, Michigan
Attention: Dr. O. Laporte

University of Minnesota
Department of Aeronautical Engineering
Minneapolis 14, Minnesota
Attention: Professor J. D. Akerman

University of Minnesota
Department of Aeronautical Engineering
Minneapolis 14, Minnesota
Attention: Dr. C. C. Chang

University of Minnesota
Department of Aeronautical Engineering
Minneapolis 14, Minnesota
Attention: Dr. R. Hermann

University of Minnesota
Department of Mechanical Engineering
Division of Thermodynamics
Minneapolis, Minnesota
Attention: Dr. E. R. G. Eckert

New York University
Department of Aeronautics
University Heights
New York 53, New York
Attention: Dr. J. F. Ludloff

New York University
Institute of Mathematics and Mechanics
45 Fourth Street
New York 53, New York
Attention: Dr. R. W. Courant

North Carolina State College
Department of Engineering
Raleigh, North Carolina
Attention: Professor R. M. Pinkerton

Ohio State University
Aeronautical Engineering Department
Columbus, Ohio
Attention: Professor A. Tifford

Ohio State University
Aeronautical Engineering Department
Columbus, Ohio
Attention: Professor G. L. von Eschen

University of Pennsylvania
Philadelphia, Pennsylvania
Attention: Professor M. Lessen

Polytechnic Institute of Brooklyn
Aerodynamic Laboratory
527 Atlantic Avenue
Freeport, New York
Attention: Dr. A. Ferri

Polytechnic Institute of Brooklyn
Aerodynamic Laboratory
527 Atlantic Avenue
Freeport, New York
Attention: Dr. P. Libby

Princeton University
Princeton, New Jersey
Attention: Dr. Sin I. Cheng

Princeton University
Forrestal Research Center
Princeton, New Jersey
Attention: Library

Princeton University
Aeronautics Department
Forrestal Research Center
Princeton, New Jersey
Attention: Professor S. Bogdonoff

Princeton University
Aeronautics Department
Forrestal Research Center
Princeton, New Jersey
Attention: Dr. L. Crocco

Princeton University
Aeronautics Department
Forrestal Research Center
Princeton, New Jersey
Attention: Professor Wallace Hayes

Princeton University
Palmer Physical Laboratory
Princeton, New Jersey
Attention: Dr. W. Bleakney

Purdue University
School of Aeronautical Engineering
Lafayette, Indiana
Attention: Librarian

Purdue University
School of Aeronautical Engineering
Lafayette, Indiana
Attention: Professor H. DeGroff

Rensselaer Polytechnic Institute
Aeronautics Department
Troy, New York
Attention: Dr. R. P. Harrington

Rensselaer Polytechnic Institute
Aeronautics Department
Troy, New York
Attention: Dr. T. Y. Li

Rouss Physical Laboratory
University of Virginia
Charlottesville, Virginia
Attention: Dr. J. W. Beams

University of Southern California
Engineering Center
3518 University Avenue
Los Angeles 7, California
Attention: Dr. R. Chuan

University of Southern California
Aeronautical Laboratories Department
Box 1001
Oxnard, California
Attention: Mr. J. H. Carrington,
Chief Engineer

Stanford University
Department of Mechanical Engineering
Palo Alto, California
Attention: Dr. D. Bershader

Stanford University
Department of Aeronautical Engineering
Palo Alto, California
Attention: Professor Walter Vincenti

University of Texas
Defense Research Laboratory
500 East 24th Street
Austin, Texas
Attention: Professor M. J. Thompson

University of Washington
Department of Aeronautical Engineering
Seattle 5, Washington
Attention: Professor F. S. Eastman

University of Washington
Department of Aeronautical Engineering
Seattle 5, Washington
Attention: Professor R. E. Street

University of Wisconsin
Department of Chemistry
Madison, Wisconsin
Attention: Dr. J. O. Hirschfelder

Institute of the Aeronautical Sciences
2 East 64th Street
New York 21, New York
Attention: Library

Midwest Research Institute
4049 Pennsylvania
Kansas City, Missouri
Attention: Mr. M. Goland, Director
for Engineering Sciences

National Science Foundation
Washington 25, D. C.
Attention: Dr. J. McMillan

National Science Foundation
Washington 25, D. C.
Attention: Dr. R. Seeger

Industrial Companies

Aeronutronic Systems, Inc.
1234 Air Way
Glendale, California
Attention: Dr. J. Charyk

Aeronutronic Systems, Inc.
1234 Air Way
Glendale, California
Attention: Dr. L. Kavanau

Aerophysics Development Corp.
P. O. Box 689
Santa Barbara, California
Attention: Librarian

Allied Research Associates, Inc.
43 Leon Street
Boston, Massachusetts
Attention: Dr. T. R. Goodman

ARO, Inc.
P. O. Box 162
Tullahoma, Tennessee
Attention: Dr. B. Goethert

ARO, Inc.
P. O. Box 162
Tullahoma, Tennessee
Attention: Librarian,
Gas Dynamics Facility

AVCO Manufacturing Corp.
2385 Revere Beach Parkway
Everett 49, Massachusetts
Attention: Library

AVCO Manufacturing Corp.
2385 Revere Beach Parkway
Everett 49, Massachusetts
Attention: Dr. A. Kantrowitz

AVCO Manufacturing Corp.
Advanced Development Division
2385 Revere Beach Parkway
Everett 49, Massachusetts
Attention: Dr. F. R. Riddell

Bell Aircraft Corp.
Aerodynamics Section
P. O. Box 1
Buffalo 5, New York
Attention: Dr. Joel S. Isenberg

Boeing Airplane Company
P. O. Box 3107
Seattle 14, Washington
Attention: Mr. G. Snyder

Chance Vought Aircraft, Inc.
P. O. Box 5907
Dallas, Texas
Attention: Mr. J. R. Clark

CONVAIR
A Division of General Dynamics Corp.
San Diego 12, California
Attention: Mr. C. Bossart

CONVAIR
A Division of General Dynamics Corp.
San Diego 12, California
Attention: Mr. W. H. Dorrance
Dept. 1-16

CONVAIR
A Division of General Dynamics Corp.
San Diego 12, California
Attention: Mr. W. B. Mitchell

CONVAIR
A Division of General Dynamics Corp.
Fort Worth 1, Texas
Attention: Mr. W. B. Fallis

CONVAIR
A Division of General Dynamics Corp.
Fort Worth 1, Texas
Attention: Mr. E. B. Maske

CONVAIR
A Division of General Dynamics Corp.
Fort Worth 1, Texas
Attention: Mr. W. G. McMullen

CONVAIR
A Division of General Dynamics Corp.
Fort Worth 1, Texas
Attention: Mr. R. H. Widmer

Cooperative Wind Tunnel
950 South Raymond Avenue
Pasadena, California
Attention: Mr. F. Felberg

Cooperative Wind Tunnel
950 South Raymond Avenue
Pasadena, California
Attention: Mr. E. I. Pritchard

Cornell Aeronautical Laboratory
Buffalo, New York
Attention: Dr. A. Flax

Cornell Aeronautical Laboratory
Buffalo, New York
Attention: Mr. A. Hersberg

Cornell Aeronautical Laboratory
Buffalo, New York
Attention: Dr. F. K. Moore

Douglas Aircraft Company
Santa Monica, California
Attention: Mr. J. Gunkel

Douglas Aircraft Company
Santa Monica, California
Attention: Mr. Ellis Lapin

Douglas Aircraft Company
Santa Monica, California
Attention: Mr. H. Luskin

Douglas Aircraft Company
Santa Monica, California
Attention: Dr. W. B. Oswald

General Electric Company
Research Laboratory
Schenectady, New York
Attention: Dr. H. T. Nagamatsu

General Electric Company
Missile and Ordnance Systems Dept.
3198 Chestnut Street
Philadelphia 4, Pennsylvania
Attention: Documents Library,
L. Chasen, Mgr.-Libraries

The Glenn L. Martin Company
Aerophysics Research Staff
Flight Vehicle Division
Baltimore 3, Maryland
Attention: Dr. Mark V. Morkovin

The Glenn L. Martin Company
Baltimore 3, Maryland
Attention: Mr. G. S. Trimble, Jr.

Grumman Aircraft Engineering Corp.
Bethpage, New York
Attention: Mr. C. Tilgner, Jr.

Hughes Aircraft Company
Culver City, California
Attention: Dr. A. E. Puckett

Lockheed Aircraft Corp.
Missiles Division
Van Nuys, California
Attention: Library

Lockheed Missile Systems Division
Research and Development Laboratory
Sunnyvale, California
Attention: Dr. W. Griffith

Lockheed Missile Systems Division
P. O. Box 504
Sunnyvale, California
Attention: Dr. L. H. Wilson

Lockheed Missile Systems Division
Lockheed Aircraft Corp.
Palo Alto, California
Attention: Mr. R. Smelt

Lockheed Missile Systems Division
Lockheed Aircraft Corp.
Palo Alto, California
Attention: Mr. Maurice Tucker

Marquhardt Aircraft Company
P. O. Box 2013 - South Annex
Van Nuys, California
Attention: Mr. E. T. Pitkin

McDonnell Aircraft Corp.
Lambert-St. Louis Municipal Airport
P. O. Box 516
St. Louis 3, Missouri
Attention: Mr. K. Perkins

North American Aviation, Inc.
Aeronautical Laboratory
Downey, California
Attention: Dr. E. R. Van Driest

Northrop Aircraft, Inc.
1001 East Broadway
Hawthorne, California
Attention: Mr. E. Schmued

Ramo-Wooldridge Corporation
409 East Manchester Blvd.
Inglewood, California
Attention: Dr. M. U. Clauser

Ramo-Wooldridge Corporation
409 East Manchester Blvd.
Inglewood, California
Attention: Dr. Louis G. Dunn

Ramo-Wooldridge Corporation
P. O. Box 45564, Airport Station
Los Angeles 45, California
Attention: Dr. C. B. Cohen

Ramo-Wooldridge Corporation
P. O. Box 45564, Airport Station
Los Angeles 45, California
Attention: Dr. John Sellars

The RAND Corporation
1700 Main Street
Santa Monica, California
Attention: Library

The RAND Corporation
1700 Main Street
Santa Monica, California
Attention: Dr. C. Gazley

The RAND Corporation
1700 Main Street
Santa Monica, California
Attention: Mr. E. P. Williams

Republic Aviation Corporation
Conklin Street
Farmingdale, L. I., New York
Attention: Dr. W. J. O'Donnell

United Aircraft Corporation
East Hartfort, Connecticut
Attention: Mr. J. G. Lee

Internal

Dr. Harry Ashkenas
Dr. Frank E. Goddard
Dr. James M. Kendall
Dr. John Laufer
Dr. Thomas Vrebalovich
Dr. Peter P. Wegener
Dr. Harry E. Williams
Hypersonic WT; Attn: Mr. G. Goranson
Reports Group
Jet Propulsion Laboratory
4800 Oak Grove Drive
Pasadena 2, California

Dr. W. D. Rannie
Goddard Professor
Jet Propulsion Center
California Institute of Technology

Dr. Julian D. Cole
Dr. Donald E. Coles
Dr. P. A. Lagerstrom
Prof. Lester Lees
Dr. H. W. Liepmann
Dr. Clark B. Millikan
Dr. Anatol Roshko

Aeronautics Library
Hypersonic Files (3)
Hypersonic Staff and Research Workers (20)

Foreign

via AGARD Distribution Centers